

THERMAL FUSION FOR SUTURELESS CLOSURE:
DEVICES, COMPOSITION, METHODS

by

ERIC ANTHONY KRAMER

B.S., Temple University, 2010

M.S., University of Colorado, 2013

A thesis submitted to the
Faculty of the Graduate School of the
University of Colorado in partial fulfillment
of the requirement for the degree of
Doctor of Philosophy
Department of Mechanical Engineering

2016

This thesis entitled:
Thermal Fusion for Sutureless Closure: Devices, Composition, Methods
written by Eric Kramer
has been approved for the Department of Mechanical Engineering

Dr. Mark E. Rentschler, Advisor

Dr. Virginia L. Ferguson

The final copy of this thesis has been examined by the signatories, and we find that both the content and the form meet acceptable presentation standards of scholarly work in the above mentioned discipline.

Date: _____

Abstract

Kramer, Eric A. (Ph.D., Mechanical Engineering. Department of Mechanical Engineering)

Thermal Fusion for Sutureless Closure: Devices, Composition, Methods

Thesis directed by Associate Professor Mark E. Rentschler

As minimally invasive surgical techniques progress, the demand for reliable ligation is pronounced. The surgical advantages of energy-based vessel sealing exceed those of traditional, compression-based ligatures in procedures sensitive to duration, foreign bodies, and recovery time alike. While the use of energy-based devices to seal or transect vasculature and connective tissue bundles is widespread, the breadth of heating strategies and energy dosimetry used between devices underscores an uncertainty as to the molecular nature of the sealing mechanism and induced tissue bond. Further, energy-based techniques (e.g., tissue “fusion” or tissue “welding”) exhibit promise for the closure, repair and functional recovery of soft and connective tissues in the orthopaedic, colorectal and dermal domains. To optimize and progress the use of energy-based tissue fusion, a constitutive theory of molecular bonding forces that arise in response to suprphysiological temperatures is required. While rapid tissue bonding may arise from dehydration and water transport, dipole interactions, covalent crosslinks or the coagulation of cellular proteins, long-term tissue repair requires that the reaction to thermal damage be tailored to accelerate and mimic the onset of biological healing and remodeling. The aim of this work is to supplement the findings of published thermal fusion research by exploring the contributions of primary and secondary tissue constituents to the formation of energy-based fusion bonds. Results of this work and their associated implications to the theory of energy-based surgical adhesion will encourage a molecular approach to characterization of the prevalent and promising energy-based tissue bond.

Dedication

To my family and friends, domestic and foreign, who continue to provide me with the requisite education, guidance, and inspiration to discover.

Acknowledgments

I am continually grateful for my principal advisor, Dr. Mark E. Rentschler, for his acute mentorship and comprehensive approach to a graduate education. In numerous instances, he has afforded generosity and compliance to enable me to explore the breadth of my abilities, often far beyond the prescribed path of our initial research aims. I would also like to thank my co-advisor, Dr. Virginia L. Ferguson, for likewise encouraging an international pursuit of education and for integrating my passion for healthcare with a foundation in engineering. It has been a veritable thrill to pursue this frontier of minimally invasive surgery, energy-based tissue fusion, with Dr. Rentschler and Dr. Ferguson.

Several special individuals have been instrumental to the progression of my undergraduate and graduate education. Primarily, I would like to thank Dr. George Baran and Dr. Quan Wan for their instruction and encouragement during my undergraduate entry into the field of bioengineering and biomaterials at Temple University. Likewise, Dr. David Tebbe and Dr. Andre Lutz acted as benevolent mentors and true friends during my employment at Heraeus Kulzer and Jeppesen in Germany, and during my often trepid yet surely entertaining assimilation into the German culture and language.

I would like to once more thank Dr. Mark Rentschler, in addition to Dr. Gregory Rieker for their persistent encouragement of my involvement with the graduate educational programs within Design Center Colorado. In addition to providing mentorship during my participation in the program, Dr. Rieker has consistently entrusted me to make significant contributions to the structure and orchestration of graduate courses in product design. My experiences in the

program have strengthened my confidence as an educator and designer, and have led to the next step in my career as a fellow in the Biodesign Innovation Fellowship at Stanford University.

I would also like to thank Dr. James Cezo for his warm and tireless mentorship during my orientation to the field of energy-based tissue fusion. Dr. Cezo set a continuous example of the dedication and persistence required for the execution and dissemination of “good science”. I would like to thank Nicholas Anderson for his companionship and education during late nights of data collection, and his published contributions to our investigations of tissue-device interactions in energy-based tissue fusion. I am indebted to Alex Barrett at the University of Colorado Denver for his instruction of the biochemical methods required to make novel strides towards the understanding of molecular transitions in energy-based fusion adhesion, and his assistance with the data collection instrumental to the final aim of my research. Likewise, I am thankful for Doug Fankell’s partnership in the pursuit of novel characterization metrics for fusion adhesion. I am thankful to Dr. Ken Taylor, Kelli Barnes, and Renée Merchel of ConMed Corporation for their persistent support in the shared pursuit of optimizing and advancing the field of energy-based vascular surgery, from regular meetings to companionship in animal laboratories and throughout our attendance at international conferences. I would like to acknowledge the Innovative Grant Program (IGP) at the University of Colorado Boulder for providing instrumental support to the research presented herein. Finally, I would like to thank Elizabeth Chipala at Premier Laboratory and Joe Dragavon of the Advanced Light Microscopy Core within the BioFrontiers Institute at the University of Colorado for their kind assistance in obtaining imagery of fused tissues for publication in our numerous scholarly manuscripts.

Table of Contents

ABSTRACT	III
DEDICATION	IV
ACKNOWLEDGMENTS	V
TABLE OF CONTENTS	VII
LIST OF TABLES.....	XI
LIST OF FIGURES.....	XII
CHAPTER 1. INTRODUCTION.....	1
1.1. SCOPE OF RESEARCH.....	1
<i>1.1.1. Aim 1.....</i>	<i>1</i>
<i>1.1.2. Aim 2.....</i>	<i>2</i>
<i>1.1.3. Aim 3.....</i>	<i>2</i>
CHAPTER 2. BACKGROUND AND LITERATURE REVIEW	3
2.1. BACKGROUND	3
<i>2.1.1. Surgical Benefits and Drawbacks of Thermal Fusion</i>	<i>3</i>
<i>2.1.2. Energy-Based Surgical Devices and Energy Delivery Modalities.....</i>	<i>5</i>
<i>2.1.3. Clinical Applications of Energy-Based Surgery</i>	<i>10</i>
<i>2.1.4. Prospective Applications of Energy-Based Surgery</i>	<i>11</i>
2.2. EMPIRICAL FINDINGS	12
2.2.1. <i>Device comparison studies</i>	<i>12</i>
2.2.2. <i>Tissue-device interactions.....</i>	<i>14</i>
2.2.3. <i>Strength testing of fused tissue.....</i>	<i>15</i>
2.2.4. <i>Results of experimental fusion</i>	<i>17</i>
2.3. ADHESION THEORY	22
2.3.1. <i>Collagen Structure & Denaturation</i>	<i>22</i>

2.3.2. <i>Observations of Thermal Transitions in Collagen</i>	23
2.3.3. <i>Dehydration & water transport</i>	24
2.3.4. <i>Amalgamation of cellular and extracellular non-collagenous proteins</i>	26
2.4. MOVING FORWARD	26
2.4.1. <i>Approaches to Gaps in Adhesion Theory</i>	26
2.4.2. <i>Collagen crosslinking</i>	28
2.4.3. <i>Molecular bonding of cellular and matrix proteins</i>	28
2.4.4. <i>Assessment of Tissue Viability and Functional Recovery Potential</i>	28
2.4.5. <i>Applicability to tissue engineering</i>	29
2.5. SUMMARY	29
CHAPTER 3. STRENGTH AND PERSISTENCE OF ENERGY-BASED VESSEL SEALS RELY ON TISSUE WATER AND GLYCOSAMINOGLYCAN CONTENT	30
3.1. INTRODUCTION.....	30
3.2. MATERIALS AND METHODS.....	34
3.2.1. <i>Tissue harvest and storage</i>	34
3.2.2. <i>Tissue preparation and treatment</i>	34
3.2.3. <i>Alteration of water content</i>	35
3.2.4. <i>Alteration of GAG content</i>	35
3.2.5. <i>Seal Rehydration</i>	36
3.2.6. <i>Measurement of water content</i>	36
3.2.7. <i>Strength testing by bursting pressure</i>	36
3.2.8. <i>Quantification of GAG content</i>	37
3.2.9. <i>Histology</i>	38
3.2.10. <i>Data analysis</i>	39
3.3. RESULTS.....	39
3.3.1. <i>Water content</i>	39
3.3.2. <i>GAG Digestion</i>	41
3.3.3. <i>Seal Rehydration</i>	42

3.3.4. Histology.....	43
3.4. DISCUSSION.....	45
3.5. CONCLUSIONS	49
CHAPTER 4. EFFECTS OF HEATING RATE AND DURATION ON BOND STRENGTH IN ENERGY- BASED VESSEL SEALING.....	51
4.1. INTRODUCTION.....	51
4.2. MATERIALS & METHODS	54
4.2.1. Tissue harvest, preparation & treatment	54
4.2.2. Variation of Heating Rate	54
4.2.3. Load-Controlled Fusion Apparatus	55
4.2.4. Bursting Pressure Measurement.....	57
4.3. RESULTS.....	58
4.3.1. Load Control.....	58
4.4. DISCUSSION.....	60
4.4.1. Conclusion	63
CHAPTER 5. CROSSLINK STABILITY IN ENERGY-BASED TISSUE BONDING: MOLECULAR ANALYSIS OF COLLAGENOUS TRANSITIONS VIA RAMAN SPECTROSCOPY AND MASS SPECTROMETRY	64
5.1. INTRODUCTION.....	64
5.1.1. High-Level Bonding Theory.....	65
5.1.2. Low-Level Bonding Theory.....	67
5.1.3. Raman Spectroscopy in Fusion Research	68
5.1.4. Collagen and Elastin Crosslink Quantification	69
5.1.5. HPLC in Fusion Research	70
5.1.6. Proteomics in Fusion Research	70
5.1.7. Summary of Experimental Aims.....	71
5.2. MATERIALS & METHODS	71

5.2.1. Tissue harvest, preparation & treatment	71
5.2.2. Raman spectral Collection.....	72
5.2.3. Hydrolysis of sample.....	73
5.2.4. Preparation of CF-11 Enrichment Column	73
5.2.5. UHPLC Analysis.....	74
5.2.6. MS Data Acquisition.....	74
5.2.7. Quantification of cross-linked amino acids	75
5.2.8. Histology.....	75
5.2.9. Data Processing & Statistical Analysis	76
5.3. RESULTS.....	76
5.3.1. Histology.....	76
5.3.2. Raman Spectroscopy.....	77
5.3.3. Crosslinked Amino Acids Mass Spectrometry.....	80
5.3.4. Proteomic Analysis	82
5.4. DISCUSSION.....	83
5.4.1. Histology.....	84
5.4.2. Raman Spectroscopy.....	84
5.4.3. Cross-link quantification	85
5.4.4. Proteomics	86
5.4.5. Conclusion	86
CHAPTER 6. CONCLUSIONS AND FUTURE WORK.....	87
6.1. TISSUE HYDRATION AND GLYCOSAMINOGLYCAN CONTENT	87
6.2. HEATING RATES AND FUSION DURATION.....	88
6.3. COLLAGEN DENATURATION AND CROSS-LINKING OF EXTRACELLULAR MATRIX PROTEINS.....	88
6.4. SYNTHESIS OF OUTCOMES.....	89
6.5. CLOSURE	93
REFERENCES	94

List of Tables

Table 5.1: Principal frequencies of Raman-active vascular protein bands of interest ¹²² 69

Table 5.2: Identity, specifications and fold changes of selected proteins for proteomic analysis 82

List of Figures

Figure 2.1: Vascular sealing and cutting instruments. A) Ethicon Harmonic ACE®, b)Covidien LigaSure™, c) Olympus Thunderbeat, d)ConMed ALTRUS™	8
Figure 3.1: a) Water contents by weight of osmotically treated arteries. b) Bursting pressures of sealed arteries in corresponding treatment groups.....	40
Figure 3.2: a) Sulfated GAG content as a fraction of dry tissue weight for control and enzyme-treated arteries. b) Bursting pressures in mmHg for native (0 h) and enzyme-treated arteries. .	42
Figure 3.3: Bursting pressures of rehydrated arteries from native and GAG-digested arteries with respect to rehydration duration..	43
Figure 3.4: H&E (a,b,c) and VVG (d,e,f) -stained cross-sections of vascular seals from the hypotonic, isotonic and hypertonic treatment groups.....	44
Figure 3.5: H&E (a-e) and Light Green:SafO (f-j) - stained cross-sections of vascular seals from control and GAG-digestion treatment groups.	47
Figure 4.1: Heating rate profiles for instantaneous and progressive heating rates at a) 120 °C and b) 170 °C.	55
Figure 4.2: Tissue fusion construct for the variation of apposition pressure, heating rate, temperature and fusion duration under sustained hydration using 0.9% PBS.....	57
Figure 4.3: : Representative loading profiles for instantaneous and progressive heating rates at 100 N for a fusion duration of 9 s.	58
Figure 4.4: Bursting pressures of vessels sealed at various heating rates with 100 N force (~3.3 MPa) at a) 170 °C and b) 120 °C.	59
Figure 4.5: Bursting pressures of vessels sealed at various heating rates with 40 N apposition force (~1.3 MPa) at a) 170 °C and b) 120 °C.	60

Figure 5.1: Histology of fresh (a,c) and fused (b,d) arteries stained with picosirius red under polarized light (a,b) and H&E in brightfield (c,d). 77

Figure 5.2: Mean Raman spectra for native and thermally fused arterial tissue..... 78

Figure 5.3: : Raman peak intensities and ratios for crosslink species of interest. 79

Figure 5.4: Normalized peak area for the Amide III and Amide I Raman bands..... 80

Figure 5.5: Normalized peak areas of bivalent (collagen, immature), trivalent (collagen, mature) and tetravalent (elastic) collagen crosslinks detected by HPLC/MS for native and fused tissue. 81

Chapter 1. Introduction

1.1. Scope of Research

For millennia, wound closure has relied on the mechanical stability of sutures. Despite centuries of surgical progression, departures from foreign-body mechanical closure remain rare to this day. The advent of energy-based tissue coaptation, however, has spawned a surge in device development and has nearly replaced mechanical closure with a biological “nano-suture” for vascular ligation and hemostasis. The concept of energy-based tissue coaptation or “tissue fusion” revolves around the dehydration, denaturation and thermal coagulation of vascular proteins. While thermal fusion excels in permanent vascular closure, this system of adhesion has the potential to join and repair cellular tissues in the vascular, dermal, gastric and colorectal surgical domains among others, which may render foreign-body mechanical closure obsolete and greatly accelerate the fields of open and minimally invasive surgery. This research is centered at the characterization and exploitation of thermal bonding mechanisms for the expansion of tissue fusion into instantaneous, watertight and functionally recoverable tissue closure. Through investigations of constitutive bonding forces, biochemical characterizations thereof and an evaluation of long-term healing potential in fused tissues, the broadening potential of thermal tissue repair is presented.

1.1.1. Aim 1

Aim 1 of this research targets the contribution of specific vascular constituents to the strength of adhesion between fused vascular tissue layers. Specifically, water content and glycosaminoglycan content were varied prior to fusion; fusion strengths as quantified by vascular bursting pressure were used to assess the influence of varied arterial composition on the formation of fusion bonds. Likewise, the rehydration of vascular seals post-fusion was

investigated as a measure of a bond's dependence on the vaporization of water, as well as its resilience with exposure to a hydrated environment. The objective of Aim 1 is to initiate a constitutive model of adhesion forces for use in predicting the fusion potential of a given tissue type based upon its chemical composition.

1.1.2. Aim 2

The second Aim of this work is to characterize the effect of tissue-device interactions on the induced strength outcomes in fused vascular tissues. Specifically, heating rates and durations are investigated for vascular sealing using a clinically approved fusion device, in attempts to validate and leverage the findings of Aim 1 for enhanced bond strength, with the goal of maintaining tissue hydration and tissue viability for functional recovery in such prospective fusion applications as vascular anastomosis.

1.1.3. Aim 3

Aim 3 of this work concerns the quantification of collagenous crosslinks present in pre- and post-fusion vascular tissue samples. As crosslinking is a primary component of published fusion adhesion theory despite minimal supporting data, the empirical determination of Collagenous crosslinks' contribution to fusion adhesion is a critical step in the formation of a robust bonding theory. As with Aims 1 and 2, Aim 3 intends to clarify existing discrepancies on the nature of the fusion bond, allowing for improved predictions of the chemical conditions required for thermal tissue adhesion.

Chapter 2. Background and Literature Review

Following is a discussion of the anatomy and physiology of fused vascular tissue, and research performed to date concerning the characterization of bonding forces, the response of tissues to supraphysiological temperatures, device performance and tissue damage as they relate to the clinical and prospective applications of thermal tissue fusion.

2.1. Background

2.1.1. Surgical Benefits and Drawbacks of Thermal Fusion

Vascular tissue fusion has gained traction in clinical ligation for its decreased invasiveness, reduced infection rates and ease of surgical implementation relative to sutures, staples, clips and adhesives^{36,108}. Classical fusion devices have roots in the late 19th and early 20th century, when they saw success in the fulguration of tumors, specifically those with excessive vascularity¹²¹. The immediate coagulation of transected vessels prevented the removal of growths that would otherwise have caused terminal hemorrhaging. Applications of the technique quickly spread from neurosurgery to gynecologic surgery and microsurgery, where precise coagulation and ligation was required. Modern instruments have been optimized for minimally invasive surgical procedures; many devices now incorporate cutting blades to transect desiccated but intact tissues. Further, the use of energy-based devices offers significant reductions in procedural time and surgical dexterity; a single ligature takes only seconds to complete relative to the dexterous operation of passing and tying vascular sutures. Likewise, surgical fusion devices leave behind no foreign bodies, whereas the equally swift staple and clip applicators rely on stainless steel or titanium fragments that remain permanently at the ligation site: detachment and blood loss are two associated risks that the use of fusion averts⁷⁹. A myriad of open and minimally invasive surgical procedures now benefit from the efficacy vascular

thermal fusion such as hysterectomy, adrenalectomy, splenectomy, colorectal ligation, cholecystectomy and nissen fundoplication^{60,94}.

A primary drawback to the use of thermal fusion is the lateral spread of thermal energy and associated tissue destruction to untargeted tissues. While fusion represents only a portion of electro-surgical techniques, an estimated 40,000 patients experience electro-surgery-related injuries each year¹²¹. With exposure to thermal energy above 60°C, primary structural proteins such as collagen are irreversibly denatured¹¹⁴, causing permanent conformational changes in heated tissues. This can result in tissue necrosis leading to loss of tissue function; in vascular tissues this is assumed, yet loss of neurological function can be an unintended consequence of misplaced fusion energy due to lateral thermal spread, device misuse or inadvertent device activation. In response to the rapid development of energy-based surgical devices, the Society of American Gastrointestinal and Endoscopic Surgeons (SAGES) has founded a program to research and develop appropriate training and compliance methods for surgeons, hospitals and energy-based device firms, dubbed the Fundamental Use of Surgical Energy (FUSE)¹²¹.

An additional drawback to the use of fusion devices is smoke production. In endoscopic surgical procedures, visibility of the surgical space is critical to procedural execution, and endoscope lens cleaning is a regular occurrence due to fluid buildup and tissue deposits accumulating on the scope. As smoke is a byproduct of any electro-surgical device, endoscopic visualization is invariably compromised. While active and passive filtration systems have been developed to reduce this interference, none of the currently available systems provide a satisfactory solution to this problem. Surgeons must be careful to maintain adequate visualization for the operation of electro-surgical devices, in addition to considering the potentially harmful byproducts of high-energy tissue vaporization¹²¹.

While a number of vessel sealing instruments are approved for clinical use, a common criticism of these instruments by surgeons and investigators is the variability in device performance, particularly in bond strength of fused vessels^{78,121}. Given the empirical nature of device development, devices operate on fundamentally different physical principles and deliver varying degrees of energy to anatomically distinct vessels, resulting in unpredictable sealing and cutting performance. This reality is a primary motivation for this research; surgical fusion occurs by biophysical methods that are speculative, poorly or under-characterized and generally unknown to the scientific community. As such, the use of fusion remains restricted in its clinical applications, and progression into neighboring surgical and therapeutic fields remains experimental. A robust, constitutive theory of biophysical bonding forces is the greatest barrier to the expansion of thermal fusion, and the intention of this work is to supplement existing literature on the nature of the fusion bond. With detailed knowledge of bonding constituents and tissue responses to thermal and electrical energy, a known tissue's potential for fusion may be swiftly evaluated.

2.1.2. Energy-Based Surgical Devices and Energy Delivery Modalities

Monopolar & bipolar radiofrequency current

The advent of monopolar electrosurgery in early laparoscopy enabled the integration of hemostasis with tissue cutting at the interface of hydrated tissue and a charged, active electrode. The dispersing of a high density of electrons at the active electrode creates an-impedance based thermal effect, whereby the presence of water and ions within the tissue and its embedded cells induces an ionic oscillation and the subsequent conversion of electrical energy into heat. A well-grounded return electrode prevents thermal burns, and creates a concentration of thermal energy and an increase in temperature at the contact point of tissue and active electrode. As with thermal

cautery dating millennia, the desiccation and induced tissue damage have been leveraged in a series of monopolar tools for blunt tissue dissection, contact coagulation and the hemostasis of small blood vessels in open and laparoscopic surgeries.

As monopolar cautery was combined with device pressure for the hemostasis of small veins and arteries, the advancement of minimally invasive surgical techniques demanded a reliable energy-based tool for ligation of larger vessels. Bipolar radio frequency (RF) electrocautery was commercially introduced in 1955 as a single device containing a high-current, low-voltage active electrode, a return electrode and grasping pressure for vessel sealing in laparoscopic surgery¹²¹. Energy delivery for RF devices is controlled with feedback by measure of tissue impedance, a function of tissue water content. Once a tissue is coagulated and desiccated, impedance rises to a critical level and current is removed, a process lasting an average of 2–4 seconds⁶⁴. While these devices have gained significant clinical traction in recent years for vascular cutting and dissection, radiofrequency energy for use in nervous tissue bonding has been shown to interfere with the transmission of nerve impulses during and subsequent to the application of RF current¹⁰⁷. Persistent clinical RF devices include the LigaSure instruments (Medtronic–Covidien, Boulder, CO), ENSEAL[®] G2 end-articulating tissue sealers (Ethicon, Somerville, NJ), JustRight[™] Surgical Vessel Sealer (JustRight Surgical[™], Louisville, CO), HiQ+ (Olympus, Center Valley, PA).

Direct contact heating

Vessel sealing by direct conductive heating between device platens and target tissue provides temperature-controlled energy, in contrast to the impedance-based feedback of RF devices. Rapid heating cycles and varying heating algorithms for cutting and sealing procedures are designed to minimize lateral thermal tissue damage. A primary advantage of the direct

conduction approach in devices like the ConMed ALTRUST™ (ConMed, Centennial, CO) is its ability to operate in fluid environments. Additional features include a parallel closure for uniform device pressure and a bladeless cut function, which allows for the clean transection of target tissue without the addition of jamming-prone mechanical moving parts.

Ultrasonic oscillation

In attempts to localize device heating and tissue cutting to within the jaws of a vessel sealing device, manufacturers introduced ultrasonic oscillation and the mechanical heating of an active grasper against a stationary base. The Harmonic ACE®+ Shears (Ethicon, Somerville, NJ) oscillate a titanium blade at 55.5 kHz to seal, coagulate and cut tissue. Various power settings and blade pressures are used to induce the desired tissue effect⁹⁴, and recent device iterations have integrated an impedance-based biofeedback mechanism similar to that used in RF devices for the determination of energy dosimetry. A similar ultrasonic device is the Sonicbeat (Olympus). A variety of blade shapes have been implemented; straight blades have been proven more effective for hemostasis in vessel sealing, where tissue dissection is accelerated with the use of a curved blade, providing increased longitudinal movement⁹⁴. An additional advantage of ultrasonic oscillation is the production of less smoke and plume⁹⁴, which is ideal for laparoscopic surgery in which field visualization is critical. Recently, an attempt to merge the rapid dissection of ultrasonic oscillation and the reliable hemostasis of RF fusion has resulted in the Thunderbeat sealing and cutting device (Olympus). To the authors' knowledge, objective reports of Thunderbeat performance have yet to be published.

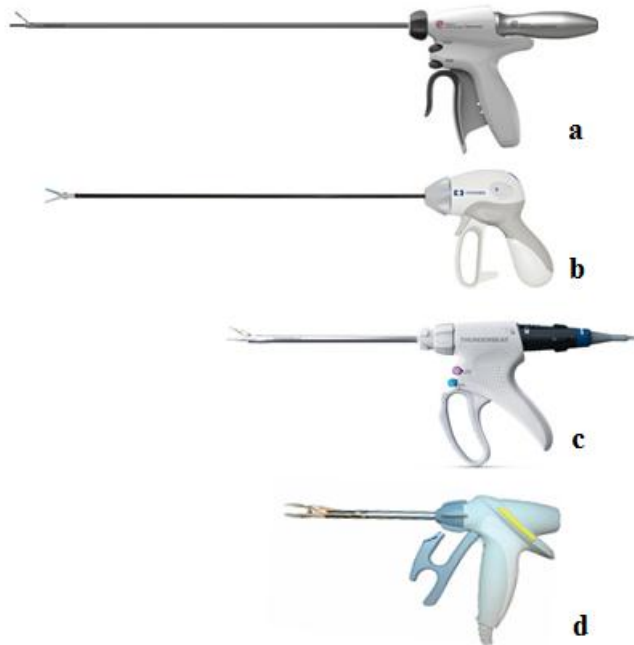


Figure 2.1: Vascular sealing and cutting instruments. A) Ethicon Harmonic ACE®, b)Covidien LigaSure™, c) Olympus Thunderbeat, d)ConMed ALTRUS™

Laser welding

The use of laser light for tissue coaptation represents a precise, controllable method for energy dosimetry with the ability for superficial and deep incidence in dermal^{3,38}, vascular⁷⁵ and colorectal tissues, with additional reports of biological attachment on the cellular level⁴⁴. Laser tissue fusion, more commonly known as laser “welding”, may be categorized by either photothermal or photochemical methods.

Photothermal welding is achieved by subjecting a closely approximated surgical incision or defect to incident laser light, generally at a wavelength that aligns to an absorption band of interstitial and bound water within the tissue (e.g., 1455 nm)⁹⁹. Near infrared (NIR) welding induces a transient rise in water temperature and the associated thermal effects in heated tissues

(e.g., protein denaturation, desiccation, and cavitation), as have been discussed for RF, ultrasonic and direct heat tissue fusion. Laser light may be pulsed or continuous, and has been applied to dermal tissues at optimized power, scanning rates, exposure area and duration for a full-thickness weld capable of mechanical characterization by tensile testing.

Photochemical tissue bonding refers to the use of chromophores and/or biological compounds to enhance the absorption and spread of optical energy, and thus thermal bonding, in targeted tissues. Photochemical compounds are often referred to as “solders” when used activated by photothermal laser light. Photochemical tissue bonding is unique in that it enables the augmentation and “doping” of solders with biological and synthetic agents to facilitate post-welding tissue regeneration⁷. Most common doping agents include albumin, fibrinogen, and collagen^{23,54,55}.

Biological and Synthetic adhesives

BioGlue is an FDA-approved surgical adhesive for the hemostasis of large vessel suture lines, reinforcement of degraded tissues, and blood loss prevention through puncture and suture lines, largely in cardiovascular surgery⁷⁵. Composed of 45% Bovine Serum Albumin (BSA) and 10% Glutaraldehyde, BioGlue is a compound biological and synthetic adhesive that provides chemical crosslinking of its self-contained BSA with native tissue proteins (e.g., collagen). Aqueous glutaraldehyde has also been used for the chemical stabilization of thermally fused aorta with minimal apposition pressure³⁰, in efforts to encourage functional recovery of fused tissue sections for the manufacture of bioprosthetic cardiac valves. Similar biocompatible and biodegradable glues have been used for the sealing and repair of transected peripheral nerves, yet the rigidity, cytotoxicity and potential for infection make them suboptimal for nerve repair⁷. Fibrin glues are designed to mimic the end stages of the clotting cascade of the healing response;

a fibrin adhesive may be recognized *in vivo* as a physiological blood clot⁷. Several studies using Fibrin glues have evidenced functional outcomes, quicker applications and superior histological results to those of traditional closure methods⁷. Junctions formed with fibrin-based glues are, however, characterized as having low tensile strength. Cyanoacrylate (CA) glues are likewise common in surgical tissue repair, attractive for their relative tensile strength and lower infection risks relative to those of fibrin glues. The regeneration and functional outcomes of tissue closure using CA glue are often identical to those of sutured techniques, though the setting procedure increases durations and potential mechanical complications once the glue has set⁷. While surgical adhesives provide an approved supplement to suture lines and puncture wounds during traditional, “cold” procedures (e.g., performed without the use of surgical energy), the focus of this review remains on energy-based adhesion, with or without chemical assistance.

2.1.3. Clinical Applications of Energy-Based Surgery

The clinical use of tissue fusion primarily consists of vascular ligation and transection for vessels 2–7 mm in diameter^{34,46}, inclusive of arterioles, small veins, arteries, medium-size muscular arteries and lymphatics. Sealing devices are likewise used for dissection of vascular tissue bundles to gain access to shrouded surgical sites. While many devices are designed with extended reach for endoscopic surgeries, applicable procedures fall within the endoscopic and open surgical realms of urology, thoracoscopy, plastic and reconstructive surgery, ear, nose and throat (ENT), and the general dissection, removal or resection of adhered, cancerous or otherwise pathological tissues and organs. The result is an increasing number of “lateral procedures” being cleared for use with fusion devices, often beyond the scope of the original design intent of the device. A prominent example of a lateral application is the dissection of cardinal and uterosacral ligaments during hysterectomy⁹⁴. A commonality between applicable surgical procedures is the

permanent, ablative (destructive) dissection and ligation required of them, where the targeted and often proximal adjacent tissues are rendered functionally idle due to desiccation and devitalization.

A primary method whereby energy-based devices induce fusion and cutting of a target tissue is the cavitation of intracellular contents upon conductive, oscillatory mechanical or electromagnetic vibration of intracellular ions. As temperatures reach 100 °C, intracellular volume increases in response to steam production, followed by cell rupture and the subsequent mechanical destruction of intra- and intermolecular bonds (e.g. Hydrogen bonds) within the surrounding extracellular matrix¹²¹. An analogous effect of thermal exposure to proteins is denaturation, whereby intramolecular bonds collapse and primary extracellular matrix proteins (e.g., Collagen types I and IV) dissociate or collapse from their secondary and tertiary structural arrangements. The association between protein denaturation, cavitation and other thermal effects with the formation of energy-based bonds will be discussed in *Bonding Theory*.

The desiccation of thermally treated tissues often makes dissection difficult in areas of high connective tissue content⁹⁴, where repeated device activation may be required. In the case of RF devices, cutting blades along the longitudinal axis of device jaws have been added to facilitate cutting where repeated device activation was insufficient. Similarly, rapid heating algorithms are implemented in direct conduction devices to induce a vaporization-induced cutting of grasped tissues¹²⁰, in contrast to a persistent application of heat for sealing operations.

2.1.4. Prospective Applications of Energy-Based Surgery

Of considerable interest in the design of vascular sealing tools is the minimization of lateral thermal spread in tissues adjacent to the surgical target. Several devices are designed to

limit thermal spread either by concentrated energy delivery (e.g., ultrasonic oscillation) or via a decrease in fusion temperatures⁹⁴. The consideration that less energy may be delivered as a controlled, recoverable injury to fusion candidates has been made seldom in the literature, superseded by an overwhelming majority of device comparison studies. However, recoverable fusion has been evidenced with similar advantages as those of vessel sealing relative to sutures in decreased perioperative blood loss¹⁰⁵ and minimized scarring in dermal tissue^{3,38}. Similarly, experimental fusion has been explored with promising results for a watertight union with functional recovery of such vascular, fluid-carrying tissues as the small and large bowel^{11,31,58,101}. Energy-based fusion has also been suggested and investigated for the thermal union of transected or pathological neurons without tissue deficit⁷. The use of fusion for the union and functional recovery of vascular tissues must balance bond strength with tissue hydration and cellular viability to initiate and progress a wound-healing response with biological remodeling. Results of experimental fusion techniques are discussed in *Empirical Findings*.

2.2. Empirical Findings

2.2.1. Device comparison studies

Numerous comparisons between vessel sealing devices have been published as a record of clinical device performance and surgical preference⁵². Users of the ultrasonic Harmonic ACE have reported a 23% reduction in thermal spread and 21% shorter transection times²⁵. In contrast, the RF-based LigaSure has significantly outperformed the Harmonic ACE with respect to bursting pressures of arteries ($p < 0.01$), with insignificant increases in the bursting pressure of veins equal to or less than 7mm in diameter³⁷. With regard to target size, vessels of increasing diameter have been found to require longer seal times across ultrasonic and RF devices⁶⁹. Several investigators have found veins to be more susceptible to collateral damage and wall

infiltration^{79,85}, given the decreased size of the muscular layer in venous tissues. JustRight Surgical[®] has placed design intent on providing surgeons with procedure-based, size-specific ligation tools, and is the first manufacturer to receive FDA clearance for RF fusion in pediatric cases²¹.

Concurrent with the obvious differences in device design and mode of operation, important to note in the comparison of fusion devices is variability in study design and associated outcomes of such evaluated end points as bursting pressure, seal duration, thermal damage, and failure rate. Considerations of data collection are discussed in detail in later sections, but the determination of device superiority, or inferiority, is complicated without a standardized measurement platform for the biothermomechanical effects of energy-based surgical devices. While the breadth of published literature represents the rapid advancement of a prosperous and promising surgical technique, the variation of energy delivery modalities and form factors in commercially available devices, rapid revision and combination of these modalities, and the breadth of device applicability with regard to vessel location, composition, and anatomical factors make device comparison and analysis a challenging task. Likewise, the determination of device efficacy and reliability in a clinical setting appears loosely defined and subject to user-based and environmental influences. These factors underscore the need for a bottom-up, analytical approach to energy-based surgical coaptation, fusion device development, and the regulatory approval process for tools that induce tissue-specific effects for a desired surgical outcome.

2.2.2. Tissue-device interactions

Contact Mechanics

The mechanical interaction between energy-based surgical devices and target tissues remains poorly understood⁷⁹, and is a motivational basis for research in the engineering domain of surgical device assessment. Investigations of contact mechanics of existing devices and associated tissue effects stand to optimize existing tools, and inform the development of advanced fusion applications and devices.

Fankell et al. recently developed an empirically-based parameter for the prediction of thermal bonding and cutting in arterial tissue through use of the finite element method²⁷. Using strain energy in the tissue calculated via mechanical and thermal influences, a prediction of tissue damage and the corresponding tissue effect can be made. Such models may contribute to future development of a constitutive adhesion theory, where thermomechanical responses may be assigned to each tissue constituent (e.g., water, proteins, lipids) as a predictive tool for the fusion potential of a tissue with a known composition.

Lateral thermal spread

Lateral thermal spread, defined as the “damage of tissues beyond those targeted by the surgeon”⁷⁹, has been quantified as a measure of peripheral energy spread via histopathology for vessel sealing and dissection devices of various energy delivery modalities. Hruby et al. determined the ultrasonic oscillation of Harmonic ACE to induce remarkably less thermal spread in both arteries ($p < 0.0005$) and veins ($p < 0.005$) than that of the RF-based LigaSure and a similar prototype device³⁷. Similarly, Landman et al. quantified ultrasonic thermal spread using the Harmonic ACE at < 1 mm, compared to a 3–4 mm spread using LigaSure in both arteries and veins⁵³. Philips et al. noted an increase in thermal spread in veins relative to arteries, as to be

expected in vessels with a relatively less volumetric muscular layer (*tunica media*), and they measured lateral thermal spread in 6 additional tissue types to blood vessels⁷⁹. Statistical comparisons of thermal spread in ureter, bladder, peritoneum, stomach, small bowel and colon were largely insignificant, but established baseline values of thermal spread for multiple devices in lateral procedures not directly related to sealing and cutting of blood vessels. Phillips further established that blade temperature of both ultrasonic and RF-based devices did not correlate with thermal spread; the two variables were in fact shown to be inversely correlated in all tissue types⁷⁹. This unique finding has directly relevant implications for the refinement and optimization of clinical fusion devices.

2.2.3. Strength testing of fused tissue

Ultimately, the success of vessel sealing depends on the ability of the seal to withstand pulsatile blood pressure *in vivo*. In most cases, however, the formation of fibrous clots near the fusion site provide supplemental resistance to blood flow, eventually relieving the sealed portion of the vessel from all or part of its applied pressure. The ablative, permanent nature of energy-based ligation and associated clot formation may partially explain the widespread clinical approval of sealing devices with contrasting energy delivery modalities and protocols. In spite of these variations, the clinical efficacy of many if not all energy-based ligation devices is commonly evaluated with an empirical measure of *bursting pressure*, the resistance of a vascular seal to intraluminal pressurization. Vessels sealed using clinically approved devices generally withstand pressures of up to and exceeding 3× systolic blood pressure^{14,34,85}, a safety factor determined by FDA to designate clinical efficacy of a given device¹⁰⁶.

While bursting pressure has been designated as the industry standard for the evaluation of device performance in vascular fusion, there is a significant degree of variability within and

across devices^{78,121} and data collection methods¹⁴. Within devices, the inherent biological variability in tissue constituents (e.g., nutritional effects, tissue hydration) may alter impedance and temperature measurements used by energy sources and current generators to determine the duration or magnitude (e.g., temperature) of energy application, leading to variations in even geometrically identical arteries. Surely, the approval of devices for veins and arteries of varying thickness between 2 and 7 mm in diameter makes the normalization of bond strength data to vessel size a two-dimensional task, often resulting in increased variability⁶⁹. Across devices, variations in the modality of energy delivery, duration of energy application, power specifications, jaw shape, grasping size, vessel size and associated apposition pressure may all contribute to the determination of induced bond strength and a device's clinical fitness for use.

With regard to data collection methods, a broad spectrum of bursting pressure measurement equipment is used in the published literature. Pressurization may occur automatically using saline⁹² or air¹⁶ through an unspecified size of cannula or catheter. Fixation of the open end of arteries to the chosen aperture may be achieved with an iris clamp⁹² or manually-tied waxed cord¹⁴. Pressurization rates vary from 7.5 to 120 mL/min, and bursting environments may vary from their ambient temperature to the pressure release medium. Where vessel dimensions are measured and accounted for, metrology techniques range from digital calipers⁹² to a microscope and reticle⁴. The diversity of data collection methods in bursting pressure measurements make the determination and standardization of the geometrical failure mode of fused cylindrical blood vessels extremely difficult, and call the effects of the methods for device evaluation into question.

2.2.4. Results of experimental fusion

Dermal Repair

Sriramoju et al. accomplished the water-tight re-approximation of dermal incisions *in vivo* via the minimization of power to a continuous wave fiber laser (1455 nm, 600mW) with the implementation of a dwell time, or cooling period during which a laser shutter was closed⁹⁹. Tensile strength and wound remodeling were assessed post-operatively at 0, 7, 21 and 42 days. Successful welds were obtained in 67% of incisions for all evaluated laser welding parameters, where a fluence of 13.6 kJ/cm² demonstrated the most successful welds⁹⁹. In a similar study design, Alimova et al. elaborated on this work, demonstrating a recruitment of polymorphonuclear neutrophils (a preliminary component of an inflammatory response) at the wound area 24 hours post-operation³. Relative to sutured skin, laser-welded incisions demonstrated improved visual healing as reduced scarring and a reduced deposition of abnormal tissue (hyperkeratosis) as quantified by Raman spectroscopy³. These *in vivo* studies demonstrate proof-of-concept for dermal fusion in guinea pigs; *ex vivo* fusion of porcine and human skin has also been demonstrated¹⁰⁴. The experimental fusion of dermal tissues by photothermal welding shows great clinical promise and beckons further research into the appropriate laser parameters for a fully recoverable dermal incision.

Vascular Anastomosis

The success of fusion devices in vascular ligation has led several investigators to evaluate the technique for vascular anastomosis. As early as 1983, Serure et al. obtained 100% long-term patency of CO₂ laser-welded femoral arteries in rats (70 mW, $\lambda = 10.6 \mu\text{m}$ on a 150 μm spot size) with an absence of foreign body reactions in welded relative to sutured anastomoses⁹⁰. Laser anastomoses were performed in one third of the time as sutured junctions, with less

ischemia and adequate, but not superior, tensile strengths. Due to the relatively low welding strength of strictly photothermal vascular anastomosis, mechanical and photochemical enhancements are gaining traction for clinical use of the technique. As recently as 2015, Pabittei et al achieved poly (lactic-co-glycolic acid) (PLGA) or poly (ε-caprolactone) (PCL) scaffold- and semisolid genipin solder-enhanced laser anastomoses in porcine carotid arteries. A 670 nm laser was used to spot-weld anastomoses wrapped in either solder-impregnated scaffold, with 11 laser spots on PLGA scaffold unions withstanding 923 ± 56 mm Hg of pulsatile pressure⁷⁵: a three-fold magnitude of systolic blood pressure. Solder-impregnated PCL scaffold unions also withstood supraphysiological blood pressures at 703 ± 96 mm Hg. A distinction was made between cohesive and adhesive failure, where anastomoses with PCL scaffolds failed cohesively, indicating a bond between the molecules of solder and the native tissue collagen. Adhesive failures occurred between anastomotic ends with PLGA scaffolds, indicating a superior strength in adhesive relative to cohesive bonding, as qualified by electron microscopy. While clinical implementation of this technique has been hampered by slow progress in the enhancement of welding strength, the decreased procedural time, excellent patency rate and recent *in vitro* augmentation of laser-assisted vascular anastomosis strengthens the case for an energy-based replacement of foreign-body, compression-based vascular unions.

Colorectal Fusion

In evaluation of intestinal seal adequacy, several investigators have explored the potential of surgical energy for colorectal anastomosis, a technique currently associated with dexterous technical complications and suboptimal functional outcomes⁵. Small bowel thermo-fusion has been achieved only with adequate RF energy and optimal compressive pressures⁵. Custom RF and direct heat thermal fusion devices have been developed for *ex vivo* and *in vivo* fusion and

anastomosis of colorectal tissues^{95,117}: survivable anastomotic resection of the small bowel using a custom device based on the RF LigaSure resulted in immediately water-tight, and intact seals with undisturbed healing complete with granulation tissue, newly synthesized collagen in the submucosa of joined bowel, and a re-epithelialization at seal borders. Further, animals displayed healthy and normal intestinal passage 7 days post-operative⁹⁵. Additional studies have also confirmed normal pathological healing with angiogenesis, granulation and fibroblast proliferation in anastomosed small bowel⁹¹. The thermal injury characteristics of colonic anastomoses have also been assessed using a custom RF fusion device, indicating abundant denaturation of post-fusion colonic collagen proportional to compressive pressure during the anastomosis. Increased compressive pressure also resulted in histologic “cracking” or damage of the muscular submucosa¹¹⁷, implying, in agreement with the results of small bowel thermo-fusion, an optimal compressive parameter for colorectal anastomosis. Indeed, compressive pressure has been correlated to the bursting pressures of colon ($p < 0.05$) fused using another custom RF device, with an optimum pressure of 1.13 MPa and an increase in bursting pressures for thicker colonic walls¹¹³. Experimental data on custom, direct heat anastomotic devices has yet to be published. The adequate healing responses and normal intestinal passage of energy-based anastomoses in colorectal tissues show great promise for the clinical implementation of this application of the fusion technique.

Nerve Repair

Nerve repair via sutured closure is suboptimal given the likelihood of intraneural fluid loss during regeneration⁷ let alone the technical challenges and scarring induced by the application of neural sutures. Functional recovery of nerve tissue by energy-based union has been evaluated for use with photothermal and photochemical laser welding, the latter inclusive of

protein solders as well as chromophores for an increase in laser light scattering and transmission into the nerve tissue⁷. CO₂ lasers are characterized as having low penetration and spread, which in combination with their absorption by water makes them suitable for end-to-end nerve repair⁷. The speed, reduced trauma, reduced foreign body reactions and minimally invasive nature of laser welding has made it particularly attractive to restricted neural surgery, such as in cranial nerves. Photothermal nerve repairs are often used in conjunction with stay sutures, are characterized by low tensile strength, and have reported to offer inconsistent results. As such, the use of photochemical methods have added tensile strength⁷⁰ and nerve protection to laser repairs via the addition of biological compounds such as albumin⁵⁶. Nonetheless, surgical welding induces tissue damage, and surgical adoption of laser-welded nerves is thus characterized by hesitation or reluctance for the repair of such delicate tissues as nerves⁷.

Cornea Welding

Reports of dye-assisted photochemical diode laser welding for the repair of corneal defects evidenced collagen bridges across the welding sites, with a preservation of birefringence in, and thus lack of thermal denaturation of collagenous structures⁶³. While the demonstration of laser-welding for corneal tissues adds another application to those investigated for energy-based closure, this finding holds greater implications for the development of a constitutive bonding theory of fusion adhesion to be discussed in *Adhesion Theory*.

Tendon and Cartilage Welding

In 1996, CO₂ and Argon laser welding was assessed for viability in albumin solder-assisted tendon repair. Both lasers successfully fused tendon ends immediately, yet immediately postoperative bonding was tenuous and impossible to test by conventional tensile methods.

However, 14 days of postoperative healing enabled tensile testing to within 59 and 64% of the strength of uninjured tendon for CO₂ and Argon-laser welded tendons, respectively⁴⁷.

In 2001, the attempted Argon laser fusion of Trypsin-decellularized, e.g., purified yet ultrastructurally preserved tendon collagen resulted in a failed junction of separate sections despite a sweep of laser parameters¹⁰. Only upon a decreasing in temperature and an increase in welding times were collagenous (tendon) discs able to be welded⁹³, further underlining the variability of collagenous structures' willingness to interact under a given set of fusion conditions. The implications of these results to the development of constitutive thermal bonding are discussed in *Adhesion Theory*.

Photochemical, albumin solder-enhanced laser welding has also been evaluated for use in energy-based repair of articular cartilage. An 808 nm laser was combined with albumin solder and indocyanine green, a chromophore for increased laser absorption. Resulting welds demonstrated adequate tensile strengths of 100 kPa and minimal thermal damage (< 500 μm)¹¹⁸. The use of a dye-enhanced albumin solder is thus feasible for efficient laser welding of articular cartilage in preliminary study.

The results of tendon welding attempts indicate an immediate failure of these highly collagenous tissues to fuse, yet a response to thermal injury has been observed that may hold promise for the thermal union of highly-organized, collagen-dominant connective tissues with high tensile strength, such as articular cartilage. In applying surgical energy to tissues with varying composition, we may need to closer approximate the biological assembly remodeling for long term healing to ensue, rather than applying excessive and ablative energies to fusion

candidates in hopes of increasing the denaturation, homogenization, coagulation and bonding of connective tissues.

2.3. Adhesion Theory

2.3.1. Collagen Structure & Denaturation

In debating the nature and bonding implications of collagenous transitions during fusion, one must first explore the nature of collagen assembly and stabilization. The primary structure of collagen molecules consists of an amino acid polypeptide chain of $(\text{Gly-X-Y})_n$ joined by peptide bonds¹¹⁹, where the X position is often occupied by proline, and the Y position by hydroxyproline⁸². The coiled formation of these chains, known as α -chains or α -helices, comprise collagen's secondary structure¹¹⁹. Tertiary collagen IA exists as a regular, repeating triple helix of amino acid α -chains stabilized by peptide bonds, inter-chain Hydrogen bonds^{50,119} and Hydrogen-bonded water bridges⁹⁸. These molecules stagger to form quaternary fibrils, joined after secretion by cells via intra- and intermolecular covalent crosslinks^{114,119} to form macroscopic collagen fibers, the primary structural protein unit in vertebrate connective tissues⁸⁴. Water bridges in helical collagen create a set of interactions nearly as strong as direct inter-chain Hydrogen bonds themselves⁵⁰, yet when these bonds are disrupted by exposure to heat, the stability of the molecule is compromised, leading to partial transient denaturing of collagen helices⁹⁸.

While the presence of water serves to stabilize the triple helix, the final step in collagen biosynthesis is the formation of intra- and intermolecular crosslinks. Crosslink formation begins via the lysyl oxidase-mediated conversion of lysine and hydroxylysine residues to aldehydes within the collagen molecule. These “intermediate”, bivalent crosslinks are converted during maturation into the trivalent stabilizing crosslinks: pyridinium, pyrrole and histidine-containing

compounds⁸⁶. It is understood that with exposure to the energy of fusion (~ 40 – 60 C) ^{41,114}, helical Collagen denatures into an amorphous coiled mass of peptide chains; this is thought to occur via the breaking of consecutive Hydrogen bonds between α -chains in the triple helix⁶⁶. These theories may lead investigators to point to reversible Hydrogen bonding as a primary source of fusion adhesion. Quantitative literary evidence of these transitions in thermally fused tissues, however, has remained scarce in nearly three decades of fusion research.

2.3.2. Observations of Thermal Transitions in Collagen

Early imaging work by Schober placed an interdigitation, or “homogenization” of aperiodic adventitial collagen fibrils at the origin of structural adhesion⁸⁹, implying a physical interaction between denatured collagens in thermally treated tissues. Subsequent work by White and Kopchok used imaging to observe an orientation- and apposition-dependent bonding of collagen to collagen or collagen to elastin; several bonds were observed to bridge adventitial and medial vascular layers in fused vascular tissue¹¹². In cases where welding temperatures were presumed insufficient to cause Collagen denaturation, White proposed a physiochemical crosslinking of collagen fibers to account for the observed adhesion. These high-resolution imaging studies offered qualitative evidence of collagenous transitions; biochemical evidence had yet to be provided. In evaluating the developing Collagen theory via electrophoresis, Murray and Guthrie proposed a post-fusion increase in high molecular weight, non-collagenous proteins as a potential source of crosslink-based adhesion between low molecular weight proteins^{33,68}. Only in increasing the “harshness” of the solubilization buffer were slight increases in post-fusion Collagen V beta chains and collagen IA gamma chains observed, suggesting the possible crosslinking of inferior collagens or simply an increased solubility of these proteins following thermal exposure. While these studies offered a preliminary report on the biochemical

mechanisms of vascular fusion, a definitive correlation of fusion adhesion to collagen crosslinking or renaturation was not established. Nevertheless, the assumption that thermal tissue welding was a byproduct of collagen renaturation and/or potential crosslinking prevailed in the literature to follow^{3,5,19,41,77,88,96,101,103}. In 1997, Tang observed the “roping” of parallel collagen fibers after welding; this was proposed to complement the end-to-end interdigitation observed by Schober. Ward Small subsequently reported post-fusion increases in intermediate and mature collagenous crosslinks, the first quantitative evidence of its kind to suggest covalent collagen assembly during fusion⁹³.

In 2001, Burt et al. elevated scrutiny on the collagen hypothesis, evaluating laser welding of transected digital flexor tendon (> 90 wt. % collagen) as a replacement for sutures. Despite a sweep of energy input parameters, Burt observed no adhesion and demonstrated breakdown of the irradiated region via Trypsin digestion, suggesting an absence of intermolecular crosslinks in treated tissues and that the observed success of fusion in cellular tissues may be due to non-collagenous interactions. Regarding the interdigitation and roping reported in prior studies, he proposed that the “appearance of fibril fusion is an early stage of quasicrystalline matrix melting, where fibril architecture is partly preserved”^{10,57}. Burt’s analysis indicated that the majority of evidence to suggest the thermal crosslinking of ECM proteins remained qualitative, and that the influence of collagen denaturation on the formation of fibrillar tissue “fusions” had yet to be determined.

2.3.3. Dehydration & water transport

As mentioned previously, a primary mechanism in the thermal bonding and cutting procedures, and hence a target for manipulation by fusion device developers, is the vaporization of water and thermal coagulation of hydrated cellular contents and water-stabilized extracellular

proteins. As with the desiccation and evaporation processes in instantaneous thermal bonding, the water-enabled biotransport of cells and cellular proteins is equally critical for the wound healing and biological remodeling processes. As such, much attention is paid in the literature to the influence of water in the formation and stability of energy-based tissue bonds.

Multiple studies report the dependence of fusion on a vaporization of water in interfibrillar (unbound) or bound states^{17,29-31}. Leading hypotheses posit that in native tissues, a relative increase in bound and unbound water results in increased solvent accessibility for charged groups on the polypeptide chains of collagen molecules (e.g., OH groups of proline and Hydroxyproline)¹¹⁵. Further, the thermal stability of crosslinked collagen networks has been shown to depend on intrafibrillar water content⁶⁵. In vaporizing the bound and unbound tissue water in combination with the apposition pressures of fusion, charged groups may be forced to interact with each other at sites previously occupied by Hydrogen bonds or Hydrogen-bonded water bridges^{17,30}. In 2015, this hypothesis was tested via three avenues: the alteration of tissue water content prior to fusion, the alteration of hydrophilic Glycosaminoglycan content prior to fusion, and the post-fusion rehydration of desiccated vascular seals for assessment of *in vitro* bond stability. Indeed, it was shown that an increased pre-fusion unbound tissue water content induced by osmotic equilibration and the enzymatic digestion of Glycosaminoglycans, which sequester water and prevent its transport throughout the extracellular matrix⁴⁵, resulted in significantly higher bursting pressures in fused arteries⁴⁹. Likewise, the rehydration of vascular seals post-fusion has resulted in complete loss of³⁰ or significantly reductions⁴⁹ in vascular seal strength. The involvement and dependence of water transport prior to, during, and following the fusion process shed valuable light on the nature of the fusion mechanism, and may enable predictions of fusion potential for a given tissue based on its content of bound and unbound

water. These findings may also further explain the failure of dense collagenous networks (e.g., tendon) to fuse, given their relatively low hydration levels and high concentration of glycosaminoglycans.

2.3.4. Amalgamation of cellular and extracellular non-collagenous proteins

While Collagen dominates vertebrate tissue composition, a common characteristic of successfully fused tissues is their cellularity. The earliest observations of fused tissues complemented adventitial homogenization, a collagenous transition, with a “coagulation necrosis of smooth muscle cells in the underlying media”⁸⁹. The polymerization of platelets and/or fibrin was suggested to describe the coagulum⁹⁰, which withstood microarterial pressures even when direct tissue apposition was not achieved¹¹². Imagery of nucleated cells at the fusion interface is often correlated with increased bonding strength between fused tissue layers^{4,69}. Regarding the cellularity of successful fusion candidates, Burt proposed that “(tissue welding) may reflect thermal coagulation of cytoplasmic peptides or nucleic acids liberated at the tissue interface”¹⁰. Such a mechanism of protein denaturation and subsequent cellular and tissue cooling into a “sticky coagulum” may account for the successful fusion of cellular (vascular, colorectal, reproductive and dermal) tissues, and the observed welding failure of highly collagenous, yet hypocellular tendon.

2.4. Moving Forward

2.4.1. Approaches to Gaps in Adhesion Theory

The development of a constitutive molecular bonding theory of the energy-based surgical adhesion of transected tissues will require detailed attention to tissue chemistry and composition, thermal transitions in not only the primary ECM proteins but in all constituents, and

thermomechanical tissue-device contact models including water transport and energy dosimetry. While these pursuits have been initiated by a portion of the published literature, a focus of fusion investigation remains disproportionately aimed at application-specific fusion outcomes, leading only to incremental advancements in experimental and pre-clinical uses of technique. A comprehensive database of molecular transitions and associated findings will enable target-specific development of new energy-based devices, and is likely to confer additional advantages to the development of existing tools as they continue to evolve.

A preliminary approach to the development of constitutive bonding theory is the isolation of tissue constituents either by enzymatic digestion, chemical extraction, or via the bench-top synthesis of distinct matrix proteins. The separation of individual constituents will enable the single-point investigation of thermal transitions without the effects of coupled transitions. Certain published experiments from which novel findings have emerged have partially explored this approach through the removal of individual constituents such as GAGs⁴⁹ and cellular components¹⁰, leaving simplified tissue structures behind. The decellularization of fusion candidates is of particular interest due to emerging theory placing cellular coagulation at the origins of fusion adhesion. Similarly, the enzymatic digestion of supplementary ECM proteins (e.g., elastin) may enable the validation of elastic influence⁹² in structurally preserved collagen networks.

Characterization methods of energy-based tissue transitions are frequently limited to engineering-specific diagnostic tools and equipment. An increase in the use of biochemical methods for the quantification of pre- and post-fusion constituent abundance may novel insight into the stability of a particular protein and its contributions to the formation of fusion adhesion. Techniques such as high performance liquid chromatography, mass spectrometry and proteomic

analysis are currently in use for the quantification of thermal transitions in extracellular matrix bonding during fusion⁵¹. An increase in biochemical data may provide the molecular level of detail required for characterization of thermal transitions in, and thus the potential for thermal bonding in various fusion candidates.

2.4.2. Collagen crosslinking

The literary citations of the thermal breakdown and subsequent, cooling-induced reformation of collagen crosslinks during fusion procedures are based in qualitative imagery and associated inference. While chemical additives (e.g., Glutaraldehyde, indocyanine green) and biological supplements (e.g., albumin, fibrin, fibrinogen) may aid in the semi-instantaneous stabilization of and post-operative biological recovery of energy-based bonds, these findings remain empirically-based, rather than on a detailed understanding of their benefit to thermally-induced effects in fused tissues.

2.4.3. Molecular bonding of cellular and matrix proteins

Simulations in molecular dynamics (MD) are becoming increasingly common for the prediction of temporal changes hydration and composition, as well as recovery stages of chemically influenced or pathological tissues⁵⁹. These simulations may prove useful primarily for the prediction of hydration changes and water transport in fused tissues¹, but certainly of the inflammatory and healing response of thermally injured tissues as well.

2.4.4. Assessment of Tissue Viability and Functional Recovery Potential

The assessment of functional recovery in fused tissues is certainly best completed on tissues fused *in vivo* via quantitative methods, but preliminary assessments of tissue viability and thermal stability and resilience may point investigators to the tissues with highest recovery

potentials. Histological techniques for the detection of cell viability and transport remain a direct indicator of recovery potential, while more quantitative techniques such as *in vivo* Raman spectroscopy⁹⁸ or high performance liquid chromatography³² may provide direct indications of the repair and regeneration status of prominent tissue proteins such as collagen and elastin. As an alternative to *in vivo* investigation, bio-reaction with mechanical stimulation may provide an adequate *in vitro* environment in which to assess the functional recovery potential of fused tissues.

2.4.5. Applicability to tissue engineering

The energy-based techniques detailed herein offer tissue coaptation applicable to wound healing as a superset of vessel sealing, post-operative incision closure in minimally invasive surgery and similar dermal procedures, and to general tissue repair. Thermal techniques may likewise offer a replacement for the semi-instantaneous integration of autologous, allogeneic and engineered tissues grafts. As techniques for *in vivo* implementation of many proof-of-concept procedures develop, the parallel investigation of fusion potential for tissue grafting may well confer the same advantages seen in vessel sealing to the integration and repair of damaged tissues with supplemental tissue architectures. Likewise, the investigation of thermal transitions in tissue constituents may prove advantageous to the development of novel tissue engineering synthesis and integration procedures.

2.5. Summary

Understanding the biothermomechanical behavior of the extracellular matrix requires a foundation in biochemistry, clinical medicine, heat and mass transfer and experimental engineering among others. While the effort is surely shared among researchers, it is crucial that each investigator focus on obtaining repeatable trends that can be incorporated into adjacent

(proximal) studies on the effects of applied thermal energy to proteins of the ECM (burn science, wound healing, tissue engineering and implant integration).

While the fusion literature is comprised of investigations of both clinical and experimental techniques, the remainder of this work is concerned with characterizing the primary application of surgical fusion: vascular sealing and cutting. By exploring the physical and chemical states of tissues most commonly used in energy-based surgery, this research seeks to optimize our knowledge of what currently works as a foundation for development of techniques that one day could.

Chapter 3. Strength and Persistence of Energy-Based Vessel Seals Rely on Tissue Water and Glycosaminoglycan Content

3.1. Introduction

Minimally invasive surgery has flourished in response to developments in energy-based vessel sealing. Relative to traditional, compression-based ligatures, vessel sealing offers increased biocompatibility and surgical efficiency to the circulatory, reproductive and colorectal domains^{5,24,78,94,109}. Despite these benefits to vascular surgery, the methods and mechanisms of vessel sealing remain empirically-derived, while its performance record and breadth of application remain largely unchanged over nearly two decades of use. The optimization and expansion of vessel sealing from permanent, destructive ligation to long-term healing in vascular anastomosis, for example, remains limited by uncertainties as to the origin and stability of vascular adhesion forces. By exploring the influence of tissue hydration and hydrophilic tissue components (e.g., glycosaminoglycans) on the formation and resilience of vascular seals, this work seeks to advance a constitutive model of adhesion forces in vascular thermal fusion.

Energy-based vessel sealing, a subset of tissue “fusion” or tissue “welding”, is achieved through grasping pressure and the application of heat via bipolar current, ultrasonic oscillation, photoirradiation or direct conduction. While all fusion devices deliver localized heating and induce a loss of water from fused tissues, the variety of heating strategies and energy dosimetry used in fusion underlies the uncertainty as to what causes tissue to bond^{20,87}. As a consequence, the use of vessel sealing devices is restricted to veins and arteries less than 7 mm in diameter^{34,46}, as vessels sized above 5 mm exhibit low adhesion strengths and high rates of failure⁶⁹. Investigative efforts to characterize fusion processes and improve device performance have reported protein denaturation and interdigitation¹⁰³, protein crosslinking^{68,93}, water transport³⁰, electrostatics³⁰ and the coagulation of cellular proteins^{10,69,112} as potential sources of tissue adhesion. Much of the available data and interpretations thereof appear contradictory, however, and the physiochemical processes of thermal fusion “remain obscure for lack of appropriate measurements and underlying theory”¹¹⁴. The optimization of existing surgical devices, development of long-term healing strategies and our understanding of tissue-device biothermomechanics, therefore, necessitate further investigation into a component-based adhesion theory^{78,108,114}.

Of primary interest to fusion investigators has been the thermal denaturation of vascular collagens as a precursor to tissue adhesion. Numerous studies correlate heat-induced denaturation, the breaking of inter-chain hydrogen bonds^{98,114}, to the subsequent formation of tissue bonds during cooling via chain interactions between amorphous collagens, namely renaturation¹⁰³, interdigitation^{89,103} and crosslinking^{33,68,93,112}. Many of these corollaries are based on qualitative imagery, however, and few studies present quantitative evidence of collagen-specific crosslinking, nor suggest the bonding pairs that may form the crosslinks. As

collagen-based adhesion theories gained support in the literature^{3,5,19,41,77,96,101}, increased scrutiny revealed that the thermal fusion technique was ineffective for purified collagen¹⁰, that denaturation was not critical for thermal bonding^{29,112} and that successfully fused tissues are not only collagenous but are hydrated and highly cellular¹⁰. The common composition of fused tissues gave rise to alternative adhesion theories, implicating cellular coagulation¹⁰ and tissue water transport^{29,30} in the sources of fusion adhesion. In support of ultimately establishing a thermomechanical constitutive model of adhesion forces during thermal fusion, the role of tissue hydration and hydrophilic tissue constituents (e.g., Glycosaminoglycans) in the bond formation process must be explored.

Following collagen denaturation, dehydration is the second macroscopic response of vasculature tissue to applied heat. To understand the role of water in fusion adhesion, an understanding of its role in native tissue structure is useful. The primary unit of structural protein in vertebrates is a triple helix of three (Glycine-X-Y)_n polypeptide chains, known as tropocollagen. Amino acid residues within the molecule are bound and stabilized by Hydrogen bonds⁸², and by hydrophilic residues that are well-suited for hydrogen-bonded water bridges. These bridges join either two carbonyl groups to each other [CO (Hyp)-H₂O-CO (Gly)], or a hydroxyl group to a carbonyl group [OH-H₂O-CO (Gly) or OH-H₂O-CO (Hyp)] on neighboring molecules within a chain, or between molecules of adjacent chains⁹⁸. We theorize that this “bound water” vaporizes during fusion, thereby exposing polar bonding pairs along the polypeptide chains of neighboring collagen molecules, including those that span the interface of fused tissue layers. As successful tissue fusion relies on the vaporization of water in either interfibrillar (unbound) or bound states^{17,29-31}, we hypothesize that deliberately increasing pre-fusion tissue water content will increase the strength of the fused tissue junction. Likewise, the

rehydration of fused tissue bonds should result in a decrease in bond strength, a potential result of hydrophilic residues releasing their bonding pairs in favor of water molecules.

Much of the unbound water within vascular tissue is sequestered by hydrophilic Glycosaminoglycans (GAGs) within the extracellular matrix (ECM) of the vessels. The bottle-brush structure and net negative charge of GAGs confer compression-resistant and anticoagulative properties to the tissues which they occupy⁴⁵. Through dipole interactions with water molecules, GAGs resist aqueous transport throughout the ECM, an interaction which may inhibit one theorized mechanism of thermal fusion: cellular peptide coagulation. Through alteration of the GAG content of native vessels, we seek to evaluate this theory and gain further insight into the role of aqueous and hydrophilic tissue constituents (*i.e.*, unbound water and GAGs) in the formation of energy-based tissue bonds. By enzymatically digesting GAGs from the vascular matrix, we anticipate increases in tissue porosity, aqueous transport and peptide coagulation, and a corresponding increase in tissue bond strength.

A final component of this study involves the longitudinal rehydration of vascular seals post-fusion to evaluate the persistence of fusion adhesion. Rehydration is intended to address the question of whether vascular fusion can be employed in functionally recoverable procedures such as vascular anastomosis, rather than the destructive and terminal nature of vessel sealing as is currently practiced in surgery. Thermally fused aortic tissue has been observed to lose significant adhesive strength after only 1 hour of rehydration in saline with complete adhesion loss after 24 hours³⁰. Accordingly, we expect a temporally progressive reduction in seal strength with exposure to a hydrated environment.

This study aims to clarify the influence of tissue hydration on the formation, strength and resilience of vascular fusion bonds via three avenues: the alteration of pre-fusion tissue water

content via osmotic equilibration, the enzymatic digestion of hydrophilic GAG molecules prior to fusion, and the post-fusion rehydration of native and GAG-digested vascular seals. The results of this observational study will be beneficial to two aims: 1) understanding the optimal conditions for creating resilient vascular seals in hydrated *in vivo* environments, and 2) advancement of a component-based adhesion theory of vascular thermal fusion in efforts to reveal novel applications for energy-based vascular tissue *repair* (e.g., vascular anastomosis) and the long-term functional recovery thereof.

3.2. Materials and Methods

3.2.1. Tissue harvest and storage

Porcine splenic arteries are a common analogue to human vessels in fusion research due to their size ($\varnothing 2 - 5$ mm) and availability¹⁴⁻¹⁶, and were chosen for use in this study. Spleens were obtained from a local abattoir (Innovative Foods LLC, Evans, CO), from which the splenic artery was excised within 5 hours of tissue harvest. Arteries were cut into 20 mm segments, embedded in Tissue-Tek® Optimum Cutting Temperature (OCT) compound and immersed in chilled (-160 °C) 2-Methylbutane prior to storage at -80 °C until use (< 14 days).

3.2.2. Tissue preparation and treatment

Prior to treatment and/or fusion, samples were thawed in a 37 °C bath of PBS (BP665-1, Fisher Scientific, Fair Lawn, NJ) until they moved freely in solution (≈ 15 minutes). Arteries were further rinsed in PBS for 15 minutes at 37 °C with agitation to dissociate residual OCT from their surfaces.

3.2.3. Alteration of water content

To determine the effect of tissue hydration on the strength of vascular seals, tissue water content was varied through a series of osmotic pressure treatments. 90 specimens were split evenly into three groups and immersed in one of three solutions with varying tonicity relative to biological pH: deionized water (hypotonic), 0.9% PBS (isotonic) and 9% PBS (hypertonic). Tissues were given 48 hours at 4° C to equilibrate their osmotic pressures with that of the treatment solution, after which they were brought to room temperature in a bath of their respective solutions for 30 minutes.

3.2.4. Alteration of GAG content

The contribution of GAG content to seal performance was evaluated via enzymatic digestion using Chondroitinase ABC (ChABC) (C3667, Sigma-Aldrich, Milwaukee, WI). Control arteries (n = 20) were immersed in 0.9% PBS for 120 minutes at 37 °C with agitation. Enzyme-digested arteries were immersed in 0.9% PBS with 1U/mL ChABC at 37 °C with agitation for 0.5, 1, 2, 3 or 5 hours (n = 20/gp.). Following treatment, all groups (including controls) were subjected to a 60 second enzyme inactivation period at 100 °C^{39,67}. Specimens were then rinsed three times in 0.9% PBS at room temperature for 15 minutes. At this point, each treatment group was separated into three sub-groups of n = 10, 8 and 2 specimens each for strength testing via burst pressure, GAG quantification and histology, respectively. Strength testing groups were stored in 0.9% PBS at 4 °C for 12 hours. GAG quantification groups were immersed in liquid Nitrogen and lyophilized. Histology specimens were prepared as described below.

3.2.5. Seal Rehydration

Vascular seals of both control and 2h GAG-digested arteries were progressively rehydrated in 0.9% PBS at 37°C with agitation to assess the impact of post-fusion water uptake on seal strength. A separate set of arteries was used for this experiment; each digested group was fused using the ConMed ALTRUS™^{15,16}, a direct-heat vessel sealing device, and subsequently rehydrated for 0, 3, 6, 12 or 24 hours prior to strength testing (n=10/gp.)

3.2.6. Measurement of water content

To assess the impact of osmotic equilibration and GAG digestion on tissue water content, ten 10mm specimens were selected from each hydration and GAG treatment group for measurement of water content and were not subjected to the heat or pressure of fusion. Tissue water content was measured by weighing specimens prior to and following desiccation to quantify their mass fraction of water. Specimens were pat dry with a Kimwipe™ to remove excess surface water, and weighed using a precision balance (UMX2, Mettler Toledo, Columbus, OH). Specimens were then frozen in liquid Nitrogen for 30 minutes, lyophilized (7740020, Labconco, Kansas City, MO), and weighed once more to obtain the dry mass of the tissue. The percentage of water by weight was calculated using (3.1), where m_{dry} and m_{wet} are the dry and wet tissue mass of each sample, respectively.

$$\%WaterContent = \frac{(m_{wet} - m_{dry})}{m_{wet}} \cdot 100 \quad (\text{Equation 3.1})$$

3.2.7. Strength testing by bursting pressure

Bursting pressures of arterial seals were measured using a syringe pump (280210, KD Scientific Inc., Holliston, MA), pressure transducer (PX603-0306SV, Omega Engineering Inc., Stamford, CT), data acquisition system (DAQ) (OMBDAQ-55, Omega Engineering Inc.,

Stamford, CT), software (pDaqview, Omega Engineering Inc.), an 18 gauge flat-tip cannula and a saline bath for visualization of seal failure. Specimens were fused at an open end using the ConMed ALTRUS® at 170 °C for 3 seconds, and the opposite end was tied to the cannula using waxed nylon cord. The orientation of each sealed artery in the device jaws relative to the cannula was maintained for this and all other studies; this is important due to the “Maryland-Style” crescent shape of the ALTRUS® jaw profile, which may have a directional effect on the failure modality and corresponding bursting pressure of vascular seals. To further mitigate the effects of the abnormal jaw geometry, tissue position within the device jaws was controlled using a custom fixture. The same ALTRUS® handpiece and energy source were used for the duration of the study. Upon cannulation, sealed arteries were pressurized with air at a rate of 120 mL/min until rupture. The maximum pressure achieved prior to seal failure was recorded as the bursting pressure. Bursting pressures of specimens with arterial wall failure, partial seal failure or with any failure mode other than catastrophic through-seal failure were discarded (< 10% of all specimens).

3.2.8. Quantification of GAG content

Sulfated GAG (sGAG) content was quantified using the DMMB assay as reported by Farndale et al²⁸, with minor modifications. Lyophilized arteries were weighed and recorded prior to digestion in a Papain/L-Cysteine HCl buffer (P4762 and C1276, Sigma-Aldrich). Specimens were incubated at 60 °C for 24 hours, vortexed intermittently. Standard concentrations of Chondroitin Sulfate (C9819, Sigma-Aldrich) were prepared from 0 – 150 µg/mL for calibration of sample readings. 250 µL of standard or digested sample was allowed to react in a 96-well round-bottomed plate with 10 µL of DMMB solution as prepared by Barbosa et al⁶. Wells were gently mixed via micropipette to promote complete DMMB-GAG complexation, and absorbance

was read at 570 nm by an absorbance reader (ELx800, BioTek Instruments, Inc., Winooski, VT) within one minute to avoid temporal degradation of the GAG-DMMB complex²⁸. Mean sGAG concentrations were calculated via interpolation of sample absorbance readings to the Chondroitin sulfate standard curve. sGAG mass fractions were calculated by normalization of mean sGAG concentrations (8 readings/specimen) to the dry tissue weight as shown in (3.2), where C is the concentration of sGAG in the sample well ($\mu\text{g/mL}$), V_{digest} is the volume of the digested sample in papain (mL), and W_{dry} is the dry weight of lyophilized tissue in μg . The reduction of sGAG content in treated arteries is represented as the percentage of sGAG content digested relative to original sGAG content (as measured in the control group), calculated using (3.3), where $mf_{control}$ and $mf_{treated}$ are the sGAG mass fractions of the dry tissue weight of control and treatment groups, respectively.

$$mf = C \frac{(V_{digest})}{W_{dry}} \quad (\text{Equation 3.2})$$

$$\% \text{ sGAG Loss} = \frac{mf_{control} - mf_{treated}}{mf_{control}} \cdot 100 \quad (\text{Equation 3.3})$$

3.2.9. Histology

Histology was conducted on control, hydration and GAG-digestion treatment groups for qualitative analysis of seal composition and morphology. For each group, three specimens were fused using the ALTRUS® and prepared for visualization of the treated arterial cross-section in an attempt to evaluate morphology, and for the GAG-digestion groups, the extent and locations of GAG digestion. Specimens were fixed in 10% neutral-buffered formalin, dehydrated, and impregnated with paraffin. Fused arteries were then cut longitudinally to expose the fusion cross-section, and embedded in paraffin. Specimens were sectioned, mounted and stained at 5

µm using Hematoxylin and Eosin (H&E), Verhoeff's Van-Gieson (VVG) or Light Green: Safranin O (SAFO). H&E stains nuclear content dark blue/violet, muscular cytoplasm in dark red, and Collagen in pale pink. VVG is used to visualize elastic fibers and cell nuclei in black, collagen in pale pink and cytoplasm in yellow. Light Green and Safranin O (SafO) are used as a background stain and proteoglycan counter-stain, respectively, resulting in red GAGs on a green background. Micrographs were taken at five times magnification using a light microscope (AXIOSKOP 40, Zeiss, Oberkochen, Germany) equipped with a digital camera (14.2 Color Mosaic, Diagnostic Instruments, Sterling Heights, MI).

3.2.10. Data analysis

One-way analysis of variance (anova1) and Tukey-Kramer multiple comparison (multcompare) within the Matlab software (Matlab R2014a, MathWorks, Inc., Natick, MA) were used to evaluate significance ($p < 0.05$) between treatment groups of water content, GAG content and bursting pressure data. Hydration data consists of one measurement per specimen and 10 specimens per sample (*i.e.*, treatment group). GAG quantification data consists of eight measurements per specimen, and eight specimens per sample. Bursting pressure data represents several repeated measures ($n = 10 - 12$) per treatment group, such that the mean of these repeated measures constitutes the bursting pressure for that sample. The mean standard deviation of bursting pressure for all repeated measures was also calculated, which is a measure of inter-animal variability. All data are presented as mean \pm standard deviation.

3.3. Results

3.3.1. Water content

Pre-fusion water content for each hydration group significantly decreased as the tonicity of the treatment solution was increased ($p < 0.0001$, Figure 3.1a). Vessels in the hypotonic

solution contained the most water at 83.1 ± 1.9 weight %, those in isotonic solution weighed in at 78.8 ± 1.1 % water, while the hypertonic group expelled all but 72.5 ± 0.9 % of its weight in water during osmotic equilibration in concentrated (9%) PBS. Artery dimensions across the three hydration groups showed no statistical differences in circumference (6.51 ± 0.90 mm, N.S.) or in wall thickness (0.55 ± 0.10 mm, N.S.).

Hydration correlated positively with bursting pressures of the hypotonic group relative to the iso- and hypertonic treatment groups (Figure 1b). No difference was observed between seal strengths in the iso- and hypertonic treatment groups. Bursting pressures of the hypo-, iso- and hypertonic hydration groups were measured as 607.6 ± 83.2 , 332.6 ± 44.7 and 348.7 ± 44.0 mmHg, respectively.

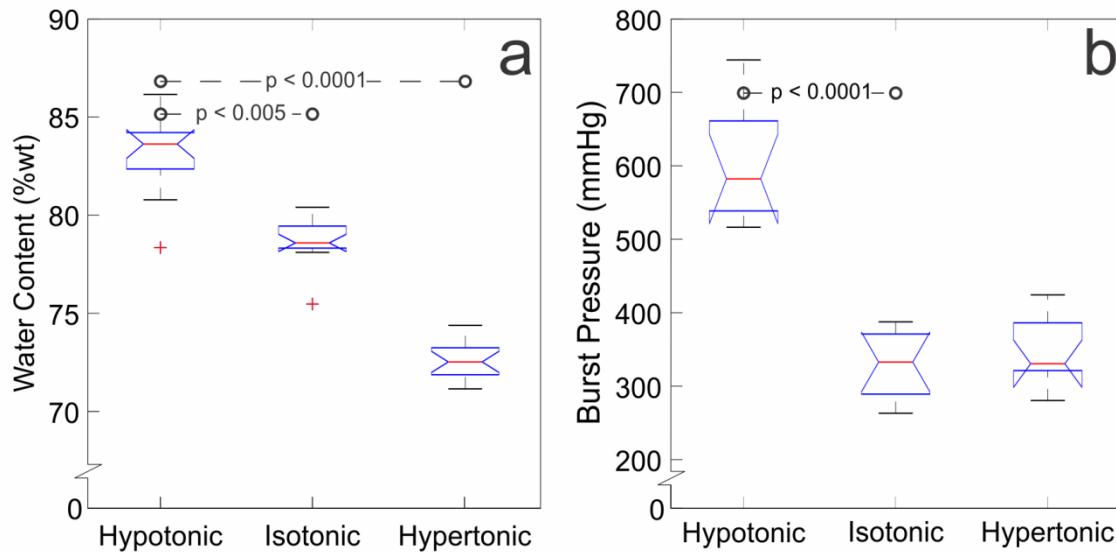


Figure 3.1: a) Water contents by weight of osmotically treated arteries. b) Bursting pressures of sealed arteries in corresponding treatment groups. Red lines indicate median values, blue lines above and below the median indicate the upper and lower quartiles, the difference between which is the interquartile range. The data range is designated by black lines; red crosses represent outliers ($\geq 2\sigma$). Statistical differences were evaluated using ANOVA1 and the Tukey-Kramer multiple comparison test.

3.3.2. GAG Digestion

Sulfated GAG content decreased significantly relative to controls (0 h) starting at 30 minutes of ChABC digestion (20.0 ± 22.6 % sGAG loss, $p < 0.05$), beyond which all groups maintained statistical decreases in GAG content relative to controls (Figure 2a). Beyond one hour of digestion, % sGAG loss became insignificant, indicating a maximum of GAG digestion being approached a 1 hour in ChABC. Maximum sGAG loss relative to controls occurred at 5 hours in solution (% sGAG loss= $72.6 \pm 8.2\%$, $p < 0.005$), and GAG loss had no statistically significant effect on the unbound water content of digested vessels.

A decline in GAG mass fraction led to a significant increase in bursting pressure (Figure 2b). GAG content was significantly decreased after 30 minutes in solution, but 2 hours of digestion were required to observe significant gains in bursting pressure relative to controls ($+68.5 \pm 51.7$ %, $p < 0.001$). Further, increases in bursting pressure become insignificant beyond 2 hours of GAG digestion, indicating that a maximum increase in seal strength is approached after 2 hours in solution; this result correlates to the asymptotic decline of GAG digestion observed at and beyond 1 hour of enzymatic exposure.

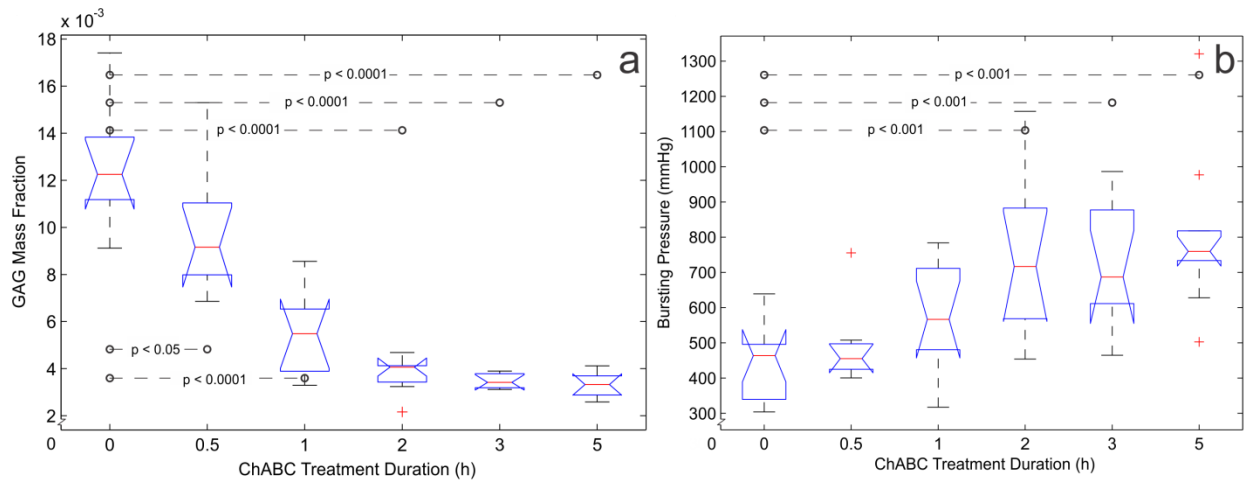


Figure 3.2: a) Sulfated GAG content as a fraction of dry tissue weight for control and enzyme-treated arteries. b) Bursting pressures in mmHg for native (0 h) and enzyme-treated arteries. Statistical differences are shown between groups; analysis was performed using ANOVA1 and the Tukey-Kramer multiple comparison test.

3.3.3. Seal Rehydration

Rehydrated seals of both untreated and GAG-digested tissues displayed a significant decrease in bursting pressure relative to controls (Figure 3.3): For native tissue, control seals resisted pressures up to 489.4 ± 112.5 mmHg, while 12 hours of rehydration significantly decreased strengths by 41.2% to 287.9 ± 74.0 mmHg ($p < 0.05$). GAG-digested seals burst at 520.9 ± 139.9 mmHg when pressurized immediately after fusion, 24 hours of rehydration decreased strengths by 44.0% to 291.8 ± 62.6 mmHg ($p < 0.001$).

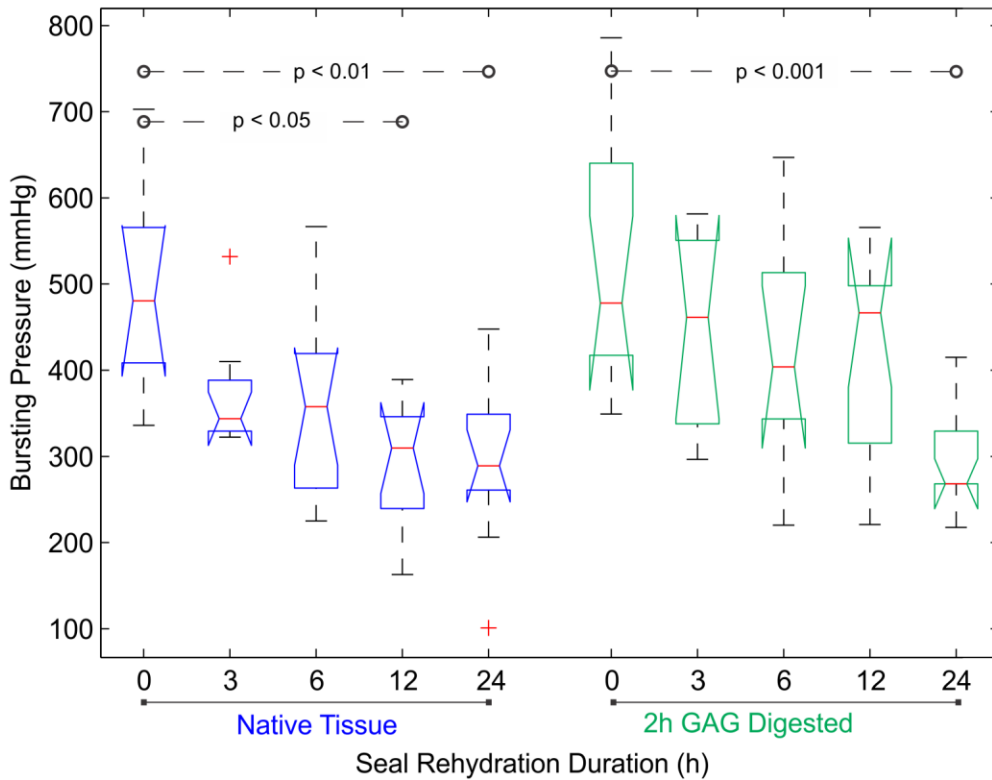


Figure 3.3: Bursting pressures of rehydrated arteries from native and GAG-digested arteries with respect to rehydration duration. Seal strengths were significantly reduced after 12 hours of rehydration for Native arteries, and after 24 hours of rehydration for GAG-digested arteries.

3.3.4. Histology

Hydration groups were stained using H&E and VVG to visualize collagen, elastin and nuclear structures (Figure 4); ChABC groups were stained using H&E for morphology as well as Light Green: SafO to visualize the location and extent of GAG digestion (Figure 5). In tissues subjected to hypotonic pretreatment, the fused media is laminated between adventitial layers, and the surrounding tissue displays a high degree of porosity. Arteries fused following isotonic pretreatment also display porosity in the adventitia, but exclude the media from the fusion region, indicating its pressure-induced separation and retraction from the fusion region. Hypertonic arteries display minimal porosity along with a pronounced separation of adventitia

and media layers. VVG-stained specimens display accentuated adventitial porosity relative to H&E-stained arteries. The VVG stain allows for visualization of the tunica intima, providing insight into the method of medial retraction during clamping, and resulting morphology of the artery adjacent to a seal.

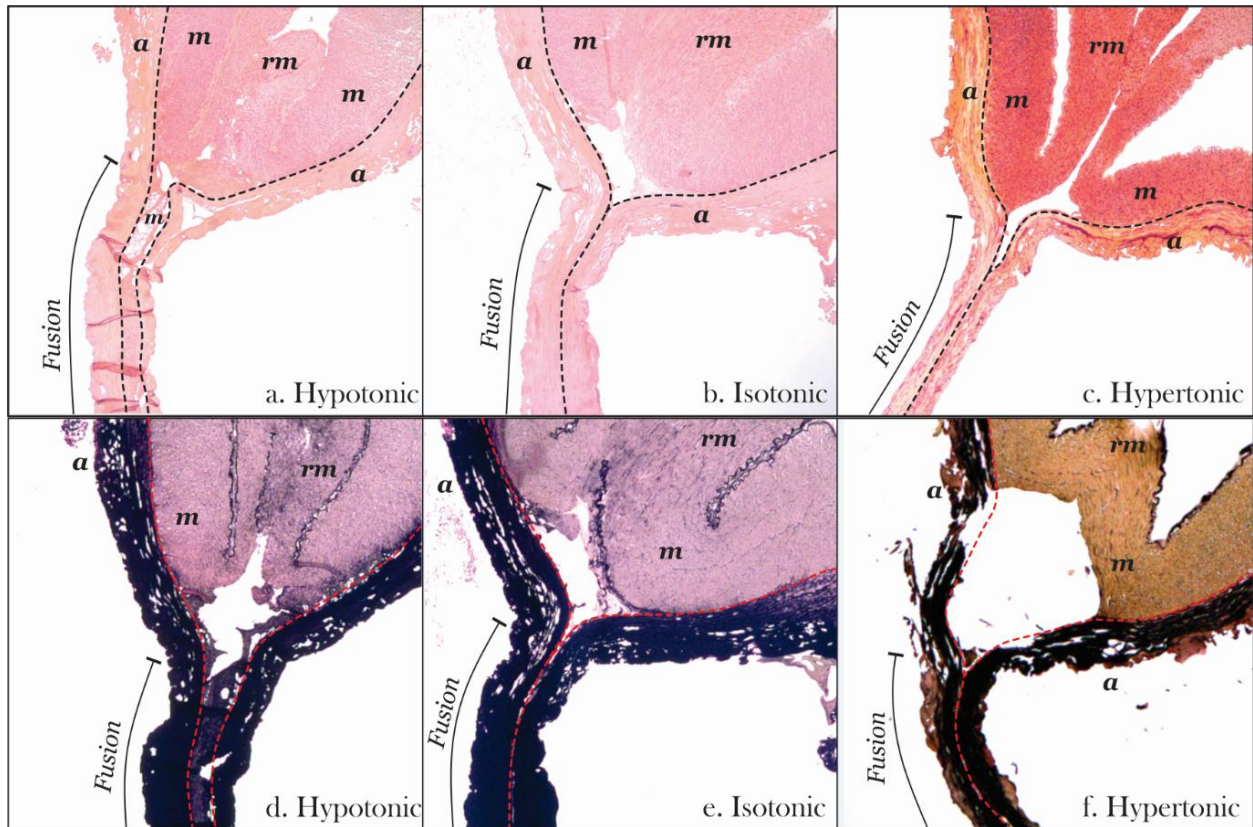


Figure 3.4: H&E (a,b,c) and VVG (d,e,f) -stained cross-sections of vascular seals from the hypotonic, isotonic and hypertonic treatment groups. Dashed lines indicate the border between adventitia (a) and medial (m) layers, where a solid line indicates the region of tissue clamped and fused with the ConMed ALTRUSTM. All image tiles are oriented with the fused portion of the artery near the bottom left and the adjacent, unaltered portion of the artery in the upper right corner of the tile. Noteworthy is the involvement of the medial layer in the fused region of Hypotonic arteries, which exhibited the highest bursting pressures of all osmotically treated arteries. Isotonic and Hypertonic arteries display a medial layer that has severed and retracted from the fusion region under pressure from the device jaws. Both hypotonic and isotonic adventitial layers exhibit large pores near the seal, likely due to the vaporization of adventitial water during fusion. The hypertonic adventitia displays a pronounced separation of adventitia from media and fewer, smaller pores in the adventitia.

Similar to the isotonic control arteries of the hydration group, control arteries of the GAG-digestion group display no medial involvement in the seal and a complete delamination and retraction of the medial layer from the fusion region (Figure 3.5). GAG-digested arteries displayed a progression of medial involvement in the fusion region as exposure to ChABC was prolonged. The extremely low GAG concentration of arteries (< 1.0 % by weight) results in a faint red stain where GAGs are present. GAG-digested arteries show GAGs retention in the laminated medial layer within the fusion region. Arteries exposed to ChABC for 30 minutes show concentrated GAGs in the adventitia; 5 hours in ChABC appears to have visibly decreased adventitial GAG concentration.

3.4. Discussion

Thermal tissue fusion has reformed the practice of surgical vessel ligation and transection, and holds potential to replace sutures in the resection, repair and functional recovery of vascular tissues. A primary barrier to progression of the technique has been that we lack a detailed understanding of the physiochemical mechanisms that give rise to thermal tissue adhesion. This study presents an empirical investigation of vascular seal strength as influenced by tissue composition via: (1) the alteration of tissue water content prior to fusion, (2) the digestion of vascular GAGs prior to fusion, and (3) the longitudinal study of rehydration post-fusion for native and GAG-depleted vascular seals. Energy-based vessel sealing relies on the evaporation of water, making pre-fusion water content, hydrophilic GAG molecules and post-fusion rehydration ideal targets for investigating the aqueous nature of the fusion mechanism. We observed that tissue water and glycosaminoglycans had considerable influence on the bursting pressures of sealed porcine arteries. These findings provide novel perspective of the

critical role of tissue hydration, and support a constitutive bonding theory of adhesion forces in the energy-based fusion of vascular tissues.

It is suggested that the heat-induced unfolding or denaturation of Type I collagen may be due to the breaking of long sequences of hydrogen bonds (both direct and water-bridged) that stabilize the molecule *in vivo*^{97,114}. Likewise, the creation of vascular seals has been attributed to the cooling-induced reformation of covalent and non-covalent bonds (molecular crosslinks, hydrogen bonds and dipole interactions) between tissue proteins^{8,68,77,89}, accompanied by a coagulum and a water vapor byproduct⁶⁹. Finally, high quality tissue welds have shown a dependence on maintained tissue hydration during the welding process⁹⁷. These findings underscore the utility of tissue water in the bond formation process, and highlight the need to better understand the aqueous nature of the fusion mechanism. The results of this present study imply that upon vaporization, bound and free tissue water may reveal polar bonding sites along extracellular matrix protein chains (*e.g.*, Collagen I polypeptides) that interact to form a dehydration-dependent tissue junction. The implication is that rather than forming permanent, insoluble covalent bonds as has been hypothesized in the literature, the fusion reaction forms interactions reliant on water vaporization, which appear to be partially soluble with longitudinal exposure to a hydrated environment. It remains to be determined whether or not the reliance of tissue seals on water loss corresponds specifically to the formation of a cellular coagulant, molecular crosslinks or electrostatic interactions.

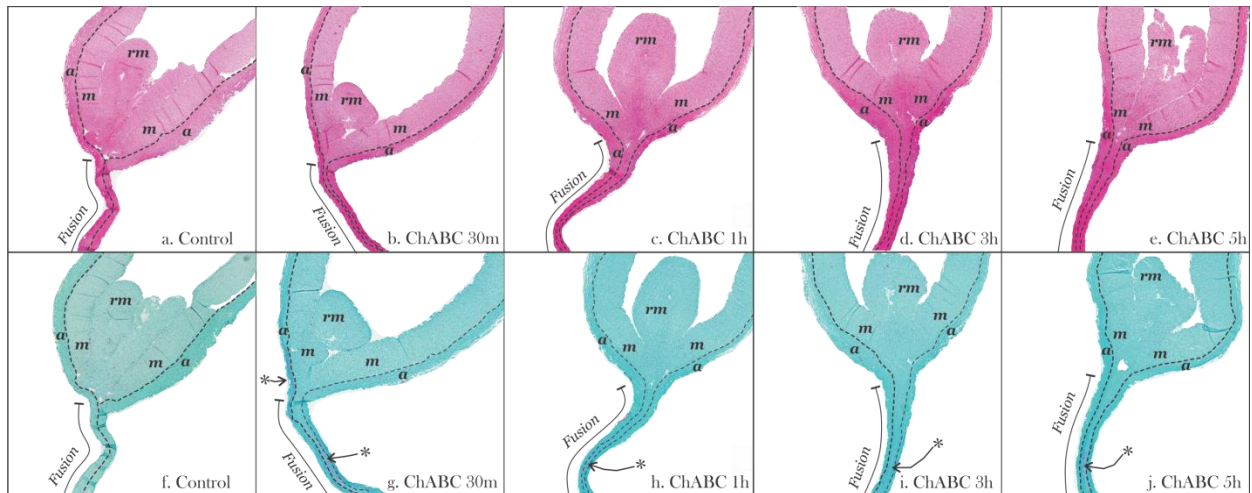


Figure 3.5: H&E (a-e) and Light Green:SafO (f-j) - stained cross-sections of vascular seals from control and GAG-digestion treatment groups. Marking and notation corresponds to that of Figure 4; “rm” indicates portions of the medial layer that have delaminated from the adventitia and retracted from the fusion region. A star indicates regions of increased GAG density. Noteworthy again is the presence of the media in the fusion region in GAG-digested arteries; these specimens withstood increased bursting pressures relative to controls.

By altering the pre-fusion content of tissue water, we sought to elucidate the role vaporization-induced water transport in promoting fusion adhesion. It is reasonable to assume that by increasing tissue water content via tonicity treatments, we are effectively changing the thermal stability of the collagen in the arterial extracellular matrix^{61,65,82,111}. For the hypotonic tissue treatment, imbibing of interfibrillar water by the extracellular matrix is presumed to have created additional water bridges in the collagen, which would result in a thermal destabilization. As fusion temperatures rise in the device jaws, the transition of an ordered polymer triple helix to a random coiled structure and the vaporization of excess water bridges may reveal additional charged residues, previously occupied by water molecules, between which polar interactions may form. Increased water content may thus impart peptide chain mobility before fusion, where dehydration of this water during fusion may increase the binding potential of coiling peptides by sheer frequency of interaction. While polar interactions have yet to be directly measured in fused

tissues, this mechanism is theorized in the previous literature⁹⁸ and may contribute to the increased adhesive strength of seals formed in hypotonic (super-hydrated) tissues observed in this study.

In removing hydrophilic GAG molecules from within the ECM, the porosity of the resultant matrix was increased³⁵, and the resistance of the matrix to water transport was decreased. This is consistent with the histology findings in this study, which depict increased porosity and vacuole formation in groups with greatest seal strengths. A lateral consequence of GAG digestion and increased porosity is a reduction in peak stress and modulus of the digested tissue³⁵. While not measured in this study, any detriment to tissue strength appears to have been superseded by the increased bond strength of digested tissue seals. Additionally, GAGs are known to possess anticoagulative properties⁴⁵, which may have a detrimental effect on any fibrin/platelet polymer coagulant that may form during fusion in tissues not subjected to digestion. While clinical digestion of GAGs prior to fusion may be impractical, the results of this study demonstrate that GAGs are inhibitory to the bond formation process, indicating that relatively low-GAG content tissues may form stronger fusion bonds. Finally, a shared characteristic of hypotonic and GAG-digested tissues is the maintenance of the tunica media, a network of smooth muscle cells, in the fusion region. It will thus be beneficial in the future to assess the influence of cell presence and cellular proteins on the process as well.

The effects of rehydration after fusion demonstrate a loss in bursting strength as tissues are allowed to recapture any water lost during fusion. This finding is in agreement with studies performed on thermally fused bovine aorta, in which brief and extensive bond rehydration resulted in moderate and complete losses of bond strength, respectively³⁰. In relating rehydration

to existing bonding theory, the often-cited renaturation of collagen fibrils as a source of fusion adhesion occurs as dehydrated chains recover some of their primary hydration water⁶¹. This represents a physical restructuring of an amorphous coil, not the binding of one coil to another. As such, rehydration in the context of this study may allow denatured collagen fibers to regain hydration water and reconfigure into their original shape; this transformation may be a source of lost fusion adhesion. Thus the implication of rehydration for functionally recoverable tissue fusion, such as in vascular anastomosis, are that fusion-induced dehydration must be sufficient to promote adhesion but not so extensive as to prevent regeneration across the fused tissue junction. While recoverable tissue fusion has been achieved in skin with reduced scarring relative to traditional closure methods^{3,38}, direct contact with a dynamic aqueous environment confers an additional challenge to the implementation of an energy-based vascular anastomosis .

The results of this study suggest that an increase in the vaporization of tissue water and sustained seal dehydration are primary contributors to the strength and resilience of thermally fused tissue. Further, glycosaminoglycans are inhibitory to fusion bonding, and low-GAG tissues may exhibit stronger thermal bonding than lubricious, GAG-rich tissues. The effects of tissue water and glycosaminoglycans provide insight into the bond formation process in energy-based tissue fusion, allowing investigators to predict the bonding potential of a given tissue based its hydration levels and GAG content. This study presents an important step towards the characterization of fusion interactions in pursuit of novel strategies for energy-based connective tissue repair and the long-term functional recovery thereof.

3.5. Conclusions

The motivation for this work stems from the persistent uncertainty as to whether thermal tissue fusion arises from electrostatics, covalent bonding or the basic physical entanglement and

thermal coagulation of vascular proteins. While the observed system of adhesion likely combines several of these effects, a rigorous analysis of adhesive sources based on tissue composition, native assembly sequences, responses to thermal energy and their long-term stability may give rise to novel strategies for tissue repair in the orthopaedic, colorectal and dermal domains among others. While existing techniques are clinically viable for vascular fusion, their thermal energies can be destructive, and surgical professionals often question the reliability of devices which employ them. An increased understanding of the effects of thermal exposure beyond those of dehydration, denaturation and collagen shrinkage may bridge reversible thermal tissue damage with a viable adhesive scaffold across which new tissue can form. This study relates the evaporation of tissue hydration water to enhanced bonding strength during vascular fusion, and the inhibition of fusion by hydrophilic glycosaminoglycans. By further characterizing the molecular responses of tissue constituents to applied thermal energy, the potential for the long-term functional recovery of thermally bonded connective tissues may soon be clarified.

Chapter 4. Effects of Heating Rate and Duration on Bond Strength in Energy-Based Vessel Sealing

4.1. Introduction

Energy-based fusion for sutureless tissue closure offers a minimally invasive ligation technique for open and endoscopic procedures. The application of heat and pressure and resulting water-tight tissue bond is approved for clinical use in vascular tissues and tissue bundles up to 7 mm in diameter⁸⁵, and shows promise for use in vascular and cellular¹⁰ tissues in the dermal, colorectal, ocular and nervous domains^{3,5,7,43,63}. The advantages of energy-based closure include reduced surgical dexterity, shorter durations and reduced procedural costs, improved patient recovery and reduced scarring³, which may soon be conferred to a range of minimally invasive clinical and surgical procedures. The barriers to broader implementation of energy-based closure include an incomprehensive understanding of the bonding mechanism by which fusion occurs, and limited surgical adoption of fusion devices due to an associated lack of repeatability and reliability in vascular ligation devices.

Energy-based tissue fusion devices may implement laser, RF/bipolar current, ultrasonic or conductive thermal energies to seal and transect vessels which may subsequently withstand up to 3x systolic blood pressures¹². The breadth of energy delivery modalities used in fusion and the empirical nature of fusion device development underlie a persistent uncertainty surrounding the origins of fusion adhesion¹¹⁴. Nonetheless, device development and associated investigations of thermal tissue transitions and device performance date nearly three decades, with minimal improvements in applicability or reliability of the technique. It is thus critical to establish a comprehensive understanding of the physiological nature of the fusion bond (e.g., a constitutive adhesion model), as well as of the tissue-device interactions that permit its use in vascular

surgery. Prior investigation into constituent-based adhesion has identified glycosaminoglycans (GAGs) as inhibitory to the bond formation process⁴⁹, while an increase in unbound tissue water led to stronger vascular seals^{17,49}. Similarly, tissue harvest and storage for laboratory and bench top evaluation of fusion devices was determined to increase bursting pressures of thermally sealed arteries, likely due to a storage-induced imbibing of unbound water by the tissue¹⁴. As such, *ex vivo* device evaluation led to an overestimation of device performance *in vivo*. Comparisons of clinical device performance across energy delivery modalities have reported marginal increases in bond strength with the use of industry-leading vessel sealing devices that implement RF/bipolar current or ultrasonic oscillation⁶⁹ relative to competing devices, as well as those implementing direct contact heating¹⁶. Device comparison studies likewise assess speed and adequacy of the device⁷⁸, as well as peripheral tissue damage through use of the instrument for both cutting and sealing of vascular tissues and tissue bundles^{78,102}.

A breadth of empirical device assessment and optimization is performed in industry, complemented by parameter sweeps for existing tools published in the literature which include fusion temperature¹⁶, duration¹⁶ and apposition pressure⁴ in attempts to effect instantaneous and water-tight bonds with maximum resilience *in vivo*. The use of sealing devices for tissue transection presents additional design challenges for manufacturers, as sealing parameters are often inadequate for transection and once desiccated, fibrous tissues respond minimally to a repeated application of heat or electric current. Resultant modifications to fusion tools may include the integration of a cutting blade for post-seal transection; others increase energy delivery to the target tissue when a cut is desired, inducing rapid and chaotic water vapor transport and increased tissue damage. As such, few fusion devices are designed with a single application in mind, resulting in excessive thermal spread to adjacent tissues⁷⁹, limited clinical

applicability^{49,60} and the questionable reliability and repeatability of these devices in *in vivo* surgical settings¹⁴.

To better implement existing clinical fusion techniques, and to explore the potential for functional recovery in fused tissues (e.g., vascular or colorectal anastomosis), fusion research must explore two areas: 1), the molecular nature of fusion adhesion and associated viability of cells and extracellular matrix for repair in response to thermal injury, and 2), the optimized reduction of thermal damage to attain instantaneous adhesion while preserving a tissue's recovery potential *in vivo*. In other words, the bonding process must induce a controlled thermal injury that is sufficient to adhere tissue layers without complete devitalization of the target tissue. As both the bond formation process and recovery potential of bonding and bonded tissues rely on the presence of water^{1,49}, one potential approach to viable bonds with recovery potential is a rate-controlled application of heat to the target tissue. Indeed, the extent of the primary thermal transition associated with thermal bonding, collagen denaturation, has been correlated with heating rate in the treated tissue². A longer duration of thermal treatment with a progressive heating rate may sustain a bonded tissue's water content, which would allow for the biotransport of water critical to the tissue's inflammatory and healing response. Similarly, the destructive and permanent device parameters used in clinical fusion (~3.3MPa, 170 °C) are designed with tissue transection in mind, and may be superfluous for functional recovery applications. Thus, a reduction in temperature and pressure combined with the aforementioned increase in fusion duration may permit an adequate factor of safety in vessel seal strength as observed in experimentally sealed blood vessels, which is generally defined by a resistance to up to 3x systolic blood pressure^{78,106}.

The aim of this study is to evaluate the effect of heating rate on the formation and strength of fusion bonds via thermal ligation of porcine arteries. Comparisons will be made between the effects of instantaneous and progressive heating rates for a clinically relevant and conservative parameters of temperature and pressure, including those identified to form the strongest bonds using clinical devices⁴, and those intended to reduce damage and facilitate functional recovery after fusion. We hypothesize that a progressive heating rate may lead to increased fusion bond strengths in sealed vasculature, and that a longer fusion duration will likewise increase bond strengths and permit the preservation of cell and extracellular matrix viability in fused tissues.

4.2. Materials & Methods

4.2.1. Tissue harvest, preparation & treatment

Porcine splenic arteries harvested from spleens obtained from a local abattoir (Innovative Foods LLC, Evans, CO) within 5 hours of organ harvest. The size and availability of these vessels make them a common analogue to human vessels¹⁴⁻¹⁶, hence their implementation in this study. Arteries were cut into 20 mm lengths, embedded in Tissue-Tek® Optimum Cutting Temperature compound (OCT, Sakura Finetek, Torrance, CA) and immersed in chilled (-160 °C) 2-Methylbutane prior to storage at -80 °C until use (< 14 days). Prior to treatment and/or fusion, samples were thawed in a 37 °C bath of PBS (BP665-1, Fisher Scientific, Fair Lawn, NJ) until they moved freely in solution (≈ 15 minutes). Arteries were further rinsed in PBS for 15 minutes at 37 °C with agitation to dissociate residual OCT from their surfaces.

4.2.2. Variation of Heating Rate

Arteries were sealed using a custom construct based upon the ConMed ALTRUS™ thermal tissue fusion device (ConMed Corporation, Centennial, CO). The construct consisted of

two 10 mm, Teflon-coated aluminum nitride heaters with modified heating algorithms internal to the ALTRUS™ energy source, the temperature of which was controlled using proportional-integral-derivative (PID) control. During sealing, arteries were submerged in 0.9% PBS to isolate the effects of varying hydration from the investigated variables of temperature, duration, pressure and heating rate. Arteries were fused for a total duration of 3, 9 or 27 s at instantaneous and progressive heating rates for each fusion duration. The linearity of heating rates following device activation were slightly affected by the PID tuning internal to the ALTRUS™ energy source. Heating rates were approximated as a first order system of °C s⁻¹.

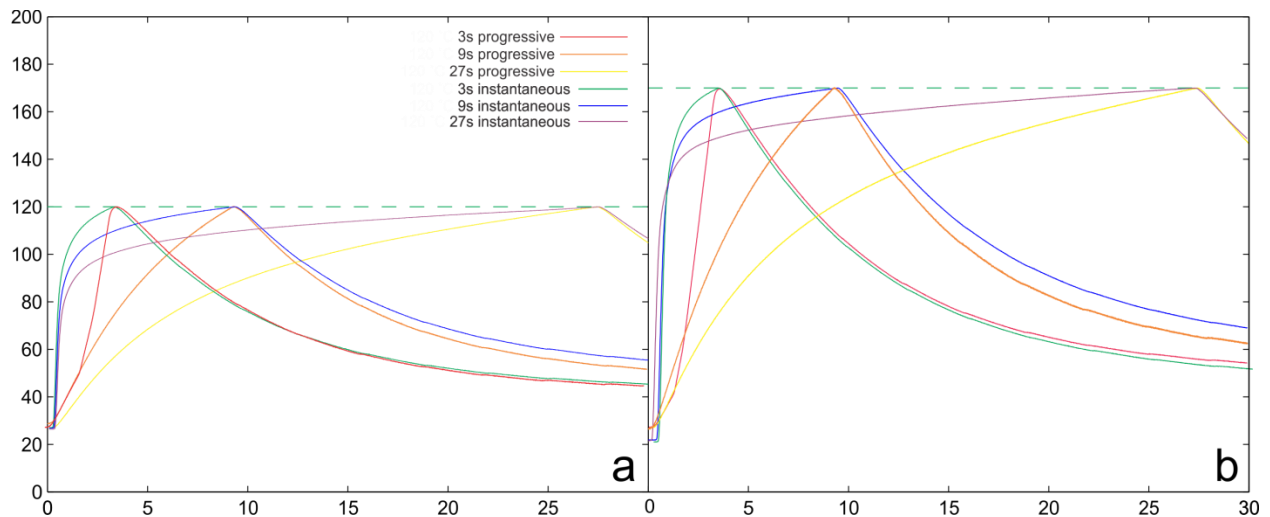


Figure 4.1: Heating rate profiles for instantaneous and progressive heating rates at a) 120 °C and b) 170 °C.

4.2.3. Load-Controlled Fusion Apparatus

Apposition pressure during fusion was controlled using PID displacement-based load control within MTS Testworks 4 software (Materials Testing Systems (MTS), Eden Prairie, MN) on a uniaxial testing system (Insight 2, MTS) via feedback from a 2kN load cell (#569327-03, MTS). The jaws of the ConMed ALTRUS™ were truncated to fit within the testing construct,

using an existing hinge pin on the device so as to maintain the geometrical approximation of the two heater surfaces as they would occur in the clinical use of the intact device. A graphite extension rod was affixed to the load cell to obtain clearance of the testing chamber, and to maintain uniaxial force delivery from the compress ALTRUS™ jaws into the load cell. Each arterial section was manually inserted into a custom tissue placement fixture designed to maintain position of the arteries at the mid-point of the fusion jaws from tip to tail. This fixture prevents variations in the cross-section of the fused tissue, and thus in the applied pressure exerted on the compressed artery due to the tapered and curved profile of the Maryland-style jaw in the ConMed ALTRUS™. Likewise, each artery was fused with the native, un-fused end distal to the concave vertical edge of the Maryland jaw, so as to avoid curvature-induced alterations in bursting pressures of fused vessels due to geometrical variations in sealing profile (Figure 4.2). Upon immersion into saline and placement of the artery within the positioner, the jaws were closed onto the artery, and the load cell and extension rod brought into close proximity with the upper surface of the ALTRUS™ top jaw. Displacement was increased linearly at a rate of 1.0 mm/s until a preload of 75% of the prescribed load was attained, at which point the displacement rate switched to 0.5 mm/s until the prescribed load of 40 or 100 N was achieved. This pre-load step in the load control method, in combination with force-controlled PID tuning, assisted in the prevention of load overshoot and the associated effects of excessive damage on the malleable layers of the artery. Once the prescribed load was attained, the fusion device was activated manually through to completion. To allow for the manual activation of the fusion device, the application of load was maintained for an additional 2 s buffer relative to the duration of fusion (3, 9 or 27 s). Following fusion, each sample was removed from saline and immediately evaluated for bursting pressure.

4.2.4. Bursting Pressure Measurement

The bursting pressure of fused arteries is used as a measure of a fused vessel's ability to withstand blood pressure *in vivo*^{14,78}. Bursting pressure was measured using a standardized testing protocol as reported previously^{4,16,49}. Briefly, fused arteries were cannulated and pressurized with air at 120 mL/min until rupture. The maximum pressure attained during the test was recorded as the bursting pressure.

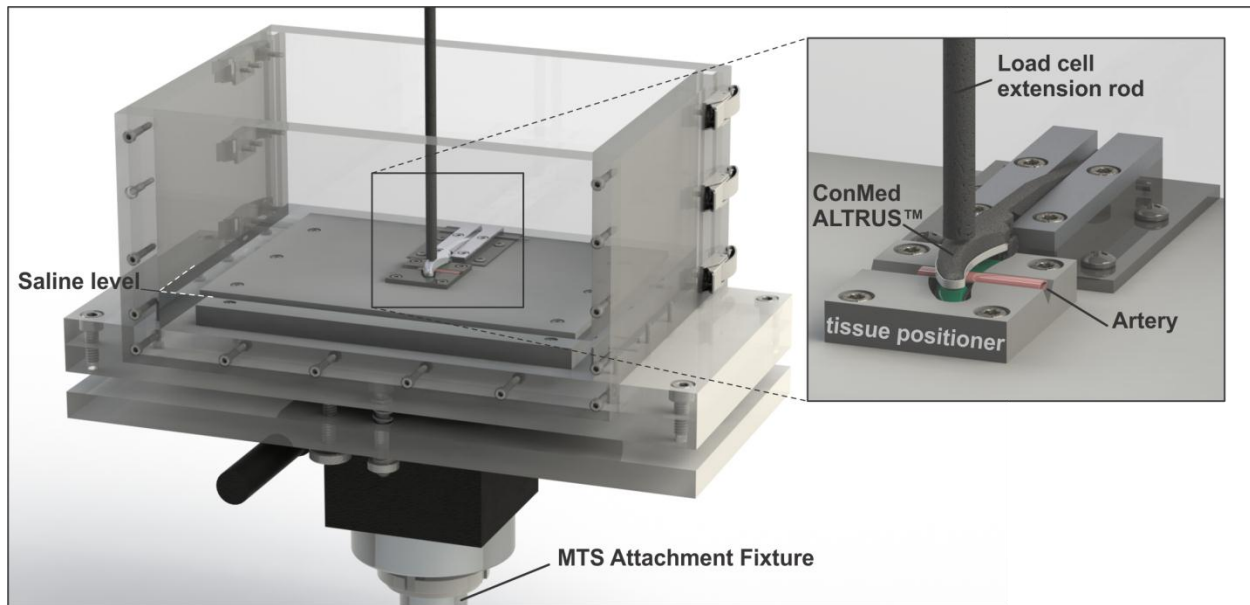


Figure 4.2: Tissue fusion construct for the variation of apposition pressure, heating rate, temperature and fusion duration under sustained hydration using 0.9% PBS.

All data are presented as mean \pm standard deviation. A one-way analysis of variance (Anova1, Matlab, Natick, MA), and a Tukey-Kramer multiple comparison test (multcompare, Matlab) were used to determine significance ($p < 0.05$) between bursting pressures for instantaneous and progressive heating rates, and for significance across treatment groups. Bursting pressure data consisted of 8 specimens per sample (i.e., combination of temperature, pressure, fusion duration and heating rate), for a total of 24 samples.

4.3. Results

4.3.1. Load Control

For each of three fusion durations, the load feedback and displacement-effected PID control maintained the desired loads of 40 and 100 N with a single anomaly. At the instance of greatest water loss, evidenced by the production of water vapor proportional to the prescribed heating rate, a drop in load and subsequent compensation by the PID control system indicates a decrease in tissue thickness as it is fused (points b and e, Figure 4.3). The observation of this phenomenon is consistent with prior work that evaluates the influence of apposition pressure on fusion bond strength⁴.

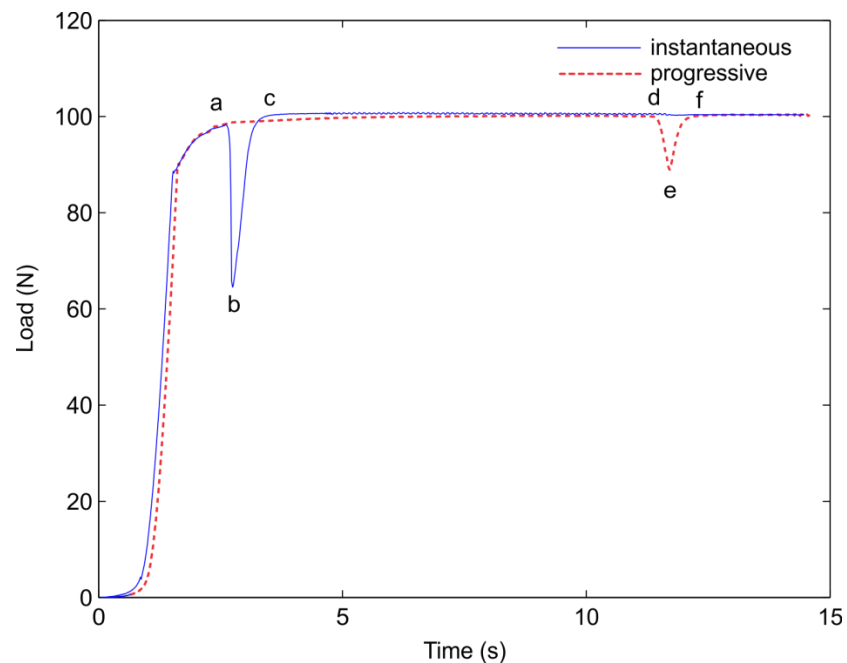


Figure 4.3: : Representative loading profiles for instantaneous and progressive heating rates at 100 N for a fusion duration of 9 s. Device activation for both rates is marked with an (a). A drop in load (b, c) and subsequent compensation by the control system (c, f) represents the point at which the prescribed temperature was achieved, and when the tissue lost the majority of its water content and thus its thickness. The same phenomenon was observed for each heating rate at 3 and 27 s fusion durations at both applied loads and temperatures.

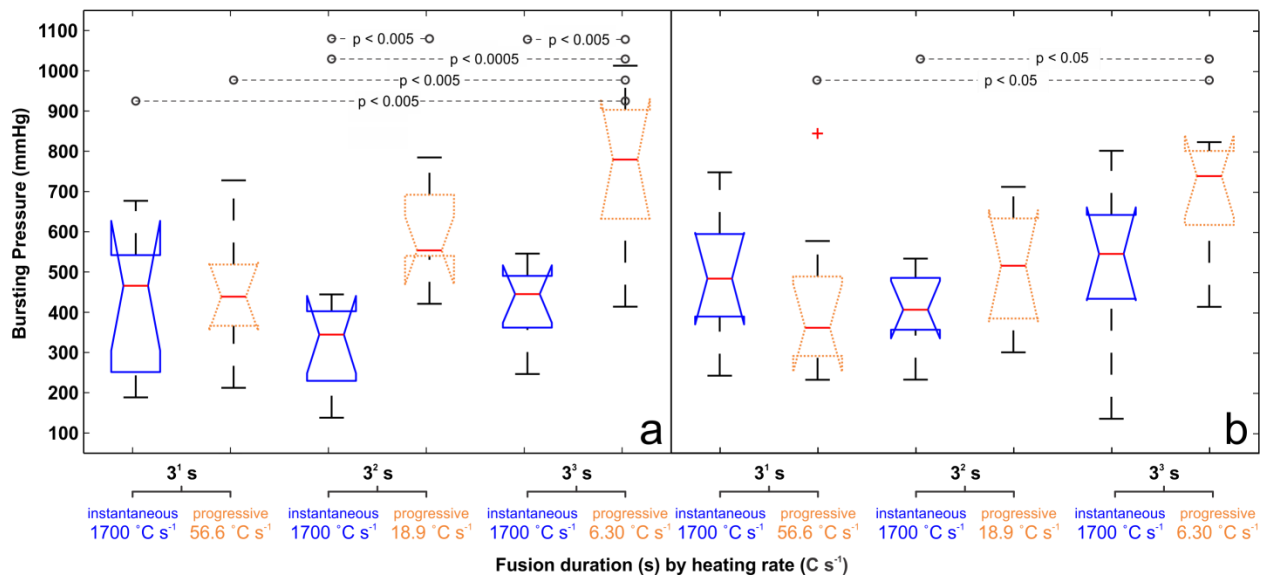


Figure 4.4: Bursting pressures of vessels sealed at various heating rates with 100 N force (~3.3 MPa) at a) 170 °C and b) 120 °C. Red lines indicate median values, black lines represent the complete data range, blue lines represent the interquartile range, and red crosses represent outliers. Significant differences between groups are indicated by order of significance on each plot.

Approximately 100 N of apposition force and an instantaneous application of 170 °C s are commonly implemented in clinical sealing devices; these parameters were used as an upper limit for device temperature and pressure in the evaluation of heating rate. Bursting pressures of seals formed at these clinically applicable parameters experienced significant increases for progressive relative to instantaneous heating rates at durations of 9 ($p < 0.005$) and 27 seconds ($p < 0.005$). At 120 °C and 100 N, no significant differences were observed between instantaneous and progressive heating rates.

For the previously-determined optimal apposition pressure of 40 N at 170 °C for 3 s using the ConMed ALTRUS™⁴, we observed a significant decrease in bursting pressure for a progressive heating rate. The remainder of sample groups collected at 40 N and 170 °C evidenced no significant differences with respect to heating rate. In stark contrast to the prior

three combinations of temperature and pressure, seals formed at 40 N and 120 °C exhibited significant decreases in bursting pressure for a progressive heating rate at all durations tested ($p < 5e^{-4}$ for all comparisons) (Figure 4.5b).

With regard to fusion duration, significant increases in bursting pressure were observed for at least two sample comparisons in all sample groups tested. In no cases were significant decreases in bursting pressure observed for an increase in fusion duration.

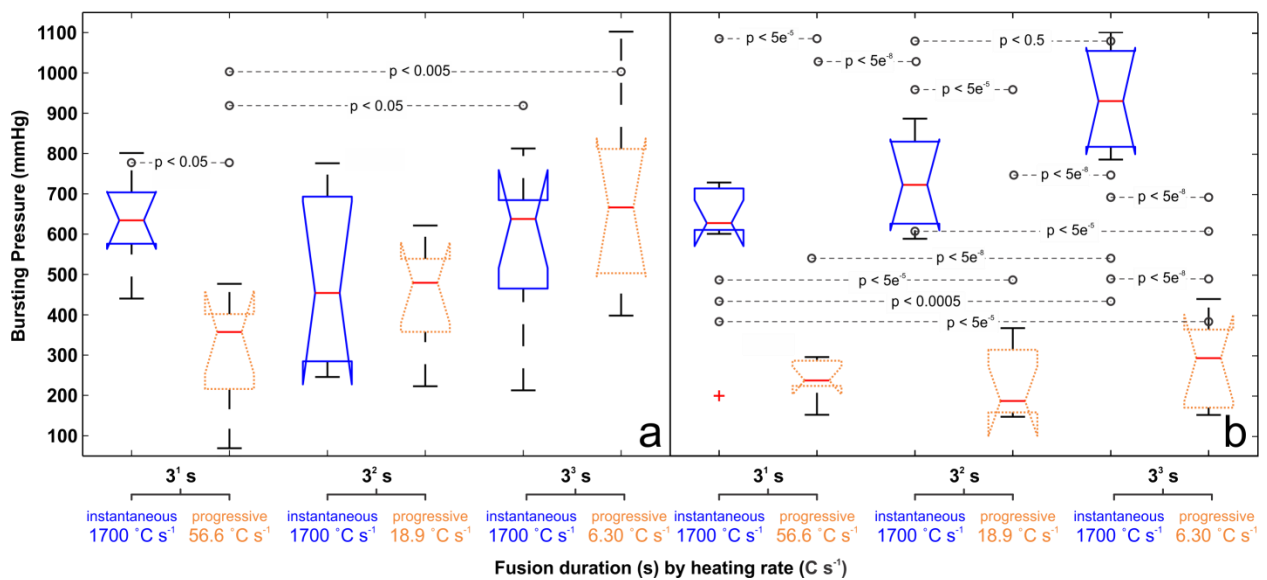


Figure 4.5: Bursting pressures of vessels sealed at various heating rates with 40 N apposition force (~1.3 MPa) at a) 170 °C and b) 120 °C.

4.4. Discussion

The temperatures, duration and pressures of thermal fusion have been investigated in depth for vascular tissues, with reported increases in bursting pressures for increasing fusion durations¹⁶ and a maximum thereof at an apposition pressure of 40 N (~1.3 MPa)⁴. To the authors' knowledge, the present work is the first published investigation of the effects of heating rate on bond strength in thermally fused tissues. The observed trends vary for each combination

of temperature and pressure, yet at clinically implemented parameters (e.g., 170 °C, 100 N) indicate that a progressive heating rate may lead to stronger seals in fused blood vessels. Contrary to the authors' hypothesis, a progressive heating rate led to drastic decreases in seal strength for low-temperature, low-pressure fusion conditions. A possible explanation for this finding is that the optimal fusion apposition force of 40 N was determined for 170° C only, thus, a 120 °C arterial surface temperature was insufficient to propagate the necessary heat and associated amalgamation of vascular constituents to form a robust seal. In pursuit of functional recovery in fused tissues such as vascular or colorectal anastomoses, further investigation will be required to identify the minimum values of tissue temperature and applied pressure required to withstand intraluminal pressures *in vivo*.

Noteworthy in the load profile is a drop in load and subsequent compensation by the MTS' PID control, as evidenced in Figure 4.3, at points b and e. This phenomenon likely corresponds to the instant of greatest water loss⁴, and thus of the greatest decrease in arterial thickness. The visible decrease in load drop for progressive heating rates may also suggest that minor, less chaotic water transport can occur for slower heating rates, leading to the formation stronger bonds under clinical parameters of temperature and pressure.

The denaturation of collagen has been positively correlated to the heating rate of tissues heated via monopolar, bipolar and laser surgical energies, where faster rates induce an increase in collagen denaturation². The thermal denaturation of collagen is certainly a byproduct of exposure to supraphysiological temperatures¹¹⁴, yet thermal fusion of collagen-rich tissues has been reported without collagen denaturation in low-temperature laser fusion²⁹. As such, the investigation into a progressive heating rate over long durations was a logical next step in determining the potential applicability of the fusion technique to functional recovery with a

limited amount of devitalized tissue. The primary goal of this study was to evaluate the effects of heating rate on the bursting pressure outcomes of fused vessels, while the corresponding variation in fusion duration served to evaluate the hypothesis that low-temperature, progressive heating may attain similar bursting pressures to those of high-temperature, instantaneous fusions of short duration. Nonetheless, the results do indicate, in agreement with published literature on fusion the effects of fusion duration¹⁶ that while it may induce additional thermal spread to adjacent tissues in the surgical space, a longer duration of fusion leads to increased bond strength in fused arteries. This increase lends further support to the notion that collagen denaturation may not be critical for thermal bonding, and that the water-assisted transport of thermally-liberated cellular and extracellular matrix components, rather than a predominantly collagenous bonding mechanism, may form the basis for instantaneous thermal tissue fusion as it is currently implemented. For clinical fusion to benefit from these changes in existing vessel sealing devices, thermal spread of the added energy would need to be mitigated with longer heating rates.

While the use of sustained hydration in this study was intended to isolate the effects of fusion temperature, pressure, and heating rate from those of varying tissue hydration during fusion, it may have demonstrated a coincidental effect of device cooling over prolonged durations. As such, the clinical use of vessel sealing may benefit from the use of surgical irrigation for device cooling and bond enhancement. Under sustained hydration, bonding increases were observed for all groups with increasing fusion duration. However, the sustained availability of saline may have decreased severity of the presented comparisons due to a constant supply of hydration to the fusion region for all samples tested; sample groups in the extremes of temperature and pressure may have experienced more or less water loss relative to each other.

Additional study of the same variables in ambient, surgical conditions may reveal increased contrast between fusion bond strength for instantaneous and progressive heating rates due to the variations in water loss during each heating modality.

4.4.1. Conclusion

Bursting pressures of vessels fused at 4 combinations of temperature and pressure were measured for 6 heating rates each. Extended fusion duration with sustained hydration in the fusion environment led to increases in fusion strength for all groups. Progressive fusion heating rates may allow for stronger bonds in current clinical applications with device parameters of high temperature and high pressure (170 °C , ~3.3 MPa) . In pursuit of functional recovery of fused tissues, low-temperature, low-pressure fusion applications (120 °C, ~1.3 MPa) may benefit from instantaneous and sustained heating, but are less responsive to a progressive heating rate than clinically-tuned fusion devices.

Chapter 5. Crosslink Stability in Energy-Based Tissue Bonding: Molecular Analysis of Collagenous Transitions via Raman Spectroscopy and Mass Spectrometry

5.1. Introduction

Vascular ligation using energy-based surgical techniques continues to reform minimally invasive surgery, despite noted uncertainty as to the origin and stability of molecular bonding forces. In removing foreign-body mechanical closure from the surgical space, energy-based vessel sealing (*i.e.*, tissue “fusion” or tissue “welding”) confers reduced surgical dexterity, shorter durations and expedited recovery to both open and endoscopic procedures. Energy-based ligation techniques implement laser, RF/bipolar current and conductive thermal energies combined with apposition pressure to form an instantaneous, water-tight seal that may withstand intraluminal pressures of greater than $3\times$ systolic blood pressure⁶⁹. While the clinical utility of vascular sealing devices is evident, the specific molecular mechanisms of energy-based tissue adhesion remain unknown. Several theories implicate alterations in the substructure of the most abundant vascular matrix protein, collagen alpha-1(Type I), such as thermal denaturation^{76,89,103}, partial renaturation¹⁰³ and/or the heat-induced breaking and reformation of intermolecular crosslinks^{33,68,93,112} in the thermal bonding process. Additional theories suggest a coagulation of cellular components in the target tissue^{10,69,112} and the interdigitation or steric entanglement of denatured proteins^{76,89,103}. While the clinical use of thermal and energy-based closure is currently limited to vascular applications, it has shown promise for use in the dermal, colorectal, oral, nervous and ocular domains^{3,5,7,43,63,83,85}. To evaluate existing theories and inform the development of advanced applications of thermal tissue bonding, this study aims to quantify thermally-induced changes in primary extracellular matrix (ECM) proteins via histopathology using polarized light, Raman spectroscopy, and quantification of ECM composition and collagen

cross-linking via ultra high performance liquid chromatography with mass spectrometry. (UHPLC/MS).

5.1.1. High-Level Bonding Theory

Comparisons of pre- and post-fusion composition in successfully fused tissues will improve our understanding of thermally-induced matrix transitions and the origins of energy-based tissue adhesion, and may lead to broader applications for sutureless tissue closure. While the influences of low-temperature thermal ablation^{2,18,110,116} and high-temperature burns^{22,81} on the substructure of various tissues have been well characterized, the relationship between surgical energy exposure and subsequent tissue bonding remains poorly understood and highly speculative. The relative abundance of collagen in vascular tissues has led many fusion investigators to focus primarily on collagen modifications that occur in response to thermal exposure. Collagen's secondary structural unit, tropocollagen, is a triple helix of three polypeptide chains (Glycine-X-Y)_n, where X and Y are often proline and hydroxyproline, respectively⁸². Amino acid residues within the chains are bound and stabilized by Hydrogen bonds⁸² and the presence of proline and hydroxyproline residues⁸². During biosynthesis, collagen acquires a number of post-translational modifications that directly affect the architecture and biophysical properties of the tissue. These include lysine modifications in the telopeptide region that are catalyzed by several groups of enzymatic proteins that complete the final step of biosynthesis – covalent intermolecular cross-linking between lysine and hydroxyl lysine residues. The types of collagen cross-links that form in normal connective tissues are determined prior to cross-link formation by the hydroxylation of specific telopeptide and helical lysine residues on collagen by lysyl hydroxylases encoded by distinct procollagen-lysine, 2-oxoglutarate 5-dioxygenase (PLOD) genes. After the imposition of these modifications, lysyl

oxidase (LOX), a copper-dependent amine oxidase, initiates the process of covalent intra- and intermolecular cross-linking of mature collagen, thereby increasing the structural integrity and strength of the vessel that contains it. Cross-links are formed between two (bivalent), three (trivalent), or four (tetravalent) mature collagen triple helices. Despite the temporal and enzymatic nature of the synthesis and maturation of fibrillar collagen in vascular tissue, thermal dissociation and subsequent reformation of LOX-mediated cross-links has been cited as a potential source of instantaneous adhesion^{33,68,93,100,112}. It is understood that collagen stability is temperature and water-dependent⁹⁸, and it has been suggested that heat-induced collagen denaturation, or unfolding of the protein, may be due to the breaking of long sequences of direct and water-bridged hydrogen bonds that stabilize the molecule *in vivo*^{97,114}. Further, bound and intrafibrillar water content in pre-fusion tissues has been shown to directly impact the integrity and resilience of thermal bonds^{17,49}, where re-hydration of bonded tissue results in a complete loss of coaptation³⁰. It is therefore pressing to re-evaluate the hypothesis that water-insoluble, thermally-stable covalent crosslinks are involved in the mechanisms of energy-based surgical adhesion.

To date, the molecular-scale characterization of fused and otherwise thermally bonded tissues has been predominantly via qualitative interpretations of imagery using either optic microscopy (histology), Scanning or Transmission Electron Microscopy (SEM, TEM). Interpretations of thermal bonding imagery have implicated end-to-end and side-to-side chemical crosslinking of collagen fibrils (“roping”) based on the visual alignment of banded (periodic) fibrils¹⁰³, or an ambiguous chemical bond based on fibrous bridging in electron micrographs³⁰. While these tools provide valuable insight into heat-induced morphological changes and the

extent of thermal damage in the treated tissue, they do not provide a quantitative metric of compositional changes and transitions during and following the fusion process.

5.1.2. Low-Level Bonding Theory

Clinical vessel sealing is currently recommended for vessels less than 7 mm in diameter^{34,46}, inclusive of arterioles, small veins and arteries and medium-sized muscular arteries. The tri-lamellar anatomical structure (*tunica intima, media and adventitia*) is shared between each class of vessel; primary structural variations include a thicker muscular (medial) layer for arteries relative to veins. Medial composition and microstructure vary with direction of blood flow and proximity to the heart, but are predominantly comprised of acellular ECM components fibrillar collagen (collagen alpha-1(I and III)), elastin, proteoglycans, and a cellular component of fibroblasts and smooth muscle cells (SMCs)⁷². As the two dominant structural proteins in each layer of vascular tissue, collagen alpha-1 (I) and elastin have been used to predict weld strength via relative abundance in fused vascular tissue, where the ratio of total collagen to elastin was directly proportional to the *bursting pressure* of the sealed artery⁹², the clinical standard for vascular seal strength¹⁰⁶. Optically, collagen denaturation has been correlated to weld formation via the measurement of a heat-induced loss of birefringence surrounding the weld area^{42,103} an optical phenomenon arising from the non-centrosymmetric structure of native collagen I networks^{42,114}. The attention paid to collagen alpha-1(I), in fusion research has led several investigators to conclude a dependence of thermal welding on the denaturation of collagen^{5,19,41,77,96,101} from their native alpha helices to lower-ordered structures (beta sheets, random coils and gelatin).

5.1.3. Raman Spectroscopy in Fusion Research

Raman spectroscopy is used to quantify changes in the secondary structure of vascular proteins often in response to disease states, but can also quantify a tissue's response to thermal injury. The prevalence of amino acids, the amide bonds between them and their secondary structure can be extracted and analyzed¹⁰⁰. A Raman spectrum comprises quantitative information on sample composition as a function of the change in energy of reflected light upon interaction with specific molecular subunits of the sample. The Raman shifts of particular spectral features (peaks) in the Raman spectra reflect this change for each species of subunit, with peak intensity being proportional to the prevalence of the subunit in the sample²⁶. As such, spectral analysis may be used to quantify molecular (and thus structural) changes in thermally treated tissue.

Prior investigation by Raman spectroscopy has concluded a dependence of thermal welding on a heat-induced formation of new tissue bonds, both instantaneous³⁰ and progressive with tissue recovery and healing³. To distinguish thermal effects from tissue recovery and restructuring, the focus of this study remains on instantaneous changes in tissue architecture. A primary indicator of instantaneous conformational changes in vascular collagen is a change in the Raman shift of the Amide I band for native α -helices ($1650\text{--}1657\text{cm}^{-1}$)^{3,122} to that of lower-ordered states (β -sheets, random coils)³. While the complete Amide I band ($1612\text{--}1696\text{ cm}^{-1}$) is the most reported collagen band, it is detected as a composite of several partially resolved species⁶² which are prominent in not only native tropocollagen helices, but immature collagen crosslinks, β -sheets or disordered secondary structures (gelatin). An amide III band ($\sim 1300\text{ cm}^{-1}$) provides complementary information on protein structure, and can be detected within collagen IA to quantify structural changes directly adjacent to proline in the $(\text{Gly-Pro-Hyp})_n$ sequence⁸⁰.

Reductions in relative peak intensity of these species can indicate degradation or damage to their structure in thermally treated tissue. Changes in the amide bands of collagen will be used to validate thermal denaturation.

Amide Band	Conformation	Principal Frequency (cm ⁻¹)	Functional Group/Vibration
Amide I	α -helix	1650–1657 ⁴⁰	C=O Stretch
	β -sheet	1670–1690 (weak)	
	Random Coil	1640–1651	
Amide III	α -helix	1270-1300	C–N Stretch, N–H Bend
	β -sheet	1229–1235	
	Random coil	1243–1253	

Table 5.1: Principal frequencies of Raman-active vascular protein bands of interest ¹²²

5.1.4. Collagen and Elastin Crosslink Quantification

The maturation of collagen and the pathological stiffening of collagen matrices are commonly quantified using the ratio of mature to immature collagen crosslinks^{40,62,73} within the tissue region of interest. The Raman spectral ratio of 1660 cm⁻¹ to 1690 cm⁻¹ has been used to indicate collagen maturity^{40,73}, and validated by Fourier Transform Infrared Spectroscopy (FTIR) to be proportional to the abundance of the trivalent (mature) crosslink pyridinoline to the bivalent (immature) crosslink dihydroxylysinoxorleucine⁶². The vibration at 815 cm⁻¹, arising from C–O–C stretching has also been associated with the divalent hydroxyl lysinoxorleucine crosslink within collagen I⁷¹. Elastic structures are indicated at 1335 cm⁻¹, representing the elastic crosslinks desmosine and iso-desmosine³. The relative intensity of each species in native and fused tissue samples may provide an indication of crosslink stability during the fusion process. We hypothesize that while generally stable at high temperature and biological pH, both immature

and mature collagen crosslinks may experience degradation at the high pressures and temperatures of thermal welding (> 3 MPa, ~170 °C). There is however unlikely to be a heat-induced increase in any collagenous or elastic crosslinks, again due to the enzymatic nature of the crosslink formation and maturity pathways.

5.1.5. HPLC in Fusion Research

HPLC has also been used, although in a single study, to quantify thermally-induced changes in immature crosslinks (Hydroxylysinoxorleucine (HLNL) and dihydroxylysinoxorleucine (DHLNL) and the mature, trifunctional product of DHLNL, hydroxypyridinium (HPyr)) of argon laser-welded tissues⁹³. The present study aims to provide a validation and supplement to these published results, while expanding upon the breadth of collagen crosslinks detected to include the bivalent, immature collagen crosslinks lysinoxorleucine (LNL) and lysino-keto-norleucine (LKNL), the mature, trivalent crosslink Lysyl-Pyridinoline (LPyr), adding the detection of elastic crosslinks Desmosine and Isodesmosine (DES/IDES), and increasing the specificity of crosslink detection via a novel method of UHPLC in tandem with MS.

5.1.6. Proteomics in Fusion Research

Similarly, HPLC in tandem with mass spectrometry has been used to report a proteomic profile of laser-irradiated Human Gingival Fibroblasts (HGF) for wound healing in periodontal therapy⁷⁴. The primary results of this study implicated an upregulation in irradiated cells of galectin-7, a modulator of cell-cell and cell-matrix interactions, as a possible contributor to the improved wound healing process in laser-irradiated tissues⁷⁴. The present study aims to provide an additional, more thorough proteomic analysis of thermally treated tissues in whole, in this

case the vasculature affected by a leading energy-based vessel sealing device, the ConMed ALTRUS™.

5.1.7. Summary of Experimental Aims

Prior work in our group has made efforts to identify precursors to, and ideal compositional and environmental conditions for, fusion adhesion with respect to tissue water content^{17,49}, hydrophilic non-collagenous proteins⁴⁹, and the implications of *ex vivo* fusion research on thermal bond strength relative to *in vivo* ligation using the same tools¹⁴. This work seeks to advance our understanding of constituent-based bonding in energy based tissue bonding via analyses of thermal denaturation as birefringence changes in histological sections, Raman spectroscopy of native and fused vasculature and UHPLC/MS of the same. We hypothesize a confirmation of reductions in the order of collagen secondary structure as measured via birefringence and Raman spectroscopy, and a possible decrease in the abundance of immature, reducible collagen crosslinks in fused tissues due to thermal damage, with no increases in collagenous or elastic crosslinks in fused tissues relative to controls as characterized by Raman spectroscopy and UHPLC/MS.

5.2. Materials & Methods

5.2.1. Tissue harvest, preparation & treatment

This study utilized porcine splenic arteries, a common analogue to human vessels due to their size (\varnothing 2 –5 mm) and availability. Splenic arteries were harvested of spleens from a local abattoir (Innovative Foods LLC, Evans, CO), within 5 hours of organ harvest. Vessels were segmented into 10 mm lengths, and subject to compression (~3.3 MPa) within the jaws of a thermal fusion device (ALTRUS™, ConMed Corporation, Centennial, CO) so as to maintain the effects of apposition pressure on the arteries which include a severed and retracted medial layer,

leaving only adventitial tissue within the jaws⁴⁹. Native arteries were removed from the jaws; the compressed tissue was separated from the artery as a 16 mm² square section and prepared for analysis via either Raman spectroscopy or mass spectrometry. Fused sections were sealed at 170 °C for 3 s, separated from their adjacent tissue into a square section and likewise prepared for analysis.

Prior to Raman spectral collection, specimens were flattened and dried between parallel glass slides under vacuum for 24–48h to prevent laser-induced tissue drying and associated adjustments in focal plane during scanning, and thus spectral accuracy. Dried specimens were mounted to AFM metal specimen discs (Ted Pella 16218, ø15mm) with cyanoacrylate glue and cured within the parallel slides, again to maintain a uniform focal plane.

Samples for analysis using mass spectrometry were collected into pooled groups of several (6–10) arterial sections for a total weight of ~10 mg per sample. 8 samples each of native and fused tissue were used for the quantification of collagen crosslinks using HPLC/MS. An additional sample of pooled tissue sections from each group weighing ~10 mg was collected for proteomic analysis. Samples were immersed in liquid nitrogen, homogenized using a ceramic mortar & pestle (Coors, Golden, CO) and stored in a micro-centrifuge tube at –80 °C prior to preparation & analysis via HPLC/MS.

5.2.2. Raman spectral Collection

Raman spectra from 700 to 1700 cm⁻¹ were collected using a confocal Raman microspectroscope (inVia Reflex, Renishaw plc, Wotton-under-Edge, UK) equipped with a 785 nm diode laser (Innovative Photonic Solutions, Monmouth Junction, NJ) at 33.2 mW coupled to a 50× objective (NA=0.75, Leica, Wetzlar, DE) on an optical microscope (DM 2700 M, Leica).

For each sample of fresh or fused tissue, spectra were collected at 8 arbitrary locations within the clamped and flattened region of the artery, for a total of 128 collected spectra. For each spectrum, ten 15s exposures were acquired and averaged. Baseline subtraction and cosmic ray removal using Renishaw software (Wire 4.2, Renishaw) were completed for all spectra prior to data processing.

5.2.3. Hydrolysis of sample

The dried sample was placed in a glass hydrolysis vessel and hydrolyzed in a volume of 6N HCl, 0.1% phenol. The hydrolysis vessel is flushed with N₂ gas, sealed, and placed in a 110°C oven for 24 hours. After hydrolysis, the dried sample is re-hydrated in 200uL of 18 mΩ H₂O for 5 minutes, then 200uL of glacial acetic acid for 5 minutes, and finally 800uL of 1-Butanol for 5 minutes. This will re-hydrate the dried sample in an organic mixture with a final ratio of (4:1:1, butanol: acetic acid: water). Importantly, 20μL of sample is removed after re-hydration in water and saved for determination of hydroxyproline content.

5.2.4. Preparation of CF-11 Enrichment Column

CF11 cellulose powder is loaded in a slurry of butan-1-ol: glacial acetic acid, water (4:1:1) solution onto a Nanosep MF GHP 0.45μm spin columns until a settled resin bed volume of approximately 5 mm is achieved. The resin is washed with 1.5 mL 4:1:1 organic mixture using an in-house vacuum manifold set up. Re-hydrated samples are then loaded onto individual columns, the vacuum is turned on, and the sample is pulled through the resin into glass collection vials. The flow through is again passed over the resin to ensure maximal binding of cross-linked amino acids and set aside. The column is then washed with 1.5 mL of fresh 4:1:1 organic mixture. A fresh collection vessel is placed under the column and 750 uL of 18 mΩ H₂O is used to elute cross-linked amino acids off of the CF-11 resin. The eluent is then placed in a centrifugal

evaporator and run until complete dryness. Dried eluent is then reconstituted in a buffer appropriate for downstream MS analysis on reversed-phase or amide HILIC UHPLC columns.

5.2.5. UHPLC Analysis

Up to 20 μ L of tissue hydrolysates were analyzed on a Vanquish UPHLC system (ThermoFisher, San Jose, CA, USA) using an Acquity UHPLC BEH Amide column (2.1 x 100mm, 1.7 μ m particle size – Waters, Milford, MA, USA). Samples were separated through a 5 minute gradient elution (55% - 40% Mobile phase B) at 250 μ L/min (mobile phase: (A) 10mM NH₄CH₃CO₂, pH 10.2, (B) 95% acetonitrile, 5% Mobile Phase A, pH 10.2, column temperature: 35°C.

5.2.6. MS Data Acquisition

The Vanquish UPHLC system (ThermoFisher, San Jose, CA, USA) was coupled online with a QExactive mass spectrometer (Thermo, San Jose, CA, USA), and operated in two different modes – 1. Full MS mode (2 μ scans) at 70,000 resolution from 75 to 600 m/z operated in positive ion mode and 2. PRM mode at 17,500 resolution with an inclusion list of in-tact cross-linked amino acid masses (Supplemental Figure), and an isolation window of 4 m/z. Both modes were operated with 4 kV spray voltage, 15 sheath gas and 5 auxiliary gas. Calibration was performed before each analysis using a positive calibration mix (Piercenet – Thermo Fisher, Rockford, IL, USA). Limits of detection (LOD) were characterized by determining the smallest injected cross-linked amino acids (LNL, DHLNL, LPyr, Desmosine/Isodesmosine) amount required to provide a signal to noise (S/N) ratio greater than three using < 5ppm error on the accurate intact mass. Based on a conservative definition for Limit of Quantification (LOQ), these values were calculated to be threefold higher than determined LODs.

MS Data acquired from the QExactive were converted from a .raw file format to .mzXML format using MassMatrix (Cleveland, OH, USA). Assignment of cross-linked amino acids was performed using MAVEN (Princeton, NJ, USA). The MAVEN software platform provides the means to look at data acquired in Full MS and PRM modes and allows user to import in-house curated peak lists for rapid validation of features. Normalization of cross-linked amino acid peak areas was performed using two parameters, 1. Hydroxy proline content and 2. Tissue dry weight pre-hydrolysis (in milligrams). Hydroxy proline content is determined by running a 1:10 dilution of the pre-enrichment sample through the Full MS mode (only) described above and exporting peak areas for each run.

5.2.7. Quantification of cross-linked amino acids

Relative quantification of cross-linked amino acids was performed by exporting peak areas from MAVEN into GraphPad (La Jolla, CA, USA) and normalizing based on the two parameters described above. Statistical analysis, including T test and ANOVA (significance threshold for p values <0.05) were performed on normalized peak areas. Total cross-link plots were generated by summing normalized peak areas for all cross-links in a given sample and comparing prophylactic to tumor tissue. The ratio of hydroxy lysine collagen cross-links (HLCC) to lysine collagen cross-links (LCC) was determined by summing normalized peak areas of HLCCs (DHLNL, dePyr, Pyr) and taking the ratio to LCCs (LNL).

5.2.8. Histology

Three specimens from each group (native, fused) were prepared for visualization of the arterial cross-section. Native arteries were clamped and removed from the ConMed ALTRUS™; fused arteries were sealed in the ConMed ALTRUS™ for 3 s at 170 ° C. Samples were fixed in formalin, dehydrated and embedded in paraffin prior to sectioning at 5µm. Hematoxylin & eosin

and Picrosirius red stains were used to visualize morphological structure and the extent of collagen denaturation via loss of birefringence, respectively. Slides were imaged at 10x magnification using differential interference contrast microscopy on a Nikon Ti-E microscope (Nikon, Minato, Tokyo Japan).

5.2.9. Data Processing & Statistical Analysis

All data are presented as mean \pm standard deviation. A one-way analysis of variance (ANOVA1, Matlab, Natick MA) ($p < 0.05$) was used to determine statistical significance between sample groups. Spectra for native and fused porcine arterial tissue (n=64) were averaged and normalized to unity as shown in Figure 5.2. Spectral intensities at 815 cm^{-1} and 1335 cm^{-1} were extracted using Matlab as indicators of the prevalence of divalent collagen crosslink hydroxylysinoxorleucine and tetravalent crosslinks desmosine and isodesmosine³, respectively; the peak at 1335 cm^{-1} represents both elastic crosslinks. The ratio of peak intensities at 1660 cm^{-1} and 1690 cm^{-1} was calculated as a representation of the relative abundance of trivalent pyridinoline to bivalent dihydroxylysinoxorleucine⁶². Peak areas for the Amide III ($1245\text{--}1270\text{ cm}^{-1}$)¹²² and Amide I ($1612\text{--}1696\text{ cm}^{-1}$) bands of collagen I were calculated as indicators of thermal degradation (denaturation) of the protein's secondary structure. Peak centers were recorded for the Amide I and Amide III bands of collagen I.

5.3. Results

5.3.1. Histology

Histology of arterial samples under polarized light using Picrosirius red indicates a loss of birefringence for thermally fused collagen in the clamped and fused region of the tissue (Figure 5.1). All samples indicate a delamination and retraction of the *tunica media* from the *tunica adventitia* due to the clamping and apposition pressure of the ConMed ALTRUSTTM.

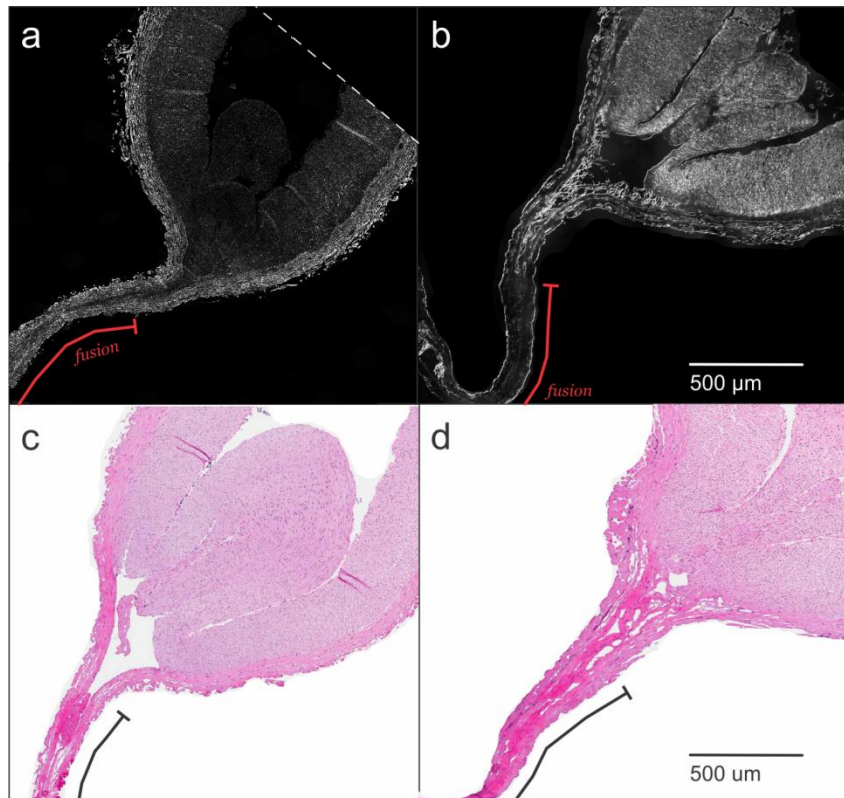


Figure 5.1: Histology of fresh (a,c) and fused (b,d) arteries stained with Picrosirius red under polarized light (a,b) and H&E in bright field (c,d). A red line indicates the fused region of the artery clamped in the device jaws. Notable is the loss of collagen birefringence in clamped and thermally fused region of the artery (b), and a delamination and retraction of the cellular tunica media from the adventitia in both fresh and fused arteries due to the clamping pressure of the ConMed ALTRUS™.

5.3.2. Raman Spectroscopy

Significant spectral differences between the investigated tissue conditions are observable only for the ratio of Raman peak intensity at 1660 cm^{-1} to that at 1690 cm^{-1} . Peak centers for the Amide I and Amide III bands were unchanged between native and fused artery.

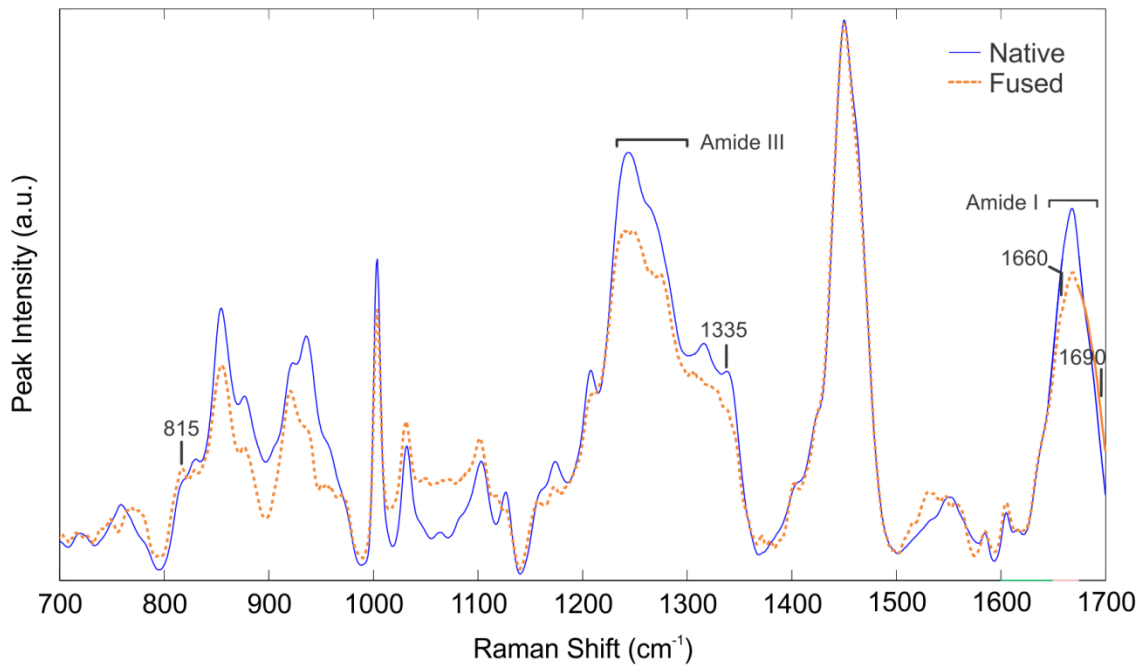


Figure 5.2: Mean Raman spectra for native and thermally fused arterial tissue.

Changes in peak intensity at 815 cm^{-1} and 1335 cm^{-1} were statistically insignificant between native and fused tissue ($p=0.45$ and $p=0.43$, respectively). A 29% decrease in the ratio of peak intensities at 1660 cm^{-1} and 1690 cm^{-1} was observed from native to fused tissue ($p < 0.0005$).

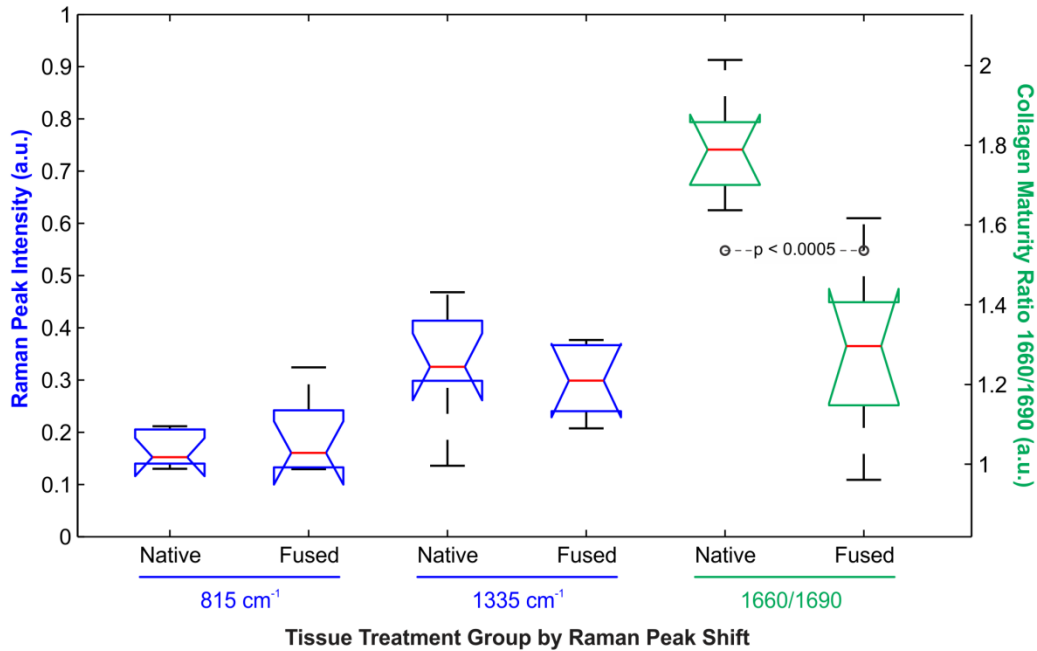


Figure 5.3: Raman peak intensities and ratios for crosslink species of interest. Red lines indicate median values, blue lines above and below the median indicate the upper and lower quartiles, the difference between which is the interquartile range. The data range is indicated by black lines.

Slight changes in normalized peak area for the Amide III and Amide I bands were detected, though statistically insignificant ($p = 0.21$ and $p = 0.46$) as shown in Figure 5.3.

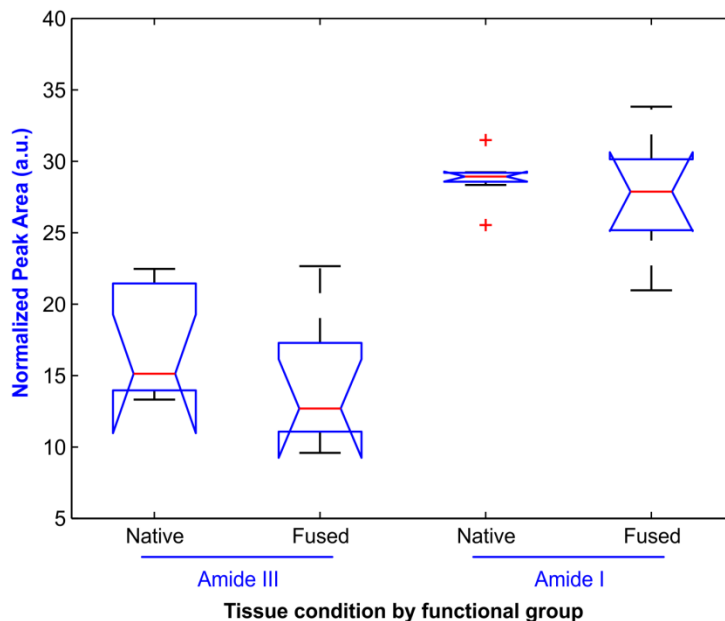


Figure 5.4: Normalized peak area for the Amide III ($p = 0.21$) and Amide I ($p = 0.46$) Raman bands

5.3.3. Crosslinked Amino Acids Mass Spectrometry

Differences in normalized peak area for all crosslink species detected remained insignificant for all comparisons with the exception of that of HLNL, the abundance of which experienced a statistically significant decrease in fused relative to native tissue ($p < 0.005$).

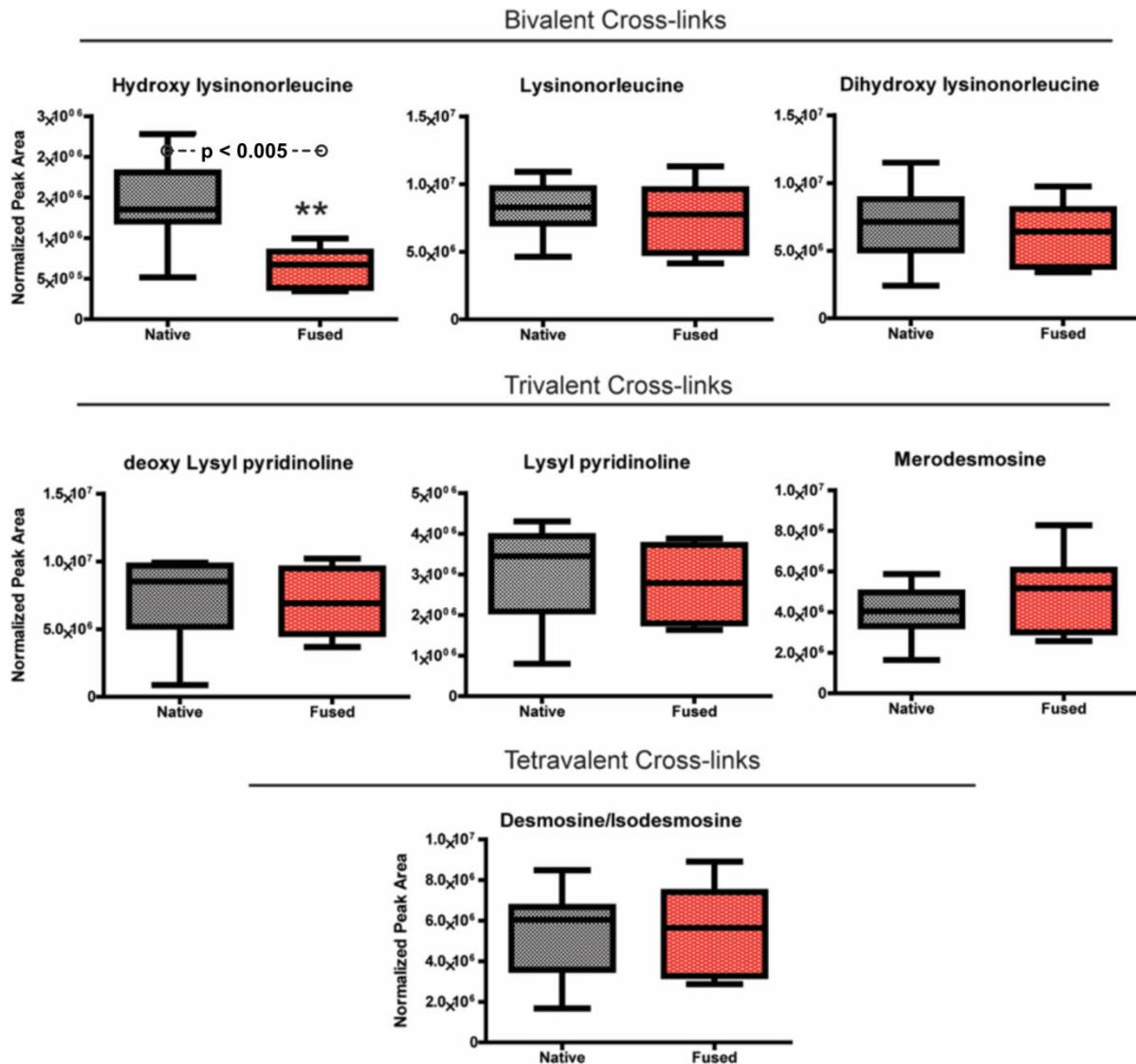


Figure 5.5: Figure 6: Normalized peak areas of bivalent (collagen, immature), trivalent (collagen, mature) and tetravalent (elastic) collagen crosslinks detected by HPLC/MS for native and fused tissue.

5.3.4. Proteomic Analysis

Protein	Functional	Matrisome	MW	Gene	Splenic Artery Pre-Laser Fusion	Splenic Artery Post Laser Fusion	Fold Change
Actin alpha-2	Cytoskeletal	Cellular	42 kDa	ACTA2	1611	1203	0.75
Alpha actinin-1	Cytoskeletal	Cellular	55 kDa	ACTA1	233	116	0.50
Annexin A2	Other ECM	ECM-affiliated	39 kDa	ANXA2	157	217	1.38
Biglycan	Structural ECM	Proteoglycan	42 kDa	BGN	224	208	0.93
Collagen alpha-1(I)	FACIT Collagen	Collagen	139 kDa	COL1A1	600	1414	2.36
Collagen alpha-1(III) chain	FACIT Collagen	Collagen	139 kDa	COL3A1	506	1155	2.28
Collagen alpha-1(IV)	FACIT Collagen	Collagen	156 kDa	COL4A1	28	16	0.57
Collagen alpha-1(V)	Fibrillar Collagen	Collagen	182 kDa	COL5A1	36	67	1.86
Collagen alpha-1(VI)	Matricellular	Collagen	45 kDa	COL6A1	84	132	1.57
Collagen alpha-1(VIII)	Matricellular	Collagen	73 kDa	COL8A1	4	9	2.35
Collagen alpha-1(XII)	FACIT Collagen	Collagen	102 kDa	COL12A1	62	44	0.71
Collagen alpha-1(XIV)	FACIT Collagen	Collagen	193 kDa	COL14A1	210	363	1.73
Collagen alpha-2(I)	FACIT Collagen	Collagen	129 kDa	COL1A2	674	1537	2.28
Collagen alpha-2(IV)	FACIT Collagen	Collagen	161 kDa	COL4A2	53	26	0.49
Collagen alpha-2(V)	Fibrillar Collagen	Collagen	122 kDa	COL5A2	34	65	1.94
Collagen alpha-2(VI)	Matricellular	Collagen	106 kDa	COL6A2	256	345	1.35
Collagen alpha-3(VI)	Matricellular	Collagen	342 kDa	COL6A3	907	1377	1.52
Decorin	Structural ECM	Proteoglycan	40 kDa	DCN	168	188	1.12
Dermatopontin	Structural ECM	Glycoprotein	22 kDa	DPT	10	26	2.63
Fibrillin-1	Matricellular	Glycoprotein	254 kDa	FBN1	106	444	4.19
Fibrinogen alpha chain	Structural ECM	ECM-affiliated	32 kDa	FGA	11	11	1.05
Fibronectin	Structural ECM	Glycoprotein	272 kDa	FN1	152	54	0.35
Fibulin-1	Matricellular	Glycoprotein	78 kDa	FBLN1	123	52	0.42
Fibulin-5	Matricellular	Glycoprotein	50 kDa	FBLN5	28	87	3.16
Galectin	Other ECM	ECM-affiliated	15 kDa	LGALS1	289	189	0.65
Integrin beta	Structural ECM	Glycoprotein	88 kDa	ITGB1	50	39	0.78
Laminin subunit beta-2	Structural ECM	Glycoprotein	179 kDa	LAMB2	83	31	0.37
Lumican	Structural ECM	Proteoglycan	39 kDa	LUM	174	251	1.44
Lysyl oxidase like-1 protein	ECM regulator	ECM regulator	65 kDa	LOXL1	0	14	
Matrix Gla protein	Structural ECM	Glycoprotein	12 kDa	MGP	3	4	1.25
Nidogen-2	Structural ECM	Glycoprotein	152 kDa	NID2	41	12	0.29
Periostin	Matricellular	Glycoprotein	93 kDa	POSTN	16	4	0.26
Perlecan	Structural ECM	Proteoglycan	195 kDa	HSPG2	156	69	0.44
Peroxiredoxin-2	Matricellular	Other ECM	22 kDa	PRDX2	30	28	0.95
Prelamin-A/C	Other ECM	Cellular	65 kDa	LMNA	113	103	0.91
Protein-lysine 6-oxidase	ECM regulator	ECM regulator	47 kDa	LOX	4	0	0.00
Tenascin-C	Matricellular	Glycoprotein	191 kDa	TNC	103	36	0.34
Transglutaminase	Matricellular	ECM regulator	77 kDa	TGM2	99	76	0.77
Versican	Matricellular	Proteoglycans	178 kDa	VCAN	21	25	1.19
Vimentin	ECM regulator	Cellular	54 kDa	VIM	517	455	0.88

Table 5.2: Identity, specifications and fold changes of selected proteins for proteomic analysis.

Proteomic analysis of fused vascular tissue indicates changes in numerous cellular and extracellular matrix proteins. In regards to the primary extracellular matrix protein class of fibrillar collagens, proteomic analysis indicates that 90% of fibrillar collagen is evident in extractions of soluble and insoluble extracellular matrix constituents, where 8% occurs in the

cellular extraction fraction. In fused tissues, we observe a statistically significant increase in incidence of fibrillar collagen to 41% in the cellular extraction fraction ($p < 0.0005$).

5.4. Discussion

The quantification of collagenous transitions in thermally fused tissues may shed light on existing theories regarding the bonding mechanisms of tissue fusion, as well as on the potential for application of the fusion technique to sutureless closure in avascular tissues. The long-standing prevalence of collagen-based bonding theories in the fusion literature demands their validation, and the limited clinical applications of the fusion technique beckon a component-based adhesion theory. Thus far, the failure of tendon collagen to fuse in response to a sweep in laser energy parameters¹⁰ has challenged the collagen bonding hypotheses, pointing rather to the hydration and relative cellularity of successfully fused tissues. Likewise, we have shown tissue hydration and proteoglycan content to promote^{17,49} and inhibit^{48,49} the formation of instantaneous fusion bonds, respectively. Each of these results supports the aforementioned failure of tendon collagen, a dense network of collagen alpha-1(I) high in proteoglycan content, to fuse. Finally, the dissolution of fused tissues with exposure to longitudinal hydration refutes the proposed formation or reformation of water-insoluble covalent crosslinks during the fusion process⁴⁹. These findings support the notion that the coagulation of cellular proteins (e.g., fibrin, fibronectin) within a denatured matrix of fibrous proteins may form the basis for a water-soluble bioadhesive in fused tissues¹⁰. The present study aims to detail the thermal transitions of collagenous crosslinks during fusion via quantitative analyses of cross-link abundance via Raman spectroscopy and UHPLC/MS. The evidenced dissociation of a single species of immature covalent crosslink with exposure to supraphysiological temperatures (~ 170 °C) and

pressures (~3.3 MPa) lends further support to the study of the biothermomechanics and associated adhesion of hydrated and cellular connective tissues.

5.4.1. Histology

A loss of collagen birefringence in fused tissue was confirmed in the present study, indicating a disruption in collagen secondary structure in the fusion region via thermal denaturation. The delamination and retraction of the *tunica media* from the clamped and fused region of each artery is consistent with previous findings^{4,49}, and makes an important distinction that the present analysis of tissue architecture is constrained to that of the vascular *tunica adventitia*. The use of high apposition pressure (~3.3 MPa) ensures complete vascular ligation and enables tissue transection using higher energy in fusion devices, but may not result in the strongest possible vascular seal⁴. Due to the high proportion of smooth muscle cells in the *tunica media* relative to the adventitia, analyses of fused tissue that include the laminated medial layer may provide additional insight into thermal modifications of collagen crosslinks and of cellular protein abundance.

5.4.2. Raman Spectroscopy

Raman spectroscopy for the analysis of collagen crosslinks in bone is prevalent in the literature^{40,73} and has reported the ratio of 1660 cm⁻¹ to 1690 cm⁻¹ as proportional to the relative abundance of the collagen crosslinks pyridinoline (mature, trivalent) and dihydroxylysinonorleucine (immature, divalent)⁶². However, the several components that comprise the Amide I peak are measured as changes in collagen secondary structure, rather than direct measurements of crosslink abundance, as few collagenous crosslinks are sufficiently abundant to scatter a distinctly identifiable Raman signal⁶². While 1660/1690 may indicate relative abundance of Pyr to DHLNL, a shift in peak intensity towards the higher frequencies of

the Amide I band has been reported in mechanically-damaged^{9,13} and thermally denatured³ collagen, which would likewise effect a decrease in the collagen maturity ratio. Accordingly, the observed decrease in 1660/1690 for fused vascular tissue may be attributed to a damage-induced increase in the higher frequencies of Amide I¹³, rather than a decrease in abundance of Pyr, or increase in that of DHLNL.

In addition to the quantification of collagen crosslinks, Raman spectroscopy has been used to evidence degradation (denaturation) of native collagen helices^{3,30} following thermal exposure. While reductions in intensity for several bands are visible in the mean Raman spectra of fused tissues, these changes were statistically limited to a decrease in the intensity of the band at 1,000 cm⁻¹, which is in agreement with prior findings³⁰ that may indicate a change in the secondary structure of proteins in sheet conformation³. Raman spectroscopy is reported to be effective on soft, hydrated tissues^{3,30} due to the relative Raman inactivity of water¹²², yet most of the published literature on Raman-characterized collagen crosslinks is in reference to bone. To the authors' knowledge, this study represents the third investigation by Raman spectroscopy of thermally fused connective tissue, and the second in reference to fused arteries.

5.4.3. Cross-link quantification

Prior investigation by HPLC of argon laser-welded vascular tissue (incised femoral veins and arteries) indicated decreased levels of HLNL, DHLNL and HPyr in welded tissues relative to control vessels⁹³. The present work affirms a thermal degradation of HLNL alone, with insignificant, if minor decreases in the mean values of DHLNL and HPyr. One possible explanation for the decrease in immature crosslinks alone is an increased lability, and thus decreased thermal stability, of bivalent (immature) to tri- and tetravalent (mature) crosslinks. These findings are in support our hypothesis that contrary to published theory, the instantaneous

bonding observed in thermal fusion is not owed in whole or part to the formation of collagenous crosslinks. To the authors' knowledge, this study presents the first quantitative measure of elastin crosslinks in fused tissues.

5.4.4. Proteomics

Recently, proteomic analysis has been gaining increasing usage in medical realms for the detection of novel biomarkers in various diseases⁷⁴. Three extraction fractions of fused tissues are of interest in determining the effects of fusion on arterial tissues. First, a high-salt cellular fraction (HS) provides evidence of thermally induced changes in cellular proteins. Second, a urea-soluble extracellular matrix fraction (sECM) affords the determination of changes in abundance of matrix proteins that may be modified *in vivo* during remodeling and aging processes. Lastly, an insoluble extracellular matrix fraction (iECM) can be quantified to evidence changes in insoluble extracellular matrix proteins induced by exposure to extreme heat during fusion. In fused splenic artery, the observed increase in the abundance of fibrillar collagen to 41% relative to 8% in fresh tissues may indicate a fusion-induced increase in the solubility of fibrillar collagens (e.g., collagen alpha-1(I)). A potential explanation for an increase in solubility is the denaturation of native collagen helices as well as the destruction of collagen crosslinks, thus, the proteomic analysis is in agreement with the findings of polarized histology, Raman spectroscopy and cross-link quantification.

5.4.5. Conclusion

The clinical objective of energy-based vessel sealing is an instantaneous, water-tight ligature in lieu of mechanical alternatives such as sutures, staples, and clips. The use of fusion for bonding and functional recovery in native tissues (e.g., vascular or colorectal anastomosis) may require the same instantaneous bonding, yet is equally dependent on the wound healing

response of thermally devitalized tissue. While collagen synthesis and subsequent cross-linking may be stimulated by the weld process⁴¹ *in vivo*, we conclude that the instantaneous effects of thermal bonding are limited to a dissociation of native secondary collagen structures and of a single immature crosslink species, hydroxylysinoxidized collagen. These findings represent a first quantification of collagen and elastin crosslink stability in thermally fused tissues via UHPLC, and promote further investigation into the immediate and temporal response of cellular proteins within and adjacent to fused tissues.

Chapter 6. Conclusions and Future Work

6.1. Tissue Hydration and Glycosaminoglycan content

The determined influence of tissue hydration on the formation and stability of vascular seals carries numerous implications for the field of energy-based tissue fusion, relevant to both permanent and recoverable vascular closure. Instantaneous and permanent bonds may benefit from a vaporization-induced amalgamation of cellular and extracellular proteins, but without supplemental bonding (e.g., via the formation of blood clots due to stagnation in adjacent blood vessel sections), vascular seals and cuts are susceptible to degradation via rehydration in contact with biological fluids *in vivo*. While many surgeons assume this risk in the use of vessel sealing and transection devices, the long-term implementation of vessel sealing may require supplemental bonding of sealed and transected vessels to avert such risks. In recoverable fusion, the maintenance of tissue water for the initiation of a response to thermal injury demands an optimization of water loss with bond strength, which has yet to be achieved in experimental or

clinical fusion. Future work may entail the determination of this balance and the development of biological feedback-based methods for its attainment in vascular and similarly hydrated tissues.

6.2. Heating Rates and Fusion Duration

In evaluating progressive heating rates for vascular sealing, we demonstrated the sensitivity of a clinical fusion performance metric (e.g., bursting pressure) to the rate at which water is forcibly desiccated from fused tissues. Likewise, we established a reference values at which high-temperature, low-load vascular fusion may be used to achieve adequate bonding strengths with minimal damage for implementation in functionally recoverable vascular anastomosis. The use of a progressive heating rate over extended durations was demonstrated to increase bond strength for clinically implemented fusion temperatures (170 °C); this approach may prove useful in exploring functional recovery potential of fused tissues. Future work may incorporate assessments of tissue damage and associated recovery viability at these parameters, as the presented work did not directly collect or assess measures of tissue damage.

6.3. Collagen Denaturation and Cross-linking of Extracellular Matrix Proteins

The use of UHPLC in conjunction with established mass spectrometry techniques for the detection of thermal transitions in collagen, elastin, and cellular proteins has resulted in a detailed, constituent-based report of vascular fusion-induced changes in molecular and molecular bond abundance– the first data of its kind. In establishing a constitutive model of fusion adhesion, it is these small-scale, energy-induced transitions that form the building blocks for a predictive ability of which tissues hold the potential for energy-based fusion, and how strong of a bond they may form under a given set of fusion parameters. While detailed proteomic abundance data was collected for fresh and fused tissue, the determination of which cellular and

extracellular matrix proteins are of the highest influence in fusion formation remains a great challenge, as primary constituents (e.g., collagen, elastin) continue to draw the most attention. We believe that to truly progress constitutive bonding theory, these techniques must be utilized first on synthetic, isolated tissues with a simplified composition to determine the true players in fusion adhesion.

6.4. Synthesis of Outcomes

Over three decades of research and development in energy-based tissue treatment have elicited a plethora of observations, theories, and assumptions about the nature of the fusion bond. Many instances of published fusion research reference previously documented suppositions or hypotheses that have yet to be substantiated in controlled study. Most importantly, the clinical efficacy of FDA-approved surgical devices has been demonstrated using data obtained in laboratory settings that are misrepresentative of the devices' relevant clinical environments. The goal of this body of work has thus been to illuminate discrepancies in clinical vs. benchtop device validation, and to seek and support a fundamental understanding of energy-based transitions in biological tissue that give rise to the observed clinical utility of energy-based tissue fusion devices.

The early foundations for this work aimed to characterize device performance in vascular ligation across a broad spectrum of fusion parameters, as well as to describe tissue-device interactions that may shed light on potential areas for bond strength optimization and increased applicability of the fusion technique. A precedent for fusion device “parameter sweeps” was set by early members of the tissue fusion project, who investigated effects of fusion temperature and duration on the outcome of vascular bond strength¹⁶. In collecting data for this and parallel studies, we noticed that tissue storage in chilled isotonic saline, a common storage medium, may

have been affecting bursting pressure outcomes of sealed vessels. Formal investigation of these effects led to the publication of a direct comparison between device performance *in vivo* and that following tissue harvest and storage in an *ex vivo* environment¹⁴. The findings of this study began to support the notion that tissue water content, be it bound or free, native or imbibed during storage, played a significant role in the formation and bonding strength of vascular seals. This insight supported further exploration of water's contributions to fusion, especially in a sea of literature that seemed to be largely complacent with established assumptions that implicated collagen "transitions", side-to-side and end-to-end cross-links of collagen fibers, or otherwise broadly defined bonding traits observed in qualitative imaging studies. As such, we directly pursued the alteration of tissue water content as an independent variable in assessing fusion strength in Aim 1. Likewise, hydrophilic GAG molecules were digested longitudinally, and sealed vessels from both dehydrated and GAG-digested tissues were subsequently rehydrated to evaluate the "solubility" of bonded tissue in an aqueous environment. As discussed in Aim 1, we hypothesized that the thermally-induced transport of water vapor during fusion may contribute to a chaotic entanglement of denatured collagen fibers during fusion. Further, we hypothesized that upon cooling, these fibers may be inclined to interact with each other via Hydrogen bonds, supported by the breakdown in bond integrity with exposure to water. While it is chemically challenging to measure the presence of hydrogen bonding in physical tissue samples, it may be worthwhile to pursue a controlled model of such an interaction via molecular dynamics simulation in the future. To establish that fusion adhesion relies largely on water-soluble bonding forces may greatly alter the perception of its clinical applicability relative to the covalent cross-linking structure that has been described, not proven, in the literature.

A second hypothesis resulting from the analysis of Aim 1 outcomes and observations in the literature is that fusion of collagenous tissues may not be feasible without a cellular component to the target tissue. Empirical investigation has shown that blood vessels, colorectal and reproductive vascular tissue, and skin respond favorably to energy-based joining, while highly collagenous, acellular tissues such as tendon and cartilage require supplemental adhesives to achieve tenuous bonding at best. The insight is critical, as fused tissues may ultimately be regarded as a fibrous matrix of denatured proteins (collagen, elastin) joined in part not only by entanglement, but by a “polymer” component of lysed and coagulated cellular material (fibrin, fibronectin, lipids, cytoskeletal and other adhesive proteins). Perhaps primary tissue constituents by mass (e.g. collagen) were only a precursor to fusion, but independent of cells would not allow for any adhesion. This theory may be tested in the future via longitudinal decellularization of native tissues that would normally demonstrate successful fusion.

It is commonly accepted that while energy-based fusion is useful for clinical ligation, that these sealed vessels are permanently damaged and rendered functionally useless to the circulatory system. As such, the utility of fusion for long-term healing and functional recovery may be regarded with skepticism. After all, why would a tissue repair or reconstruction strategy begin with thermal injury? Our hypothesis is that such an injury may not only enable water-tight junctions in lieu of leaky foreign-body closure, but in fact induce and accelerate the onset of inflammation and subsequent tissue remodeling that may lead to functional recovery. The key to this pursuit is balancing tissue damage for the purpose of bond strength with its ability to react to thermal injury, and continue to transmit the appropriate molecular signals (e.g., heat-shock proteins), and recruit and provide transport for the cells that facilitate new tissue deposition and functional recovery of the injured vessel. While clinical fusion devices aspire to minimized

thermal damage surrounding the target tissue, Aim 2 revealed that fusion must not occur on short time scales, and that in conjunction with the findings of Aim 1, prolonging the transport period of water vapor and denatured proteins may be a logical approach to achieving closure while preserving tissue integrity for the purposes of functional recovery. The burden on subsequent fusion research is to quantify tissue damage via established techniques such as cell viability assays, and potentially allow for the *in vivo* restoration of an energy-based anastomosis via custom device construction and implementation of *in vitro* bioreaction, or an animal model.

We recognize that the assumption of covalent crosslinking during thermal fusion has great implications for the potential of vascular fusion, but without direct evidence we felt compelled to prove or disprove this long-standing assumption. During the time of writing of these conclusions, Winter 2016, investigators in academia continue to cite this assumption of collagen crosslinking as a basis for investigation into anastomosis for microvascular supply networks to “free flap” tissue transplants. As might be expected, instantaneous tissue adhesion in an *ex vivo* laboratory setting is easily demonstrable; immediate perfusion may likewise be obtained. We remain concerned, however, about the bond integrity and vascular patency of such an anastomosis in the long term, due to the results of Aim 2, specifically the effects of aqueous bond rehydration. Empirical evidence has enabled the approval of devices for destructive ligation, but as mentioned throughout this work, both academia and industry continue to push this technique forward into functional recovery despite blindness to the underlying adhesive mechanisms. The results of Aim 3 have shown that covalent crosslinks are not increasing in abundance during thermal fusion, and that only 1 immature crosslink species has been shown to be labile during fusion. As such, we can no longer rely on this assumption to support our empirical investigations. Having challenged and disproven a commonly cited assumption on the

nature of the fusion bond, we believe the burden on the field of fusion to lie in utilizing instantaneous adhesion with limited energy to achieve tissue bonding, while focusing future research efforts on the observation of cellular activity adjacent to and across the bonding interface of fused tissues.

6.5. Closure

The state of clinical and experimental energy-based tissue fusion lies between the empirical investigation of existing surgical devices and the analytical assessment of thermal transitions in the myriad components of biological tissues. This work has affirmed several published observations of contributors to fusion adhesion, identified a novel antagonist to the formation of energy-based surgical bonds, and has refuted a long-standing hypothesis related to the nature of the instantaneous, watertight fusion bond. While the surgical advantages of the fusion technique remain evident and should continue to be explored, it is our hope that the utilization of surgical energy for sutureless closure of biological tissues will one day rest on a sound understanding of the chemical, biological, and mechanical pathways that empower it.

References

1. Aksan, A., A. Hubel, and J. C. Bischof. Frontiers in biotransport: water transport and hydration. *J. Biomech. Eng.* 131:74004, 2009.
2. Aksan, A., J. J. McGrath, and D. S. Nielubowicz Jr. Thermal damage prediction for collagenous tissues part I: a clinically relevant numerical simulation incorporating heating rate dependent denaturation. *J. Biomech. Eng.* 127:85–97, 2005.
3. Alimova, A., R. Chakraverty, R. Muthukattil, S. Elder, A. Katz, V. Sriramoju, S. Lipper, and R. R. Alfano. In vivo molecular evaluation of guinea pig skin incisions healing after surgical suture and laser tissue welding using Raman spectroscopy. *J. Photochem. Photobiol. B* 96:178–183, 2009.
4. Anderson, N., E. Kramer, J. Cezo, V. Ferguson, and M. E. Rentschler. Tissue Bond Strength as a Function of Applied Fusion Pressure. *J. Med. Devices* 8:30925, 2014.
5. Arya, S., N. Hadjievangelou, S. Lei, H. Kudo, R. D. Goldin, A. W. Darzi, D. S. Elson, and G. B. Hanna. Radiofrequency-induced small bowel thermofusion: an ex vivo study of intestinal seal adequacy using mechanical and imaging modalities. *Surg. Endosc.* 27:3485–3496, 2013.
6. Barbosa, I. Improved and simple micro assay for sulfated glycosaminoglycans quantification in biological extracts and its use in skin and muscle tissue studies. *Glycobiology* 13:647–653, 2003.
7. Barton, M. J., J. W. Morley, M. A. Stoodley, A. Lauto, and D. A. Mahns. Nerve repair: toward a sutureless approach. *Neurosurg. Rev.* 37:585–595, 2014.
8. Bass, L. S., N. Moazami, J. Pocsidio, M. C. Oz, P. Logerfo, and M. R. Treat. Changes in type I collagen following laser welding. *Lasers Surg. Med.* 12:500–505, 1992.
9. Bruce G. Frushour and Jack L. Koenig. Raman Scattering of Collagen, Gelatin, and Elastin. *Biopolymers* 14:379–391, 1975.
10. Burt, James D., Siddins, Mark, and Morrison, Wayne. Laser Photoirradiation in Digital Flexor Tendon Repair. *Plast. Reconstr. Surg.* 108:688–694, 2001.
11. Campbell, P. A., A. B. Cresswell, T. G. Frank, and A. Cuschieri. Real-time thermography during energized vessel sealing and dissection. *Surg. Endosc.* 17:1640–1645, 2003.
12. Carbonell, A. M., C. S. Joels, K. W. Kercher, B. D. Matthews, R. F. Sing, and B. T. Heniford. A comparison of laparoscopic bipolar vessel sealing devices in the hemostasis of small-, medium-, and large-sized arteries. *J. Laparoendosc. Adv. Surg. Tech. A* 13:377–380, 2003.
13. Carden, A., R. M. Rajachar, M. D. Morris, and D. H. Kohn. Ultrastructural Changes Accompanying the Mechanical Deformation of Bone Tissue: A Raman Imaging Study. *Calcif. Tissue Int.* 72:166–175, 2003.
14. Cezo, J. D., E. A. Kramer, J. A. Schoen, V. L. Ferguson, K. D. Taylor, and M. E. Rentschler. Tissue storage ex vivo significantly increases vascular fusion bursting pressure. *Surg. Endosc.* 1999–2005, 2015. doi:10.1007/s00464-014-3900-4
15. Cezo, J. D., E. Kramer, K. D. Taylor, V. Ferguson, and M. E. Rentschler. Temperature Measurement Methods During Direct Heat Arterial Tissue Fusion. *IEEE Trans. Biomed. Eng.* 60:2552–2558, 2013.
16. Cezo, J. D., A. C. Passernig, V. L. Ferguson, K. D. Taylor, and M. E. Rentschler. Evaluating temperature and duration in arterial tissue fusion to maximize bond strength. *J. Mech. Behav. Biomed. Mater.* 30:41–49, 2014.
17. Cezo, J.D., Kramer, E.A., Taylor, K.D., Ferguson, V.L., and Rentschler, M.E. Tissue Fusion Bursting Pressure and the Role of Tissue Water Content., 2013.

- 18.Chen, R. K., M. W. Chastagner, R. E. Dodde, and A. J. Shih. Electrosurgical Vessel Sealing Tissue Temperature: Experimental Measurement and Finite Element Modeling. *IEEE Trans. Biomed. Eng.* 60:453–460, 2013.
- 19.Chen, R. K., M. W. Chastagner, J. D. Geiger, and A. J. Shih. Bipolar Electrosurgical Vessel-Sealing Device With Compressive Force Monitoring. *J. Biomech. Eng.* 136:61001, 2014.
- 20.Cilesiz, I. Controlled temperature photothermal tissue welding. *J. Biomed. Opt.* 4:327–336, 1999.
- 21.David Krause. JustRight Surgical Vessel Sealing System. , 2016.
- 22.Despa, F., D. P. Orgill, J. Neuwalder, and R. C. Lee. The relative thermal stability of tissue macromolecules and cellular structure in burn injury. *Burns* 31:568–577, 2005.
- 23.Elvin, C. M., A. G. Brownlee, M. G. Huson, T. A. Tebb, M. Kim, R. E. Lyons, T. Vuocolo, N. E. Liyou, T. C. Hughes, J. A. M. Ramshaw, and J. A. Werkmeister. The development of photochemically crosslinked native fibrinogen as a rapidly formed and mechanically strong surgical tissue sealant. *Biomaterials* 30:2059–2065, 2009.
- 24.Entezari, K., P. Hoffmann, M. Goris, A. Peltier, and R. Van Velthoven. A review of currently available vessel sealing systems. *Minim. Invasive Ther. Allied Technol. MITAT Off. J. Soc. Minim. Invasive Ther.* 16:52–57, 2007.
- 25.Ethicon. Harmonic ACE+ Shears., Web. June 2016. <http://www.ethicon.com/healthcare-professionals/products/advanced-energy/harmonic/harmonic-ace-plus>
- 26.Ewen Smith, and Geoffrey Dent. Modern Raman Spectroscopy: A practical approach. John Wiley & Sons, 2005.
- 27.Fankell, D. P., E. Kramer, J. Cezo, K. D. Taylor, V. L. Ferguson, and M. E. Rentschler. A Novel Parameter for Predicting Arterial Fusion and Cutting in Finite Element Models. *Ann. Biomed. Eng.* 44(11): 3295-3306, 2016. doi:10.1007/s10439-016-1588-4
- 28.Farndale, R. W., D. J. Buttle, and A. J. Barrett. Improved quantitation and discrimination of sulphated glycosaminoglycans by use of dimethylmethylene blue. *Biochim. Biophys. Acta BBA-Gen. Subj.* 883:173–177, 1986.
- 29.Fenner, J. W., W. Martin, H. Moseley, and D. J. Wheatley. Dehydration: a model for (low-temperature) argon laser tissue bonding. *Phys. Med. Biol.* 39:2147–2160, 1994.
- 30.Figueiredo, R. L. P., M. S. S. Dantas, and R. L. Oréfice. Thermal welding of biological tissues derived from porcine aorta for manufacturing bioprosthetic cardiac valves. *Biotechnol. Lett.* 33:1699–1703, 2011.
- 31.Floume, T., R. R. A. Syms, A. W. Darzi, and G. B. Hanna. Optical, thermal, and electrical monitoring of radio-frequency tissue modification. *J. Biomed. Opt.* 15:18003-18003–10, 2010.
- 32.Gineyts, E., O. Borel, R. Chapurlat, and P. Garnero. Quantification of immature and mature collagen crosslinks by liquid chromatography–electrospray ionization mass spectrometry in connective tissues. *J. Chromatogr. B* 878:1449–1454, 2010.
- 33.Guthrie, C. R., L. W. Murray, G. E. Kopchok, D. Rosenbaum, and R. A. White. Biochemical mechanisms of laser vascular tissue fusion. *J. Investig. Surg. Off. J. Acad. Surg. Res.* 4:3–12, 1991.
- 34.Harold, K. L., H. Pollinger, B. D. Matthews, K. W. Kercher, R. F. Sing, and B. T. Heniford. Comparison of ultrasonic energy, bipolar thermal energy, and vascular clips for the hemostasis of small-, medium-, and large-sized arteries. *Surg. Endosc.* 17:1228–1230, 2003.
- 35.Henninger, H. B., C. J. Underwood, G. A. Ateshian, and J. A. Weiss. Effect of sulfated glycosaminoglycan digestion on the transverse permeability of medial collateral ligament. *J. Biomech.* 43:2567–2573, 2010.

- 36.Ho, Y.-H. Techniques for colorectal anastomosis. *World J. Gastroenterol.* 16:1610, 2010.
- 37.Hruby, G. W., F. C. Marruffo, E. Durak, S. M. Collins, P. Pierorazio, P. A. Humphrey, M. M. Mansukhani, and J. Landman. Evaluation of surgical energy devices for vessel sealing and peripheral energy spread in a porcine model. *J. Urol.* 178:2689–2693, 2007.
- 38.Hu, L., Z. Lu, B. Wang, J. Cao, X. Ma, Z. Tian, Z. Gao, L. Qin, X. Wu, Y. Liu, and others. Closure of skin incisions by laser-welding with a combination of two near-infrared diode lasers: preliminary study for determination of optimal parameters. *J. Biomed. Opt.* 16:38001–38001, 2011.
- 39.Ishii-Nozawa, R., T. Naito, M. Mita, K. Miyazaki, Y. Matsuda, and K. Takeuchi. Effect of Chondroitinase on Dermatan Sulfate-Facilitated Arginine Amidase Released from Rabbit Ear Artery. *Biol. Pharm. Bull.* 33:150–152, 2010.
- 40.Iwasaki, Y., J. J. Kazama, H. Yamato, and M. Fukagawa. Changes in chemical composition of cortical bone associated with bone fragility in rat model with chronic kidney disease. *Bone* 48:1260–1267, 2011.
- 41.Jing Tang, David O’Callaghan, Simone Rouy, and Guilhem Godlewski. Quantitative Changes in Collagen Levels Following 830-nm Diode Laser Welding. *Lasers Surg. Med.* 22:207–211, 1998.
- 42.John A. Pearce, Sharon Thomsen, Helen Vijverberg, and Todd Magnusen. Quantitative measures of thermal damage: Birefringence changes in thermally coagulated collagen. *Adv. Bioheat Mass Transf.* 141–144, 1993.
- 43.Johnson, T. S., A. C. O’Neill, P. M. Motarjem, C. Amann, T. Nguyen, M. A. Randolph, J. M. Winograd, I. E. Kochevar, and R. W. Redmond. Photochemical Tissue Bonding: A Promising Technique for Peripheral Nerve Repair. *J. Surg. Res.* 143:224–229, 2007.
- 44.Katchinskiy, N., R. Godbout, H. R. Goetz, and A. Y. Elezzabi. Femtosecond laser-induced cell-cell surgical attachment: Femtosecond Laser Cell-Cell Attachment. *Lasers Surg. Med.* 46:335–341, 2014.
- 45.Katsumi Murata, Koji Nakazawa, and Akio Hamai. Distribution of acidic glycosaminoglycans in the intima, media and adventitia of bovine aorta and their anticoagulant properties. *Atherosclerosis* 21:93–103, 1975.
- 46.Kennedy JS, Stranahan PL, Taylor KD, and Chandler JG. High burst-strength, feedback-controlled bipolar vessel sealing. *Surg. Endosc.* 12:876–878, 1998.
- 47.Kilkelly, M. A. J., C. P. T. Choma, N. Popovic, M. A. J. Miller, and D. E. Sweet. Tendon repair by laser welding: a histologic and biomechanical comparison and suture repair with CO2 and argon lasers. *Lasers Surg. Med.* 19:487–491, 1996.
- 48.Kramer, E. A., N. S. Anderson, K. D. Taylor, V. L. Ferguson, and M. E. Rentschler. The role of glycosaminoglycans in tissue adhesion during energy-based vessel sealing. , 2015.doi:10.1117/12.2081082
- 49.Kramer, E. A., J. D. Cezo, D. P. Fankell, K. D. Taylor, M. E. Rentschler, and V. L. Ferguson. Strength and Persistence of Energy-Based Vessel Seals Rely on Tissue Water and Glycosaminoglycan Content. *Ann. Biomed. Eng.* 44(11): 3421-3431, 2016.doi:10.1007/s10439-016-1657-8
- 50.Kramer, R. Z., J. Bella, P. Mayville, B. Brodsky, and H. M. Berman. Sequence dependent conformational variations of collagen triple-helical structure. NATURE AMERICA INC 345 PARK AVE SOUTH, NEW YORK, NY 10010-1707 USA, 1999, 454–457 pp.
- 51.Kramer, E. A. Crosslink stability in energy-based tissue bonding: molecular analysis of collagenous transitions via Raman spectroscopy and mass spectrometry. *Unpubl. Res.* , 2016.

- 52.Lamberton, G. R., R. S. Hsi, D. H. Jin, T. U. Lindler, F. C. Jellison, and D. D. Baldwin. Prospective comparison of four laparoscopic vessel ligation devices. *J. Endourol. Endourol. Soc.* 22:2307–2312, 2008.
- 53.Landman, J., K. Kerbl, J. Rehman, C. Andreoni, P. A. Humphrey, W. Collyer, E. Olweny, C. Sundaram, and R. V. Clayman. Evaluation of a vessel sealing system, bipolar electrosurgery, harmonic scalpel, titanium clips, endoscopic gastrointestinal anastomosis vascular staples and sutures for arterial and venous ligation in a porcine model. *J. Urol.* 169:697–700, 2003.
- 54.Lauto, A., D. P. Poppas, and G. A. C. Murrell. Solubility study of albumin solders for laser tissue-welding. *Lasers Surg. Med.* 23:258–262, 1998.
- 55.Lauto, A., R. Trickett, R. Malik, J. Dawes, and E. Owen. Laser-activated solid protein bands for peripheral nerve repair. *Lasers Surg Med* 21:134–141, 1997.
- 56.Lauto, A, Dawes, JM, Piper, JA, and Owen, ER. Laser nerve repair by solid protein band technique II: assessment of long-term nerve regeneration. *Microsurgery* 18:60–64, 1998.
- 57.Lawrence S. Bass, and Michael R. Treat. Laser Tissue Welding: A comprehensive review of current and future clinical applications.pdf. *Lasers Surg. Med.* 17:315–349, 1995.
- 58.Lim, C., R. Goldin, D. Elson, A. Darzi, and G. Hanna. In vivo thermography during small bowel fusion using radiofrequency energy. *Surg. Endosc.* 24:2465–2474, 2010.
- 59.Lorenzo, A. C., and E. R. Caffarena. Elastic properties, Young’s modulus determination and structural stability of the tropocollagen molecule: a computational study by steered molecular dynamics. *J. Biomech.* 38:1527–1533, 2005.
- 60.Lorenzo, N. D., L. Franceschilli, M. E. Allaix, A. Asimakopoulos, P. Sileri, and A. L. Gaspari. Radiofrequency versus ultrasonic energy in laparoscopic colorectal surgery: a metaanalysis of operative time and blood loss. *Surg. Endosc.* 26:2917–2924, 2012.
- 61.Luescher, Madeline, Ruegg, M., and Schindler, P. Effect of Hydration upon the Thermal Stability of Tropocollagen and its Dependence on the Presence of Neutral Salts. *Biopolymers* 13:2489–2508, 1974.
- 62.Mandair, G. S., and M. D. Morris. Contributions of Raman spectroscopy to the understanding of bone strength. *BoneKEy Rep.* 4:620, 2015.
- 63.Matteini, P., F. Rossi, L. Menabuoni, and R. Pini. Microscopic characterization of collagen modifications induced by low-temperature diode-laser welding of corneal tissue. *Lasers Surg. Med.* 39:597–604, 2007.
- 64.Medtronic, Covidien. Vessel Sealing., Web, June 2016. <http://www.medtronic.com/covidien/products/vessel-sealing>
- 65.Miles, C. A., N. C. Avery, V. V. Rodin, and A. J. Bailey. The Increase in Denaturation Temperature Following Cross-linking of Collagen is Caused by Dehydration of the Fibres. *J. Mol. Biol.* 346:551–556, 2005.
- 66.Miles, C. A., T. V. Burjanadze, and A. J. Bailey. The kinetics of the thermal denaturation of collagen in unrestrained rat tail tendon determined by differential scanning calorimetry. *J. Mol. Biol.* 245:437–446, 1995.
- 67.Morriss-Kay, G., and F. Tuckett. Immunohistochemical localisation of chondroitin sulphate proteoglycans and the effects of chondroitinase ABC in 9-to 11-day rat embryos. *Development* 106:787–798, 1989.
- 68.Murray, L. W., L. Su, G. E. Kopchok, and R. A. White. Crosslinking of extracellular matrix proteins: a preliminary report on a possible mechanism of argon laser welding. *Lasers Surg. Med.* 9:490–496, 1989.

69. Newcomb, W. L., W. W. Hope, T. M. Schmelzer, J. J. Heath, H. J. Norton, A. E. Lincourt, B. T. Heniford, and D. A. Iannitti. Comparison of blood vessel sealing among new electro-surgical and ultrasonic devices. *Surg. Endosc.* 23:90–96, 2009.
70. Ngeow, W. C. Scar less: a review of methods of scar reduction at sites of peripheral nerve repair. *Oral Surg. Oral Med. Oral Pathol. Oral Radiol. Endodontology* 109:357–366, 2010.
71. Nguyen, T. T., C. Gobinet, J. Feru, S. B. -Pasco, M. Manfait, and O. Piot. Characterization of Type I and IV Collagens by Raman Microspectroscopy: Identification of Spectral Markers of the Dermo-Epidermal Junction. *Spectrosc. Int. J.* 27:421–427, 2012.
72. O’Connell, M. K., S. Murthy, S. Phan, C. Xu, J. Buchanan, R. Spilker, R. L. Dalman, C. K. Zarins, W. Denk, and C. A. Taylor. The three-dimensional micro- and nanostructure of the aortic medial lamellar unit measured using 3D confocal and electron microscopy imaging. *Matrix Biol.* 27:171–181, 2008.
73. Oest, M. E., B. Gong, K. Esmonde-White, K. A. Mann, N. D. Zimmerman, T. A. Damron, and M. D. Morris. Parathyroid hormone attenuates radiation-induced increases in collagen crosslink ratio at periosteal surfaces of mouse tibia. *Bone* 86:91–97, 2016.
74. Ogita, M., S. Tsuchida, A. Aoki, M. Satoh, S. Kado, M. Sawabe, H. Nanbara, H. Kobayashi, Y. Takeuchi, K. Mizutani, Y. Sasaki, F. Nomura, and Y. Izumi. Increased cell proliferation and differential protein expression induced by low-level Er:YAG laser irradiation in human gingival fibroblasts: proteomic analysis. *Lasers Med. Sci.* 30:1855–1866, 2015.
75. Pabittei, D. R., M. Heger, S. van Tuijl, M. Simonet, W. de Boon, A. C. van der Wal, R. Balm, and B. A. de Mol. Ex vivo proof-of-concept of end-to-end scaffold-enhanced laser-assisted vascular anastomosis of porcine arteries. *J. Vasc. Surg.* 62:200–209, 2015.
76. Pearce, J. A., S. L. Thomsen, H. Vijverberg, and T. J. McMurray. Kinetics for birefringence changes in thermally coagulated rat skin collagen. , 1993.at <<http://proceedings.spiedigitallibrary.org/proceeding.aspx?articleid=1006899>>
77. Pearce, John A., and Thomsen, Sharon. Kinetic Models of Laser-Tissue Fusion Processes. *Biomed. Sci. Instrum.* 29:355–60, 1993.
78. Person, B., D. A. Vivas, D. Ruiz, M. Talcott, J. E. Coad, and S. D. Wexner. Comparison of four energy-based vascular sealing and cutting instruments: A porcine model. *Surg. Endosc.* 22:534–538, 2008.
79. Phillips, C. K., G. W. Hruby, E. Durak, D. S. Lehman, P. A. Humphrey, M. M. Mansukhani, and J. Landman. Tissue response to surgical energy devices. *Urology* 71:744–748, 2008.
80. PL Privalov, EI Tiktopulo, and VM Tischenko. Stability and mobility of the collagen structure. *J. Mol. Biol.* 127:203–216.
81. R. C. Lee, and R. D. Astumian. The physicochemical basis for thermal and non-thermal “burn” injuries. *Burns* 22:509–519, 1996.
82. Ramachandran, G. N., and Kartha, G. Structure of Collagen. *Nature* 174:269–70, 1954.
83. Rasca, E., C. Nyssen-Behets, M. Tielemans, A. Peremans, N. Hendaoui, D. Heyselaer, U. Romeo, and S. Nammour. Gingiva Laser Welding: Preliminary Study on an *Ex Vivo* Porcine Model. *Photomed. Laser Surg.* 32:437–443, 2014.
84. Richard O. Hynes, and Kenneth M. Yamada. Extracellular Matrix Biology. Cold Spring Harbor Press, 2012, 397 pp.
85. Richter, S., O. Kollmar, E. Neunhoeffler, M. K. Schilling, M. D. Menger, and G. Pistorius. Differential response of arteries and veins to bipolar vessel sealing: evaluation of a novel reusable device. *J. Laparoendosc. Adv. Surg. Tech. A* 16:149–155, 2006.

86. Robins, S. P. Biochemistry and functional significance of collagen cross-linking. *Biochem. Soc. Trans.* 35:, 2007.
87. Rodney A. White, George Kopchock, Carlos Donayre, Patrick Abergel, Richard Lyons, Stanley R. Klein, Richard M. Dwyer, and Jouni Uitto. Comparison of Laser-Welded and Sutured Arteriotomies. *Arch. Surg.* 121:1133–35, 1986.
88. Santini, M., G. Vicidomini, A. Baldi, G. Gallo, P. Laperuta, L. Busiello, M. P. Di Marino, and V. Pastore. Use of an electrothermal bipolar tissue sealing system in lung surgery. *Eur. J. Cardio-Thorac. Surg. Off. J. Eur. Assoc. Cardio-Thorac. Surg.* 29:226–230, 2006.
89. Schober, R., F. Ulrich, T. Sander, H. Dürselen, and S. Hessel. Laser-induced alteration of collagen substructure allows microsurgical tissue welding. *Science* 232:1421–1422, 1986.
90. Serure, Alan, Edward H. Withers, S. Thomsen, and J. Morris. Comparison of carbon dioxide laser-assisted microvascular anastomosis and conventional microvascular sutured anastomosis. *Surg. Forum* 34:634–636, 1984.
91. Shields, Chelsea A., Schechter, David A., Tetzlaff, Phillip, Baily, Ali L, and Dycus, Sean. Method for creating ideal tissue fusion in soft-tissue structures using radio frequency (RF) energy. *Surg. Technol. Int.* 13:49–55, 2004.
92. Sindram, D., K. Martin, J. P. Meadows, A. S. Prabhu, J. J. Heath, I. H. McKillop, and D. A. Iannitti. Collagen–elastin ratio predicts burst pressure of arterial seals created using a bipolar vessel sealing device in a porcine model. *Surg. Endosc.* 25:2604–2612, 2011.
93. Small IV, W., P. M. Celliers, G. E. Kopchok, K. M. Reiser, N. J. Heredia, D. J. Maitland, D. C. Eder, R. A. London, M. Heilbron, F. Hussain, R. A. White, L. B. Da Silva, and D. L. Matthews. In-vivo argon laser vascular welding using thermal feedback: Open- and closed-loop patency and collagen crosslinking. , 1997.
94. Smith, R., and R. Pasic. The role of vessel sealing technologies in laparoscopic surgery. *Surg. Technol. Int.* 17:208–212, 2008.
95. Smulders, J. F., I. H. J. T. de Hingh, J. Stavast, and J. J. Jackimowicz. Exploring new technologies to facilitate laparoscopic surgery: creating intestinal anastomoses without sutures or staples, using a radio-frequency-energy-driven bipolar fusion device. *Surg. Endosc.* 21:2105–2109, 2007.
96. Sooklal, Valmiki, McClure, Jesse, Hooper, Luke, and Larson, Michael. A laser device for fusion of nasal mucosa. , 2011.
97. Sriramoju, V., and R. R. Alfano. Management of heat in laser tissue welding using NIR cover window material. *Lasers Surg. Med.* 43:991–997, 2011.
98. Sriramoju, V., and R. R. Alfano. In vivo studies of ultrafast near-infrared laser tissue bonding and wound healing. *J. Biomed. Opt.* 20:108001–108001, 2015.
99. Sriramoju, V., H. E. Savage, A. Katz, R. Chakraverty, Y. Budansky, R. Podder, N. Davatgarzadeh, U. Kartazayev, R. B. Rosen, and R. R. Alfano. NIR-laser tissue welding in an in vivo guinea pig animal model</title>>, 2008.doi:10.1117/12.760044
100. Su, L., K. L. Cloyd, S. Arya, M. A. B. Hedegaard, J. A. M. Steele, D. S. Elson, M. M. Stevens, and G. B. Hanna. Raman spectroscopic evidence of tissue restructuring in heat-induced tissue fusion: New technology for tissue fusion characterization. *J. Biophotonics* 7:713–723, 2014.
101. Su, L., M. B. Fonseca, S. Arya, H. Kudo, R. Goldin, G. B. Hanna, and D. S. Elson. Laser-induced tissue fluorescence in radiofrequency tissue-fusion characterization. *J. Biomed. Opt.* 19:15007–15007, 2014.

102. Sutton, P. A., S. Awad, A. C. Perkins, and D. N. Lobo. Comparison of lateral thermal spread using monopolar and bipolar diathermy, the Harmonic Scalpel and the Ligasure. *Br. J. Surg.* 97:428–433, 2010.
103. Tang, J., G. Godlewski, S. Rouy, and G. Delacrétaz. Morphologic changes in collagen fibers after 830 nm diode laser welding. *Lasers Surg. Med.* 21:438–443, 1997.
104. TAPAN K. GAYEN, A. KATZ, HOWARD E. SAVAGE. Aorta and Skin Tissues Welded By Near-Infrared Cr⁴⁺:YAG Laser. *J. Clin. Laser Med. Surg.* 21:259–269.
105. Targarona, E. M., C. Balague, J. Marin, R. B. Neto, C. Martinez, J. Garriga, and M. Trias. Energy sources for laparoscopic colectomy: a prospective randomized comparison of conventional electro-surgery, bipolar computer-controlled electro-surgery and ultrasonic dissection. Operative outcome and costs analysis. *Surg. Innov.* 12:339–344, 2005.
106. Valleylab. 510(k) Notification. Summary of Safety and Effectiveness Information: LigaSure Vessel Sealing System. , 2004.
107. Vladimirova, I. A., Y. N. Lankin, I. B. Philyppov, L. F. Sushiy, and Y. M. Shuba. Frequency dependence of excitation–contraction of multicellular smooth muscle preparations: the relevance to bipolar electro-surgery. *J. Surg. Res.* 186:119–125, 2014.
108. Wallwiener, C. W., T. K. Rajab, W. Zubke, K. B. Isaacson, M. Enderle, D. Schälller, and M. Wallwiener. Thermal conduction, compression, and electrical current--an evaluation of major parameters of electro-surgical vessel sealing in a porcine in vitro model. *J. Minim. Invasive Gynecol.* 15:605–610, 2008.
109. Ward Small IV. Thermal and Molecular Evaluation of Laser Tissue Welding. , 1998.
110. Watanabe, H. Temperature Dependence of Thermal Conductivity of Liver Based on Various Experiments and a Numerical Simulation for RF Ablation. *32nd IEEE EMBS Proc.* , 2010. at <<http://ieeexplore.ieee.org/stamp/stamp.jsp?tp=&arnumber=5627200>>
111. Weir, Charles E. Rate of shrinkage of tendon collagen: Heat, entropy and free energy of activation of the shrinkage of untreated tendon; Effect of acid, salt, pickle, and tannage of the activation of tendon collagen. *J. Res. Natl. Bur. Stand.* 42:Research Paper RP1947, 1949.
112. White, R. A., G. Kopchok, S.-K. Peng, R. Fujitani, G. White, S. Klein, and J. Uitto. Laser vascular welding—how does it work? *Ann. Vasc. Surg.* 1:461–464, 1987.
113. Winter, Hanno, Holmer, Christoph, Buhr, Heinz-Johannes, Lindner, Gerd, Lauster, Roland, Kraft, Marc, and Ritz, Jörg-Peter. Pilot study of bipolar radiofrequency-induced anastomotic thermofusion -exploration of therapy parameters ex vivo. *Int J Colorectal Des* 25:129–133, 2010.
114. Wright, N. T., and J. D. Humphrey. DENATURATION OF COLLAGEN VIA HEATING: An Irreversible Rate Process. *Annu. Rev. Biomed. Eng.* 4:109–128, 2002.
115. Xu, D., C.-J. Tsai, and R. Nussinov. Hydrogen bonds and salt bridges across protein-protein interfaces. *Protein Eng.* 10:999–1012, 1997.
116. Yang, D., M. C. Converse, D. M. Mahvi, and J. G. Webster. Expanding the Bioheat Equation to Include Tissue Internal Water Evaporation During Heating. *IEEE Trans. Biomed. Eng.* 54:1382–1388, 2007.
117. Zhao, L., C. Zhuo, C. Song, X. Li, Y. Zhou, and D. Shi. Histological characteristics of collagen denaturation and injuries in bipolar radiofrequency-induced colonic anastomoses. *Pathol. - Res. Pract.* 211:214–218, 2015.
118. Züger, B. J., B. Ott, P. Mainil-Varlet, T. Schaffner, J.-F. Clémence, H. P. Weber, and M. Frenz. Laser solder welding of articular cartilage: tensile strength and chondrocyte viability. *Lasers Surg. Med.* 28:427–434, 2001.

119. The Extracellular Matrix: an Overview. Berlin, Heidelberg: Springer Berlin Heidelberg, 2011. at <<http://link.springer.com/10.1007/978-3-642-16555-9>>
120. Conmed Electrosurgery., Web, May 2011. http://www.conmed.com/index_electrosurgery.php
121. The SAGES Manual on the Fundamental Use of Surgical Energy (FUSE). New York, NY: Springer New York, 2012. at <<http://link.springer.com/10.1007/978-1-4614-2074-3>>